

1-1-2007

# Supramolecular Usefulness Of Hexamethylenetetramine

Philius Daka

*Eastern Illinois University*

This research is a product of the graduate program in [Chemistry](#) at Eastern Illinois University. [Find out more](#) about the program.

---

## Recommended Citation

Daka, Philius, "Supramolecular Usefulness Of Hexamethylenetetramine" (2007). *Masters Theses*. 75.  
<http://thekeep.eiu.edu/theses/75>

This Thesis is brought to you for free and open access by the Student Theses & Publications at The Keep. It has been accepted for inclusion in Masters Theses by an authorized administrator of The Keep. For more information, please contact [tabruns@eiu.edu](mailto:tabruns@eiu.edu).

**\*\*\*\*\*US Copyright Notice\*\*\*\*\***

**No further reproduction or distribution of this copy is permitted by electronic transmission or any other means.**

**The user should review the copyright notice on the following scanned image(s) contained in the original work from which this electronic copy was made.**

**Section 108: United States Copyright Law**

**The copyright law of the United States [Title 17, United States Code] governs the making of photocopies or other reproductions of copyrighted materials.**

**Under certain conditions specified in the law, libraries and archives are authorized to furnish a photocopy or other reproduction. One of these specified conditions is that the reproduction is not to be used for any purpose other than private study, scholarship, or research. If a user makes a request for, or later uses, a photocopy or reproduction for purposes in excess of "fair use," that use may be liable for copyright infringement.**

**This institution reserves the right to refuse to accept a copying order if, in its judgment, fulfillment of the order would involve violation of copyright law. No further reproduction and distribution of this copy is permitted by transmission or any other means.**

### THESIS REPRODUCTION CERTIFICATE

TO: Graduate Degree Candidates (who have written formal theses)

SUBJECT: Permission to Reproduce Theses

The University Library is receiving a number of request from other institutions asking permission to reproduce dissertations for inclusion in their library holdings. Although no copyright laws are involved, we feel that professional courtesy demands that permission be obtained from the author before we allow these to be copied.

PLEASE SIGN ONE OF THE FOLLOWING STATEMENTS:

Booth Library of Eastern Illinois University has my permission to lend my thesis to a reputable college or university for the purpose of copying it for inclusion in that institution's library or research holdings.

PHILIAS SAKA Pradi

July 13, 2007

Author's Signature

Date

I respectfully request Booth Library of Eastern Illinois University **NOT** allow my thesis to be reproduced because:

\_\_\_\_\_  
\_\_\_\_\_  
\_\_\_\_\_

\_\_\_\_\_

\_\_\_\_\_

Author's Signature

Date

**This form must be submitted in duplicate.**


**SUPRAMOLECULAR USEFULNESS OF  
HEXAMETHYLENETETRAMINE**

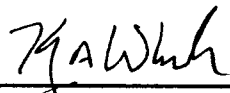
PHILIAS DAKA

This thesis has been read and approved by each member of the following  
supervisory committee:

  
\_\_\_\_\_  
Dr. Jonathan P. Blitz 7/13/07  
Date

  
\_\_\_\_\_  
Dr. Scott M. Tremain 7/13/07  
Date

  
\_\_\_\_\_  
Dr. Daniel J. Sheeran July 13, 2007  
Date

  
\_\_\_\_\_  
Dr. Craig A. Wheeler 7/13/07  
Date



## ABSTRACT

Because non-covalent contacts are important to the design and construction of materials with functional applications, efforts that seek to uncover chemical features responsible for the assembly of multimolecular arrays hold current interest. The building-block approach is one strategy that has been successfully employed for the construction of molecular assemblies. By designing molecular components with complementary functional groups, the construction of predictable supramolecular motifs is possible. Although various modes of molecular alignment have been generated using this strategy, the extension of low dimensional motifs (discrete and 1-D patterns) to 2- and 3-D patterns remain a current challenge.

Hexamethylenetetramine (HMTA) holds promise as a component for forming useful supramolecular architectures. Due to the hydrogen bond potential and tetrahedral arrangement of the four nitrogen atoms of HMTA, we envisioned that cocrystallization with various hydrogen bond donors could form extended molecular networks. As a means to explore the supramolecular behavior of HMTA, a search of the Cambridge Structural Database (CSD) for neutral HMTA complexes unveiled a diverse set of 42 crystal structures. The majority of examples in this collection include components with alcohol functions followed by carboxyl groups with only rare occurrences of amines, amides, and halides. This investigation also inspected the structures of molecular salts with hexamethylenetetraminium cations (17 structures) and uncovered a trend that

## ACKNOWLEDGEMENT

Special thanks go to my research advisor Dr. Kraig Wheeler. Not only has he been instrumental in helping me find the road to academic maturity but he has also inspired me in a number of ways. I would like also to thank my thesis committee members Dr. Scott Tremain, Dr. Jonathan Blitz and Dr. Daniel Sheeran for their valuable advice and support. Special thanks also go the Chemistry Department faculty, departmental secretary, the stock room staff and fellow graduate and undergraduate students.

Finally, it has been a great honor to be associated with numerous wonderful people during my short and rewarding stay at Eastern Illinois University. I thank them for their understanding and support they have rendered to me over the past two years.

## TABLE OF CONTENTS

ABSTRACT	i
ACKNOWLEDGEMENTS	iii
TABLE OF CONTENTS	iv
LIST OF FIGURES AND SCHEMES	vi
LIST OF TABLES	x
INTRODUCTION	1
1.1. SUPRAMOLECULAR CHEMISTRY	1
1.2. CRYSTAL ENGINEERING GOALS AND STRATEGIES	8
1.3. USEFULNESS OF HMTA AS A SUPRAMOLECULAR BUILDING BLOCK	15
CAMBRIDGE STRUCTURE DATABASE (CSD) ASSESSMENT OF HEXAMETHYLENETETRAMINE (HMTA) STRUCTURES	19
2.1 HMTA AND PURELY ORGANIC CRYSTALLINE STRUCTURES	19
2.2. HMTA-METAL ORGANIC FRAMEWORKS	23
2.3. STRUCTURAL CORRELATION OF HMTA AND NUMBER OF PROTON DONORS	26
MOLECULAR MODELING CALCULATIONS	29
CO CRYSTALLIZATION OF HMTA AND ORGANIC COMPOUNDS	34
4.1.1. BIS(1,2-DIHYDROXYBENZENE)HEXAMETHYLENETETRAMINE	34
4.1.2. CRYSTAL GROWTH, SELECTION, AND MOUNTING	35
4.1.3. INTENSITY DATA COLLECTION	36
4.1.4. INTENSITY DATA REDUCTION	37
4.1.5. STRUCTURE SOLUTION AND REFINEMENT	38
4.1.6. CRYSTAL STRUCTURE ASSESSMENT	39
4.2.1. BIS(2-HYDROXYBENZYLALCOHOL)HEXAMETHYLENETETRAMINE	42

4.2.2. CRYSTAL GROWTH, SELECTION, AND MOUNTING	42
4.2.3. CRYSTAL STRUCTURE ASSESSMENT	43
4.3.1. HEXAMETHYLENETETRAMMINIUM SULFATE	46
4.3.2. CRYSTAL GROWTH, SELECTION, AND MOUNTING	46
4.3.3. CRYSTAL STRUCTURE ASSESSMENT	47
4.4.1. BIS(5-NITROISOPHTHALIC ACID)HEXAMETHYLENE- TETRAMINE	49
4.4.2. CRYSTAL GROWTH, SELECTION, AND MOUNTING	49
4.4.3. CRYSTAL STRUCTURE ASSESSMENT	50
4.5.1. HEXAMETHYLENETETRAMINE TEREPHTHALIC ACID	53
4.5.2. CRYSTAL GROWTH, SELECTION, AND MOUNTING	53
4.5.3. CRYSTAL STRUCTURE ASSESSMENT	54
METAL ORGANIC FRAMEWORKS	58
5.1.1. [BIS( $\mu_2$ -TEREPHTHALATO)-(HEXAMETHYLENE- TETRAMINO)DIAQUA-DINICKEL (II) DIHYDRATE]	58
5.1.2. CRYSTAL GROWTH, SELECTION, AND MOUNTING	58
5.1.3. CRYSTAL STRUCTURE ASSESSMENT	59
5.2.1. [BIS( $\mu_2$ -TEREPHTHALATO)-(HEXAMETHYLENE- TETRAMINO)DIAQUA-DIZINC (II) DIHYDRATE]	61
5.2.2. CRYSTAL GROWTH, SELECTION, AND MOUNTING	61
4.2.3. CRYSTAL STRUCTURE ASSESSMENT	63
CONCLUSION	66
BIBLIOGRAPHY	71
APPENDIX	77

## LIST OF FIGURES AND SCHEMES

FIGURE 1. CONSTRUCTION OF SUPRAMOLECULAR FRAMEWORKS VIA (A-B) 1-3D MOLECULAR ASSEMBLIES AND (C) TRANSITION METAL COMPLEXES	7
FIGURE 2. SYNTHETIC SCHEME AND NANOTUBE SELF-ASSEMBLY OF BIS-UREA <b>3</b>	11
FIGURE 3. CRYSTAL STRUCTURE OF <b>3</b> SHOWING (A) MOLECULAR GEOMETRY AND (B) N-H...O SELF ASSEMBLED NANOTUBE	12
FIGURE 4. PACKING DIAGRAM OF <b>3</b> SHOWING THE ORGANIZATION OF THE NANOTUBES AND INCLUSION BEHAVIOR	12
FIGURE 5. CRYSTAL STRUCTURE OF <b>4</b> WITH AMINES (A) BENZYLAMINE, (B) 3,4-DIMETHYLANILINE, (C) ISOPROPYLAMINE AND (D) 1-OCTAMINE	14
FIGURE 6. PLOT OF METAL CONTAINING HMTA STRUCTURES SHOWING THE NUMBER OF HMTA CONTACTS (COVALENT AND NONCOVALENT) VS OCCURANCE OF HMTA CONNECTIONS	25
FIGURE 7. PLOT OF METAL CONTAINING HMTA STRUCTURES SHOWING THE NUMBER OF METAL-HMTA CONTACTS VS. OCCURRENCE OF HMTA CONNECTIONS	25
FIGURE 8. PLOT OF METAL CONTAINING HMTA STRUCTURES SHOWING THE NUMBER OF DONOR...HMTA CONTACTS VS. OCCURRENCE OF HMTA CONNECTIONS	25
FIGURE 9. GRAPH OF THE NUMBER OF HMTA CONTACTS VS. N...O DISTANCE	27
FIGURE 10. GRAPH OF NUMBER OF HMTA CONTACTS VS C-N BOND DISTANCE	28
FIGURE 11. ELECTROSTATIC POTENTIAL MAPS OF HMTA AND METHANOL/ACETIC ACID COMPLEXES	30
FIGURE 12. CARTOON REPRESENTATION OF THE ANOMERIC EFFECTS SHOWING THE CLOSE PROXIMITY OF $sp^3$ N ORBITALS	31
FIGURE 13. REPRESENTATIVE EXAMPLES OF A (A) CRYSTAL MOUNTED ON A GLASS FIBER AND (B) GONIOMETER HEAD FOR DIFFRACTION STUDIES	36
FIGURE 14. CRYSTAL STRUCTURE OF HMTA AND	40

1,2-DIHYDROXYBENZENE SHOWING ATOM LABELING SCHEME AND ATOMIC DISPLACEMENT ELLIPSOIDS AT THE 50% PROBABILITY LEVEL. DASHED LINES INDICATE HYDROGEN BONDING

- FIGURE 15. PACKING PATTERN OF **6** SHOWING THE CATEMERIC O-H...N INTERACTIONS AS DASHED LINES. H ATOMS HAVE BEEN OMITTED FOR CLARITY 40
- FIGURE 16. PROJECTION OF THE UNIT CELL CONTENTS OF **6** 41
- FIGURE 17. 3D MOLECULAR PACKING PATTERN OF **6** SHOWING INTER- AND INTRAMOLECULAR H-BONDING PATTERNS 41
- FIGURE 18. THE STRUCTURE OF THE COMPONENTS MOLECULES OF **7** SHOWING ATOM LABELING SCHEME AND ATOMIC DISPLACEMENT ELLIPSOIDS AT THE 50% PROBABILITY LEVEL 44
- FIGURE 19. VIEW OF THE PACKING PATTERN OF **7** SHOWING HETEROMERIC CATEMERIC O-H...N AND O...H-O INTERACTIONS AS DASHED LINES. H ATOMS HAVE BEEN OMITTED FOR CLARITY 44
- FIGURE 20. PROJECTION OF **7** SHOWING THE UNIT CELL AND HYDROGEN BOND NETWORK. HYDROGEN ATOMS HAVE BEEN OMITTED FOR CLARITY 45
- FIGURE 21. CRYSTAL PACKING DIAGRAM OF **7** SHOWING BOTH HYDROGEN BOND AND  $\pi$ - $\pi$  STACKING. DASHED LINES INDICATE HYDROGEN BONDS 45
- FIGURE 22. CRYSTAL STRUCTURE OF **8** SHOWING THE ASYMMETRIC UNIT, LABELING SCHEME, AND ATOMIC DISPLACEMENT ELLIPSOIDS AT THE 50% PROBABILITY LEVEL 47
- FIGURE 23. VIEW OF THE PACKING PATTERN OF **8** SHOWING CATEMERIC N-H...O AND N...H-C CONTACTS IN THE *bc* PLANE. HYDROGEN BONDS ARE SHOWN AS DASHED LINES 48
- FIGURE 24. VIEW OF THE PACKING PATTERN OF **8** SHOWING CATEMERIC N-H...O AND N...H-C IN THE *ac* PLANE. HYDROGEN BONDS ARE REPRESENTED AS DASHED LINES 48
- FIGURE 25. CRYSTAL STRUCTURE **9** SHOWING THE ASYMMETRIC UNIT, LABELING SCHEME, AND ATOMIC DISPLACEMENT ELLIPSOIDS AT THE 50% PROBABILITY. HYDROGEN BONDS ARE REPRESENTED AS DASHED LINES 51
- FIGURE 26. VIEW OF THE CRYSTAL PACKING OF **9** SHOWING CATEMERIC N-H...O INTERACTIONS AS DASHED 51

LINES. H ATOMS HAVE BEEN OMITTED FOR CLARITY

- FIGURE 27. PROJECTION OF THE UNIT CELL CONTENTS OF **9** SHOWING THE CONSTRUCTIONS OF MOLECULAR STRANDS. HYDROGEN ATOMS HAVE BEEN OMITTED FOR CLARITY. H BONDS ARE SHOWN BY DASHED LINES 52
- FIGURE 28. CRYSTAL PROJECTION OF **9** SHOWING HYDROGEN BOND SCHEME AND CLOSE HMTA-HMTA INTERACTIONS 52
- FIGURE 29. THE CRYSTAL STRUCTURE **10** SHOWING THE ASYMMETRIC UNIT, LABELING SCHEME, AND ATOMIC DISPLACEMENT ELLIPSOIDS AT THE 50% PROBABILITY LEVEL. DASHED LINES REPRESENT HYDROGEN BONDS 55
- FIGURE 30. VIEW OF THE CRYSTAL PACKING OF **10** SHOWING THE CATEMERIC N $\cdots$ H-O MOTIF IN THE *ab* PLANE. HYDROGEN BOND INTERACTIONS ARE SHOWN AS DASHED LINES 56
- FIGURE 31. VIEW OF THE PACKING PATTERN OF **10**, SHOWING THE CATEMERIC N $\cdots$ H-O CONTACTS IN THE *ac* PLANE. HYDROGEN BOND INTERACTIONS ARE SHOWN AS DASHED LINES 56
- FIGURE 32. PROJECTION OF THE UNIT CELL CONTENTS OF **10** SHOWING OF THE MOLECULAR STRANDS, H ATOMS AND OTHER ATOMS HAVE BEEN OMITTED FOR CLARITY. H BONDS ARE SHOWN BY DOTTED LINE 57
- FIGURE 33. THE STRUCTURE OF THE COMPONENT MOLECULES OF **11** SHOWING THE ATOM LABELING SCHEME AND THE DISPLACEMENT ELLIPSOIDS AT THE 50% PROBABILITY LEVEL 60
- FIGURE 34. VIEW OF THE PACKING PATTERN OF **11** SHOWING THE PROPAGATION OF HMTA $\cdots$  HMTA INTERACTIONS ALONG THE C-AXIS 60
- FIGURE 35. VIEW OF THE PACKING PATTERN OF **11** SHOWING CATEMERIC O-H $\cdots$ O AND C-H $\cdots$ O INTERACTIONS LOOKING DOWN THE A-AXIS ARE SHOWN AS DASHED LINES 61
- FIGURE 36. THE STRUCTURE OF THE COMPONENT MOLECULES OF **12** SHOWING THE ATOM LABELING SCHEME, AND DISPLACEMENT ELLIPSOIDS AT THE 50% PROBABILITY LEVEL 64
- FIGURE 37. VIEW OF THE PACKING PATTERN OF **12** LOOKING DOWN THE C-AXIS SHOWING THE ZN COORDINATION ENVIRONMENT AND WEAK CATEMERIC WATER-TERE-

PHTHALATE AND WATER-WATER (O-H...O) INTERACTIONS

- FIGURE 38. VIEW OF THE PACKING PATTERN OF **12** SHOWING  
CATEMERIC C-H...N INTERACTIONS AS DASHED  
LINES LOOKING DOWN THE A-AXIS 65
- FIGURE 39. VIEW OF THE PACKING PATTERN OF **12** SHOWING  
CATEMERIC WATER-TEREPHTHALATE AND  
WATER-WATER (O-H...O) ALONG THE *ab* PLANE  
INTERACTIONS ARE SHOWN AS DASHED LINES 65
- SCHEME A. SYNTHESIS OF HMTA 16
- SCHEME B. DEGRADATION OF HMTA 17



## LIST OF TABLES

TABLE 1. CRYSTAL GROWING TECHNIQUES	10
TABLE 2. COCRYSTALLINE COMPONENTS OF HMTA AND NUMBER OF HMTA N ATOM CONTACTS	21
TABLE 3. COCRYSTALLINE COMPONENTS OF HMTA <sup>+</sup> -H AND NUMBER OF HMTA <sup>+</sup> -H N ATOM CONTACTS	22
TABLE 4. ELECTROSTATIC POTENTIAL VALUES SHOWING HMTA AND METHANOL/ACETIC ACID COMPLEXES. SINGLE POINT ENERGY CALCULATION AT AM1 LEVEL	31
TABLE 5. CRYSTAL DATA AND STRUCTURE REFINEMENT FOR BIS(1,2-DIHYDROXYBENZENE) HEXAMETHYLENE-TETRAMINE (6)	77
TABLE 6. ATOMIC COORDINATES ( $\times 10^4$ ) AND EQUIVALENT ISOTROPIC DISPLACEMENT PARAMETERS ( $\text{\AA}^2 \times 10^3$ ) FOR BIS(1,2-DIHYDROXYBENZENE)HEXAMETHYLENETETRAMINE. U (EQ) IS DEFINED AS ONE THIRD OF THE TRACE OF THE ORTHOGONALIZED $U^{IJ}$ TENSOR	77
TABLE 7. HYDROGEN COORDINATES ( $\times 10^4$ ) AND ISOTROPIC DISPLACEMENT PARAMETERS ( $\text{\AA}^2 \times 10^3$ ) FOR BIS(1,2-DIHYDROXYBENZENE) HEXAMETHYLENE-TETRAMINE (6)	78
TABLE 8. ANISOTROPIC DISPLACEMENT PARAMETERS ( $\text{\AA}^2 \times 10^3$ ) FOR BIS(1,2 DIHYDROXYBENZENE) HEXAMETHYLENE-TETRAMINE (6). THE ANISOTROPIC DISPLACEMENT FACTOR EXPONENT TAKES THE FORM: $-2P^2 [ H^2 A^2 U^{11} + \dots + 2 H K A^* B^* U^{12} ]$	78
TABLE 9. BOND LENGTHS [ $\text{\AA}$ ] AND ANGLES [ $^\circ$ ] FOR BIS(1,2-DIHYDROXYBENZENE) HEXAMETHYLENE-TETRAMINE (6)	79
TABLE 10. TORSION ANGLES [ $^\circ$ ] FOR BIS(1,2-DIHYDROXYBENZENE) HEXAMETHYLENETETRAMINE (6)	80
TABLE 11. HYDROGEN BOND ANGLES AND DISTANCES [ $\text{\AA}$ AND $^\circ$ ] FOR BIS(1,2-DIHYDROXYBENZENE) (6)	80
TABLE 12. CRYSTAL DATA AND STRUCTURE REFINEMENT FOR BIS(2-HYDROXYBENZYLALCOHOL) HEXAMETHYLENE-TETRAMINE, (7)	80

TABLE 13. ATOMIC COORDINATES ( $\times 10^4$ ) AND EQUIVALENT ISOTROPIC DISPLACEMENT PARAMETERS ( $\text{\AA}^2 \times 10^3$ ) FOR BIS(2-HYDROXYBENZYLALCOHOL) HEXAMETHYLENETETRAMINE, (7). U (EQ) IS DEFINED AS ONE THIRD OF THE TRACE OF THE ORTHOGONALIZED $U^{IJ}$ TENSOR	81
TABLE 14. HYDROGEN COORDINATES ( $\times 10^4$ ) AND ISOTROPIC DISPLACEMENT PARAMETERS ( $\text{\AA}^2 \times 10^3$ ) FOR BIS(2-HYDROXYBENZYLALCOHOL) HEXAMETHYLENETETRAMINE, (7)	82
TABLE 15. ANISOTROPIC DISPLACEMENT PARAMETERS ( $\text{\AA}^2 \times 10^3$ ) FOR BIS(2-HYDROXYBENZYLALCOHOL) HEXAMETHYLENETETRAMINE, (7). THE ANISOTROPIC DISPLACEMENT FACTOR EXPONENT TAKES THE FORM: $-2P^2 [ H^2 A^2 U^{11} + \dots + 2 H K A^* B^* U^{12} ]$	82
TABLE 16. BOND LENGTHS [ $\text{\AA}$ ] AND ANGLES [ $^\circ$ ] FOR BIS(2-HYDROXYBENZYLALCOHOL) HEXAMETHYLENETETRAMINE, (7)	83
TABLE 17. HYDROGEN BOND ANGLES [ $\text{\AA}$ and $^\circ$ ] AND DISTANCES FOR BIS(2-HYDROXYBENZYLALCOHOL) HEXAMETHYLENETETRAMINE, (7)	84
TABLE 18. TORSION ANGLES [ $^\circ$ ] FOR BIS(2-HYDROXYBENZYLALCOHOL)HEXAMETHYLENETETRAMINE (7)	85
TABLE 19. CRYSTAL DATA AND STRUCTURE REFINEMENT FOR HEXAMETHYLENETETRAMMINIUM SULFATE (8)	85
TABLE 20. ATOMIC COORDINATES ( $\times 10^4$ ) AND EQUIVALENT ISOTROPIC DISPLACEMENT PARAMETERS ( $\text{\AA}^2 \times 10^3$ ) FOR HEXAMETHYLENETETRAMMINIUM SULFATE (8). U(EQ) IS DEFINED AS ONE THIRD OF THE TRACE OF THE ORTHOGONALIZED $U^{IJ}$ TENSOR	86
TABLE 21. BOND ANGLES AND LENGHTS FOR HEXAMETHYLENETETRAMMINIUM SULFATE (8)	87
TABLE 22. ANISOTROPIC DISPLACEMENT PARAMETERS ( $\text{\AA}^2 \times 10^3$ ) FOR HEXAMETHYLENETETRAMMINIUM SULFATE (8), THE ANISOTROPIC DISPLACEMENT FACTOR EXPONENT TAKES THE FORM: $-2P^2 [ H^2 A^2 U^{11} + \dots + 2 H K A^* B^* U^{12} ]$	89
TABLE 23. HYDROGEN COORDINATES( $\times 10^4$ ) AND ISOTROPIC DISPLACEMENT PARAMETERS( $\text{\AA}^2 \times 10^3$ ) FOR HEXAMETHYLENE-	90

TETRAMMINIUM SULFATE (8)

TABLE 24. TORSIONAL ANGLES [°] FOR HEXAMETHYLENETETRAMMINIUM SULFATE (8)	91
TABLE 25. HYDROGEN BOND ANGLES AND DISTANCES [Å and °] FOR HEXAMETHYLENETETRAMMINIUM SULFATE (8)	91
TABLE 26. CRYSTAL DATA AND STRUCTURE REFINEMENT FOR BIS (5-NITROISOPHTHALIC ACID) HEXAMETHYLENETETRAMINE (9)	91
TABLE 27. ATOMIC COORDINATES ( $\times 10^4$ ) AND EQUIVALENT ISOTROPIC DISPLACEMENT PARAMETERS ( $\text{Å}^2 \times 10^3$ ) FOR BIS(5-NITROISOPHTHALIC ACID)HEXAMETHYLENETETRAMINE (9). U(EQ) IS DEFINED AS ONE THIRD OF THE TRACE OF THE ORTHOGONALIZED $U^{IJ}$ TENSOR	92
TABLE 28. BOND LENGTHS [Å] AND ANGLES [°] FOR BIS(5-NITROISOPHTHALIC ACID)HEXAMETHYLENETETRAMINE (9)	94
TABLE 29. ANISOTROPIC DISPLACEMENT PARAMETERS ( $\text{Å}^2 \times 10^3$ ) FOR BIS(5-NITROISOPHTHALIC ACID)HEXAMETHYLENETETRAMINE (9). THE ANISOTROPIC DISPLACEMENT FACTOR EXPONENT TAKES THE FORM: $-2P^2[H^2 A^*2U^{11} + \dots + 2 H K A^* B^* U^{12}]$	96
TABLE 30. TORSION ANGLES [°] FOR BIS(5-NITROISOPHTHALIC ACID)HEXAMETHYLENETETRAMINE (9)	97
TABLE 31. TORSION ANGLES [°] FOR BIS(5-NITROISOPHTHALIC ACID)HEXAMETHYLENETETRAMINE (9)	98
TABLE 32. HYDROGEN BONDS FOR BIS(5-NITROISOPHTHALIC ACID) HEXAMETHYLENETETRAMINE (9) [Å AND °]	99
TABLE 33. CRYSTAL DATA AND STRUCTURE REFINEMENT FOR HEXAMETHYLENETETRAMINE TEREPHTHALIC ACID (10)	99
TABLE 34. ATOMIC COORDINATES ( $\times 10^4$ ) AND EQUIVALENT ISOTROPIC DISPLACEMENT PARAMETERS ( $\text{Å}^2 \times 10^3$ ) FOR HEXAMETHYLENETETRAMINE TEREPHTHALIC ACID (10). U(EQ) IS DEFINED AS ONE THIRD OF THE TRACE OF THE ORTHOGONALIZED $U^{IJ}$ TENSOR	100
TABLE 35. BOND LENGTHS [Å] AND ANGLES [°] FOR HEXAMETHYLENETETRAMINE TEREPHTHALIC ACID (10)	101

TABLE 36. ANISOTROPIC DISPLACEMENT PARAMETERS ( $\text{\AA}^2 \times 10^3$ ) FOR HEXAMETHYLENETETRAMINE TEREPHTHALIC ACID (10). THE ANISOTROPIC DISPLACEMENT FACTOR EXPONENT TAKES THE FORM: $-2P^2 [H^2 A^2 U^{11} + \dots + 2 H K A^* B^* U^{12}]$	106
TABLE 37. HYDROGEN COORDINATES ( $\times 10^4$ ) AND ISOTROPIC DISPLACEMENT PARAMETERS ( $\text{\AA}^2 \times 10^3$ ) FOR HEXAMETHYLENETETRAMINE TEREPHTHALIC ACID (10)	108
TABLE 38. TORSION ANGLES [ $^\circ$ ] FOR HEXAMETHYLENETETRAMINE TEREPHTHALIC ACID (10).	109
TABLE 39. HYDROGEN BONDS FOR TEREPHTHALIC ACID HEXAMETHYLENETETRAMINE (10) [ $\text{\AA}$ AND $^\circ$ ]	112
TABLE 40. CRYSTAL DATA AND STRUCTURE REFINEMENT FOR BIS ( $\mu_2$ -TEREPHTHALATO)-( $\mu_2$ -HEXAMETHYLENETETRAMINO)-DIAQUA-DINICKEL (II) DIHYDRATE (11).	112
TABLE 41. ATOMIC COORDINATES ( $\times 10^4$ ) AND EQUIVALENT ISOTROPIC DISPLACEMENT PARAMETERS ( $\text{\AA}^2 \times 10^3$ ) FOR BIS ( $\mu_2$ -TEREPHTHALATO)-( $\mu_2$ -HEXAMETHYLENETETRAMINO)-DIAQUA-DINICKEL (II) DIHYDRATE (11). $U(EQ)$ IS DEFINED AS ONETHIRD OF THE TRACE OF THE ORTHOGONALIZED $U^{IJ}$ TENSOR	113
TABLE 42. BOND LENGTHS [ $\text{\AA}$ ] AND ANGLES [ $^\circ$ ] FOR BIS ( $\mu_2$ -TEREPHTHALATO)-( $\mu_2$ -HEXAMETHYLENETETRAMINO)-DIAQUA-DINICKEL (II) DIHYDRATE (11)	114
TABLE 43. ANISOTROPIC DISPLACEMENT PARAMETERS ( $\text{\AA}^2 \times 10^3$ ) FOR BIS ( $\mu_2$ -TEREPHTHALATO)-( $\mu_2$ -HEXAMETHYLENETETRAMINO)-DIAQUA-DINICKEL (II) DIHYDRATE (11). THE ANISOTROPIC DISPLACEMENT FACTOR EXPONENT TAKES THE FORM: $-2P^2 [H^2 A^2 U^{11} + \dots + 2 H K A^* B^* U^{12}]$	116
TABLE 44. HYDROGEN COORDINATES ( $\times 10^4$ ) AND ISOTROPIC DISPLACEMENT PARAMETERS ( $\text{\AA}^2 \times 10^3$ ) FOR BIS ( $\mu_2$ -TEREPHTHALATO)-( $\mu_2$ -HEXAMETHYLENETETRAMINO)-DIAQUA-DINICKEL (II) DIHYDRATE (11)	117
TABLE 45. TORSION ANGLES [ $^\circ$ ] FOR BIS ( $\mu_2$ -TEREPHTHALATO)-( $\mu_2$ -HEXAMETHYLENETETRAMINO)-DIAQUA-DINICKEL (II) DIHYDRATE (11)	118

TABLE 46. HYDROGEN BONDS FOR BIS ( $\mu_2$ -TEREPHTHALATO)- ( $\mu_2$ -HEXAMETHYLENETETRAMINO)-DIAQUA- DINICKEL (II) DIHYDRATE (11) [ $\text{\AA}$ AND $^\circ$ ]	119
TABLE 47. CRYSTAL DATA AND STRUCTURE REFINEMENT FOR BIS ( $\mu_2$ -TEREPHTHALATO)-( $\mu_2$ -HEXAMETHYLENETETRAMINO) -DIAQUA-ZINC (II) DIHYDRATE (12).	119
TABLE 48. ATOMIC COORDINATES ( $\times 10^4$ ) AND EQUIVALENT ISOTROPIC DISPLACEMENT PARAMETERS ( $\text{\AA}^2 \times 10^3$ ) FOR BIS ( $\mu_2$ -TEREPHTHALATO)-( $\mu_2$ -HEXAMETHYLENETETRAMINO)- DIAQUA-DIZINC (II) DIHYDRATE (12). U(EQ) IS DEFINED AS ONETHIRD OF THE TRACE OF THE ORTHOGONALIZED $U^{IJ}$ TENSOR	120
TABLE 49. BOND LENGTHS [ $\text{\AA}$ ] AND ANGLES [ $^\circ$ ] FOR BIS ( $\mu_2$ -TEREPHTHALATO)-( $\mu_2$ -HEXAMETHYLENETETRA- MINO)-DIAQUA-DIZINC (II) DIHYDRATE (12)	121
TABLE 50. ANISOTROPIC DISPLACEMENT PARAMETERS ( $\text{\AA}^2 \times 10^3$ ) FOR BIS ( $\mu_2$ -TEREPHTHALATO) -( $\mu_2$ -HEXAMETHYLENETETRAMINO)-DIAQUA-DIZINC (II) DIHYDRATE (12). THE ANISOTROPIC DISPLACEMENT FACTOR EXPONENT TAKES THE FORM: $-2P^2[H^2 A^*2U^{11} +$ $\dots + 2 H K A^* B^* U^{12}]$	124
TABLE 51. HYDROGEN COORDINATES ( $\times 10^4$ ) AND ISOTROPIC DISPLACEMENT PARAMETERS ( $\text{\AA}^2 \times 10^3$ ) FOR BIS ( $\mu_2$ -TEREPHTHALATO)-( $\mu_2$ -HEXAMETHYLENETETRAMINO) -DIAQUA-DIZINC (II) DIHYDRATE (12)	125
TABLE 52. TORSION ANGLES [ $^\circ$ ] FOR BIS ( $\mu_2$ -TEREPHTHALATO)- ( $\mu_2$ -HEXAMETHYLENETETRAMINO)-DIAQUA- DIZINC (II) DIHYDRATE (12)	126
TABLE 53. HYDROGEN BONDS FOR BIS ( $\mu_2$ -TEREPHTHALATO)- ( $\mu_2$ -HEXAMETHYLENETETRAMINO)-DIAQUA- DIZINC(II) DIHYDRATE (12) [ $\text{\AA}$ AND $^\circ$ ]	127

## **Section1: Introduction**

### **1.1 Supramolecular Chemistry**

The chemistry of covalent bonding has been explored in depth over the last century. To the contrary, the chemistry of non-covalent bonding has only been the center of serious attention over the past few decades.<sup>1</sup> Supramolecular chemistry<sup>2,3</sup> is the science of non-covalent interactions that may be described by two vital structural attributes - molecular recognition and assembly. The design, construction, and prediction of molecular assemblies via non-covalent interactions constitute crystal engineering.<sup>4</sup> The key forces involved in the construction of molecular assemblies are largely governed by electrostatic interactions such as hydrogen bonding,  $\pi$ - $\pi$  Stacking, Halogen...Halogen, Hydrogen...Halogen, and Hydrogen...  $\pi$  Interactions.

#### **A. Hydrogen bonding**

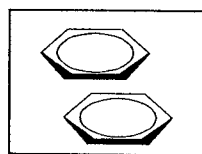
Donor-H...Acceptor

Donor = ROH, RCO<sub>2</sub>H, R<sub>2</sub>NH, R<sub>2</sub>CH  
Acceptor = R<sub>3</sub>N, C=O, ROR, RSR

Among the most exploited molecular interactions in supramolecular chemistry is hydrogen bonding.<sup>5</sup> This mode of molecular assembly has shed considerable light on the role of functional groups as an effective tool for fabricating predetermined supramolecular entities. The construction of hydrogen bonds requires at least two chemical species; the proton donor and acceptor. The proton donor is a molecule that contains an acidic H atom that is often attached to a highly electronegative element such as oxygen. The proton

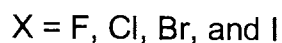
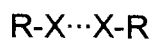
acceptor is also constructed of electronegative species that participate in hydrogen bond interactions via lone pair electrons. Hydrogen bond strengths are related to the electrostatic attraction of the two groups. It then follows that the majority of hydrogen bonds provide a cohesive force that is often stronger than such weak interactions as van der Waals forces, but weaker than covalent bonding. Although the existence of hydrogen bonds have been experimentally and computationally determined,<sup>6-8</sup> a clear comprehensive definition that describes this type of interaction is not yet possible due to the subjective interpretation of this interaction. The pursuit of understanding the hydrogen bond can be traced as far back as the 1920s.<sup>9</sup> One of its early investigators, Linus Pauling, defined a hydrogen bond as “an interaction that directs the association of a covalently bound hydrogen atom with one or more other atoms, groups of atoms, or molecules into an aggregate structure that is sufficiently stable to make it convenient for the chemist to consider it as an independent chemical species”.<sup>10</sup> This description has been elaborated over the years<sup>11-13</sup> with one of the most significant contributions by Etter and coworkers on the systematic treatment of the identification of hydrogen bonds in the 1980s<sup>14</sup>. Aakeröy and Seddon<sup>15</sup> in 1993 gave a historic account of hydrogen bond patterns and provided key insight to the predictability and application of numerous hydrogen bond connections.

### B. $\pi$ - $\pi$ Stacking



The interaction of neighboring aromatic rings occurs both biological systems e.g. DNA and in crystalline materials due to the favorable overlap of  $p$ -orbitals that leads to stabilization of molecular motifs.<sup>16</sup> The overall impact of such  $\pi$ -stacking modes to crystal organization is dependent on the relative orientation and distance of aromatic rings. In an ideal case, the two interacting rings would be positioned such that the sum of the van der Waals radii is less than 3.4 Å with all  $p$ -orbitals involved in the stabilization process.<sup>17</sup> This distance criteria produces maximum  $p$ -orbital overlap. Too short of a distance results in repulsive forces while very long distances between rings result in very weak ineffective interactions. Even if these interactions are more pronounced in biomolecules,<sup>18,19</sup> they have been extensively used in crystal engineering to produce different types of molecular frameworks.<sup>20,21</sup>

### C. Halogen...Halogen interactions

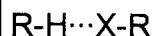


The use of halogens in crystal engineering was first reported by Schmidt and coworkers at the Weizmann Institute.<sup>22</sup> Although their work detailed the consequence of chlorine-chlorine interactions to solid-state photodimerization processes, Desiraju more recently argued that halogen-halogen contacts could be systematically used as weak attractive forces to manipulate and organize supramolecular synthons in a predictable fashion.<sup>23</sup> Investigations of the geometric preferences of halogen-halogen interactions revealed that Cl...Cl



contacts were often shorter than the sum of the van der Waals radii. Price<sup>24</sup> has shown through computational and experimental data that halogen atoms participate in these attractive interactions via non-spherical electron density distribution. Additional literature reports cite the importance of triangular halogen-halogen-halogen interactions for controlling crystal packing.<sup>25,26</sup> Though the halogen-halogen interaction was first disputed by a large cross section of the scientific community, data collected over the last several decades suggests the close assembly of halogen atoms is not a structural anomaly, but rather a bona fide electrostatic contact that has been developed as a viable supramolecular synthon.<sup>27,28</sup>

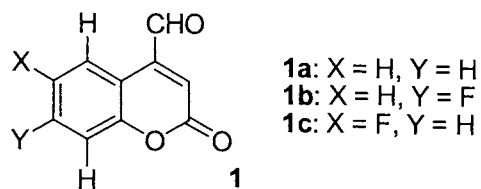
#### D. Hydrogen...Halogen interactions



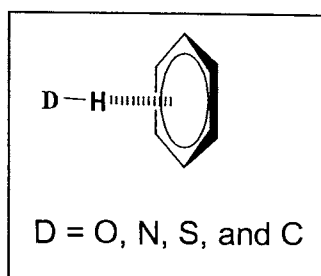
The unpaired electrons on halogens have been shown to participate in weak hydrogen-halogen interactions.<sup>29,30</sup> In this scenario, the halogen is a proton acceptor and the hydrogen atoms connected to N (amines and amides), O (alcohols and carboxylic acids), and C (alkenes and alkynes) atoms often serve as the proton donor.<sup>31</sup>

Using the C-H...F motif as a model, hydrogen-halogen interactions have been investigated extensively and identified as a weak intermolecular interaction that holds tremendous potential in different chemistry disciplines.<sup>32-35</sup> A number of crystal structures have been reported in which the hydrogen-halogen interaction furnishes the primary organizational force for the construction of

specific molecular motifs. For example, Moorthy *et al.*<sup>36</sup> investigated the homologous family of 4-formylcoumarins (**1**) and reported on the effects of fluoro substitution to crystal packing. Unlike the structure of **1a** where C-H...O contacts predominate as the major directional force for determining the crystal packing, the structures of the analogous fluoro derivatives **1b** and **1c** showed strikingly different motifs due to the occurrence of C-H...F interactions.



### E. Hydrogen... $\pi$ Interactions



Because  $\pi$  systems in aromatic compounds are rich in electrons, these species often participate in intermolecular contacts. The most common modes of association of aryl groups are  $\pi$ - $\pi$  stacking and  $\pi$ ...H contacts. Unlike conventional hydrogen bonds that are essentially derived from electrostatic interactions,  $\pi$ ...H interactions occur due to a mixture of dispersion, charge transfer as well as electrostatic forces.<sup>37</sup> Malone *et al.*<sup>38</sup> showed through theoretical and crystallographic studies that the cohesive energy associated with this interaction decreases proportionally with the electronegativity of the donor

atom. It follows then that such information is inherently useful for the design of particular supramolecular assemblies based on  $\pi\cdots\text{H}$  interactions.<sup>39,40</sup>

### **Molecular Assembly**

Taking advantage of the different weak noncovalent interactions described in the preceding sections, one can imagine the construction of a vast array of 1D - 3D molecular patterns from both organic and metal-organic building blocks. The schemes in Figure 1 provide possible scenarios of molecular recognition and assembly. These approaches illustrate the use of complementary synthons for the construction of predictable intermolecular interactions. In situations where single moieties with many sites for non-bonded contacts are desired, transition metal centers have often been utilized for this purpose due to their versatility in coordination.

Although the use of both organic and metal-organic strategies have helped advance the field of crystal engineering, these methods of molecular organization are not interchangeable.<sup>41</sup> For instance, metal-organic frameworks tend to form compounds with high thermal stability while the collection of known organic-based materials contain crystal packing patterns of greater diversity. The variety of structures classified as organic may be partially attributed to the ease of derivatization of organic molecules. Ishikawa *et al.*<sup>42</sup> illustrated this principle by cocrystalizing an *o*-bisguanidinobenzene derivative with several monosubstituted aromatic compounds (2). By systematically varying the X group on the OH containing component, a wide range of structural patterns were

observed. In fact, within this set of structures, very few motifs were common to all of the structures thus demonstrating the idea that small iterative chemical changes can, and will, produce drastically different crystal patterns.

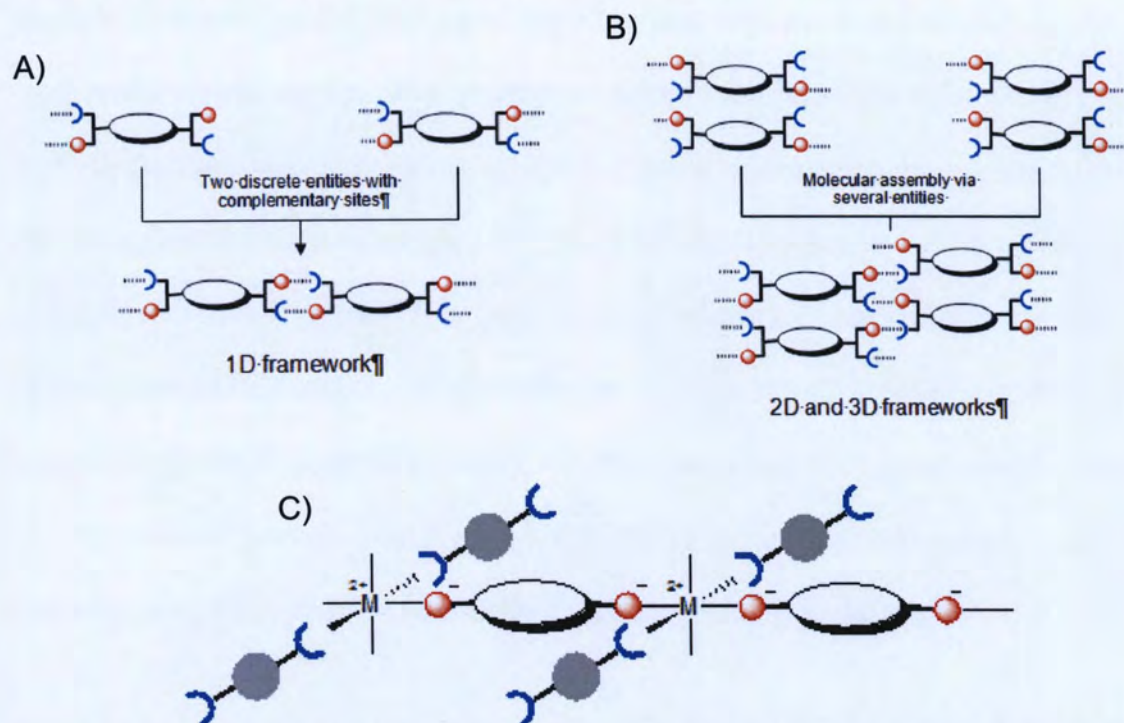
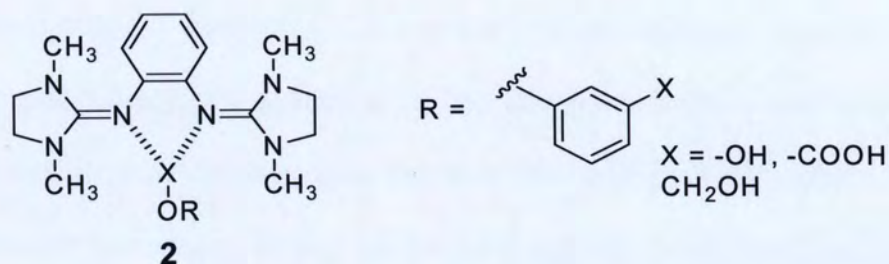


**Figure 1.** Construction of supramolecular frameworks via (A-B) 1-3D molecular assemblies and (C) transition metal complexes.



Despite many interesting structures that have been discovered using purely organic compounds, the overall objective of producing crystalline structures with industrial applications is not a common reality. A major challenge centers on the tendency of purely organic molecules to form more than one pattern of hydrogen bonds. This leads to the formation of polymorphic crystalline

structures that exhibit different physical properties.<sup>43,44</sup> Additionally, organic compounds possess unfavorable thermal and mechanical properties, which in most cases render them useless as materials for devices. In contrast, metal organic frameworks (MOFs) have high thermal and mechanical stability due to rigid metal-ligand bonds. The strength of these frameworks is reflected in shorter bond distances between atoms and other parameters such as higher oxidation states and coordination numbers.<sup>45</sup> The disadvantage posed by the rigidity of the metal-ligand bond is that they tend to be irreversible and thus materials that utilize reversibility as a key feature are not compatible with MOFs. More importantly, the irreversible nature of the metal-ligand bonds affects kinetics during crystal growth resulting in formation of many nucleation sites and consequently the products formed are microcrystalline powders.<sup>46</sup>

## **1.2 Crystal Engineering Goals and Strategies**

Prior to the 1980's only modest attention was given to furthering the field of solid-state organic chemistry. One of the first practitioners, Gerhard Schmidt, published extensively in the 1960's on the photochemistry of cinnamic acids.<sup>47</sup> This work led Schmidt to formulate the topochemical postulate which described the parameters necessary for the production of [2+2] photodimerization products in the solid-state. Arguably one of the most significant turning points in the field occurred in 1988 when the first systematic analysis of an interpenetrated structure was performed on adamantane-1,3,5,7-tetracarboxylic acid.<sup>48</sup> The nanoporous 'diamondoid' crystalline lattice of this material demonstrated for the

first time that crystal engineering had the potential to aid the design of industrial relevant applications (e.g. the construction of host-guest compounds). This study provided an important structural model that fostered the design and preparation of novel polymeric materials that possess high thermal stability. Further indication of the growth of this area occurred the following year with Gautum Desiraju's monograph on Crystal Engineering<sup>49</sup> that highlighted significant trends and discoveries in the field. The first direct application to Crystal Engineering was demonstrated in 2000 by the use of a crystalline sensor to detect SO<sub>2</sub> at ppm level.<sup>50</sup> An organoplatinum complex consisting of key chloro and phenolic groups self-assembled via intermolecular noncovalent Pt-Cl...H-O contacts to form a crystalline network. This molecular assemblage selectively bound SO<sub>2</sub> reversibly without degradation. The tight fixation of SO<sub>2</sub> to the platinum complex was attributed to Pt...SO<sub>2</sub>...Cl interactions.

Interestingly, the objectives of researchers in the field of Crystal Engineering remain the same today as they were two decades ago. These goals are to understand the packing preferences of specific chemical features and exploit known supramolecular synthons for the formation of predictable crystal structure packing. In addition to developing design strategies for the construction of new crystalline architectures, the success of such studies is often dependent on the availability of X-ray quality samples for crystallographic assessment. Several common crystal growing techniques are provided in Table 1.

**Table 1.** Crystal Growing Techniques

Crystal growing technique	Procedure
Slow evaporation	Dissolution of solute components in a compatible solvent system and allowed to evaporate over a period of time. This process is usually conducted at room temperature, but can be performed under various conditions.
Slow cooling	Crystallization sample prepared similar to slow evaporation technique, but solute should be sparingly soluble in solvent system. Dissolution occurs with heat and upon slow cooling crystals form. Frequently the rate of cooling is controlled by storing the recrystallization experiment by use of a warm Dewar flask.
Vapor Diffusion	Solute components are dissolved in solvent A. The vial containing this solution is then enclosed in a larger vial with a small portion of solvent B. Solvents A and B should be miscible, however, the solutes should be relatively insoluble in solvent B. Also, solvent B should possess a lower vapor pressure (boiling point). Diffusion of solvent B into the solution containing A promotes crystal growth by decreasing the solubility of the solutes in the solvent mixture.
Solvent Diffusion (Layering Technique)	Similar to vapor diffusion, samples are dissolved in solvent A. Solvent B (less dense and partially soluble in solvent A, solute insoluble in solvent B) is then layered on the solution containing solvent A. Liquid-liquid diffusion of the solutions results in the formation crystalline materials.
Solvothermal	Solvent and solute components sealed in a Teflon-lined high-pressure vessel. The vessel is heated at high temperatures (200-400°C) and then allowed to slowly cool to room temperature over a period of days.
Sublimation	Volatile materials are heated under reduced pressure and subsequently condensed on a cold finger to produce crystalline samples.

Using the principles outlined above, the literature contains examples in which crystal engineers have created reliable and reproducible organic networks that possess interesting properties. For example, Shimizu *et al.* generated self-assembled nanotubes from **3** using a simple synthetic procedure (Figure 2).<sup>51</sup> These materials include acetic acid guests that are only liberated at temperatures >180°C and thus show similar inclusion behavior to zeolitic compounds.

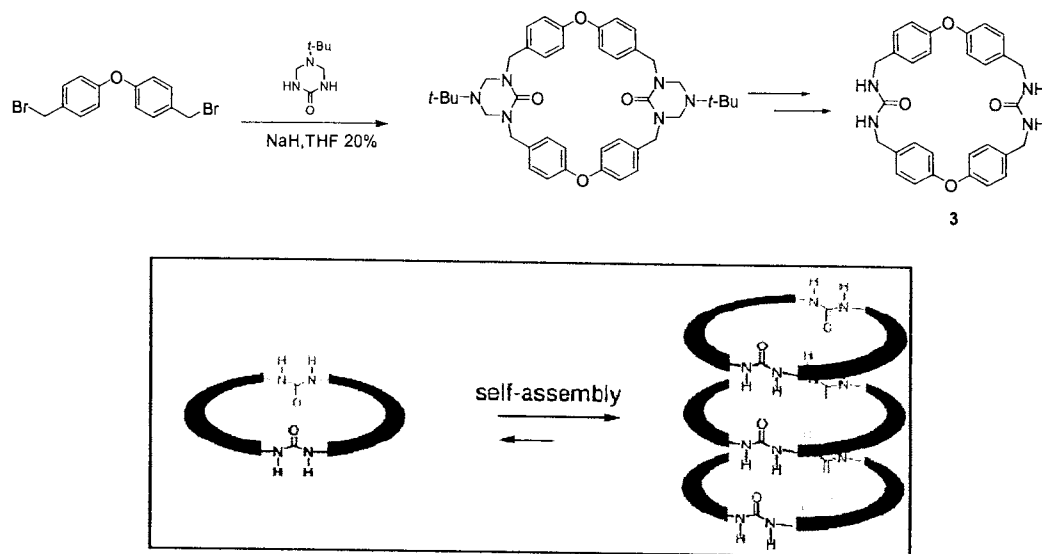
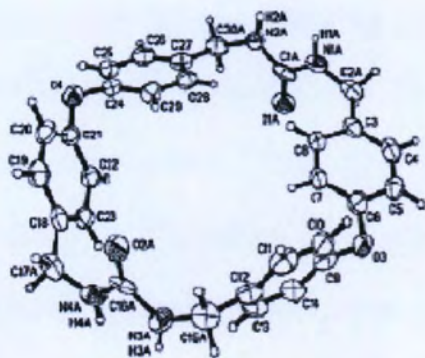


**Figure 2.** Synthetic scheme and nanotube self-assembly of bis-urea **3**.

Recrystallization of **3** in glacial acetic acid produced X-ray quality crystals that were assessed via crystallographic methods (Figure 3a). An inspection of the crystal structure shows molecules of **3** involved in  $\pi$ - $\pi$  stacking of the biphenyl ether fragments involved in extensive N-H $\cdots$ O hydrogen bonding between the urea groups. These weak noncovalent interactions produce self-assembled nanotubes with each molecule of **3** translationally organized with neighboring molecules (Figures 2 & 3b). As shown in Figure 4, the acetic acid components are incorporated into these channels without the use of strong directional forces such as hydrogen bonding.



A)



B)

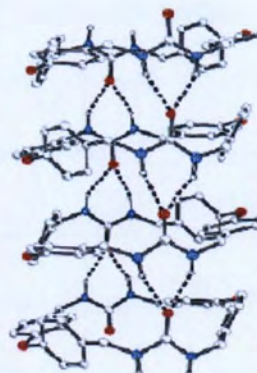


**Figure 3.** Crystal structure of **3** showing (a) molecular geometry and (b) N-H...O self-assembled nanotube.

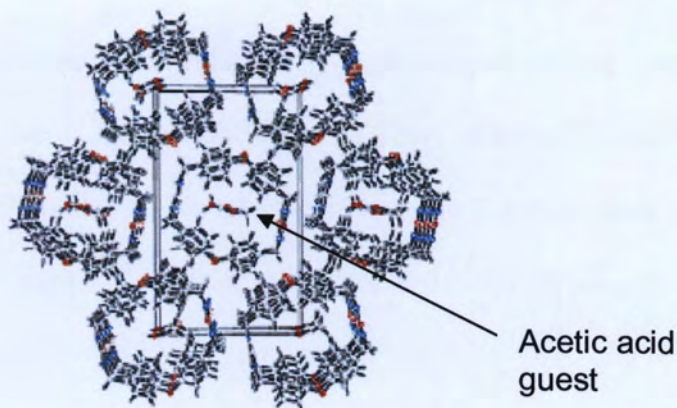


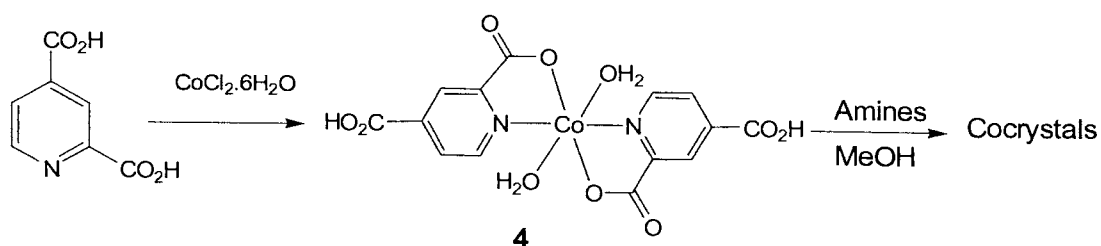
**Figure 4.** Packing diagram of **3** showing the organization of nanotubes and inclusion behavior.

The above example demonstrates the practical use of weak noncovalent interactions and the principles of molecular recognition and assembly towards the generation of complex structures that can find wide applications in chemistry, biology, and material science.<sup>52</sup>

One of the greatest challenges of crystal engineers is to formulate viable approaches for creating reliable and reproducible organic frameworks. Most

organic compounds are conformationally flexible and therefore possess large degrees of freedom compared to rigid organometallic counterparts. Due to this flexibility one substance can easily exhibit different crystal packing patterns forming polymorphs,<sup>53</sup> that show different physical and chemical properties.<sup>54</sup> To overcome this problem one strategy has been to use rigid building blocks consisting of transition metals in generating predictable frameworks.<sup>55,56</sup>

Beatty *et al.*<sup>57</sup> generated metal-containing dicarboxylic acids as building blocks for Metal Organic Frameworks (MOFs) in a reliable, reproducible and predicted manner. The procedure followed was the reaction of cobalt with dicarboxylic acids forming complexes which were the primary supramolecular building blocks. These inert neutral metal complexes designed with peripheral carboxyl groups (**4**) were cocrystallized with four different primary amines; benzylamine, 3,4-dimethylaniline, isopropylamine, and 1-octylamine. The crystal structures obtained (Figure 5) of each bimolecular compound were then assessed for any structural trends.





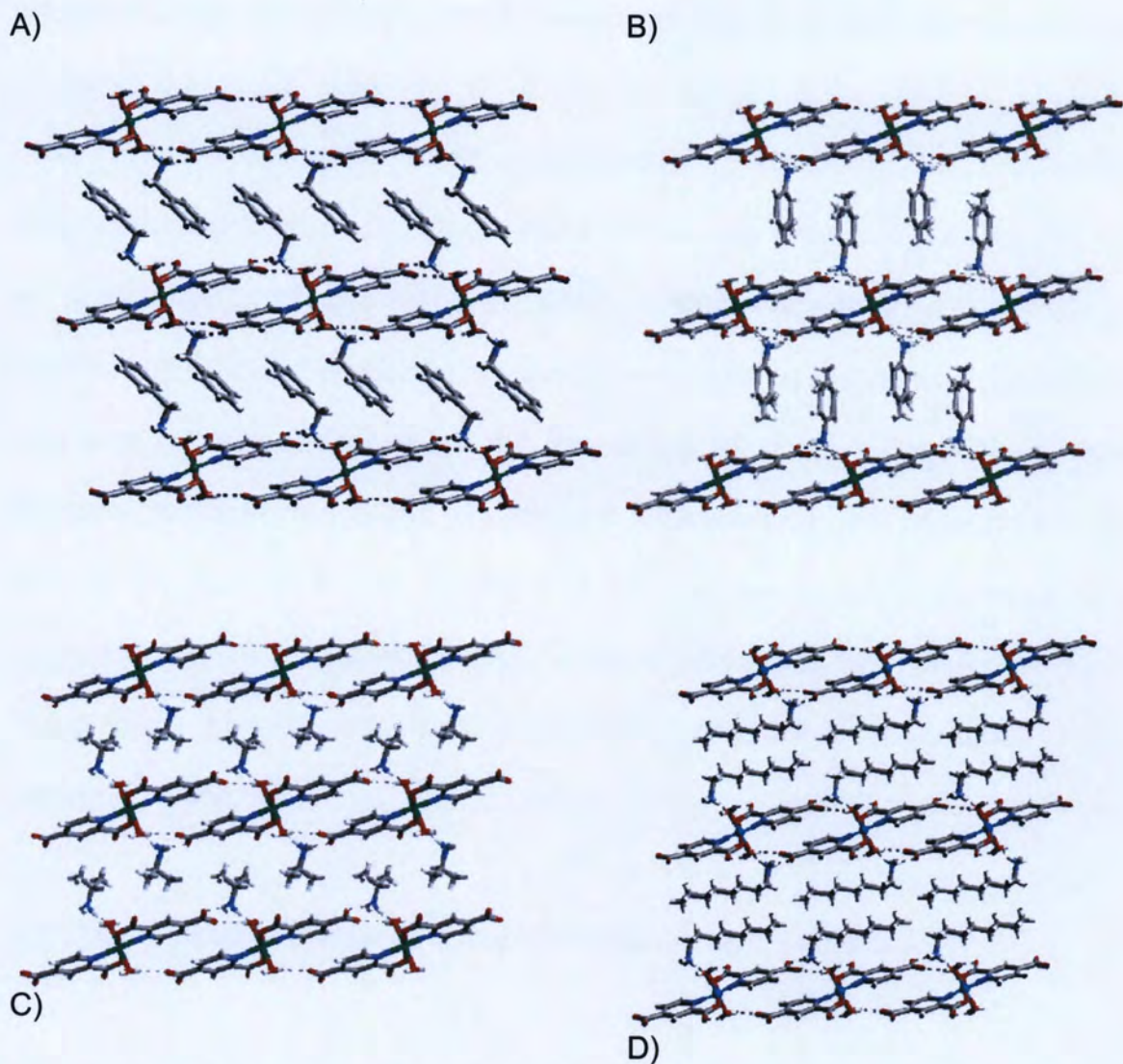


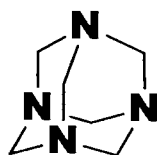
**Figure 5.** Crystal structures of **4** with amines. (A) benzylamine, (B) 3,4-dimethylaniline, (C) Isopropylamine, (D) 1-octylamine.

From a comparison of the four structures depicted in Figure 5, it was observed that this family of MOF amines form lamellar structures in a predictable and reproducible fashion. Each forms a 2-D bilayer in which the metal centers are connected by weak carboxyl-water interactions forming horizontal strands. In between these strands, the amines occupy channels and connect the metal

coordinated strands via weak amine...water and amine...carboxylate interactions as shown in Figure 5.

With this information Beatty suggested that these MOFs form motifs that are constructed from robust interactions and thus may provide a suitable avenue to predictable supramolecular synthons. More significantly, a strategic modification of the cocrystallization components (i.e., in the case of Beatty the amine and metal center) allows for fine tuning of motifs. For example, the distance between the metal coordinated strands and the strength of the interactions involved in the formation of the lamellar inorganic-organic hybrid networks can be exploited at will. Such treatments will result in facile manipulation of the electronic,<sup>58</sup> magnetic,<sup>59</sup> and optical<sup>60</sup> properties of the generated materials.

### **1.3. Usefulness of HMTA as a Supramolecular Building Block**



5

#### **Hexamethylenetetramine (HMTA)**

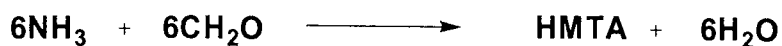
The strategies of crystal engineering requires not only an intimate understanding of conformational dynamics of a vast array of molecular frameworks and functional groups, but also the complementary nature of non-bonded contacts that are necessary to construct supramolecular assemblies. The challenge of predicting molecular arrays stems from our inability to identify

all factors responsible for crystal packing. By exploring new supramolecular motifs (patterns generated via non-bonded contacts) and the transferability of known electrostatic contacts, the field of crystal engineering has progressed at a rapid pace over the last decade.

One area that has experienced considerable attention is the formation of 3-D crystalline architectures assembled via predetermined molecular contacts. Recent successful strategies utilize building-blocks that consist of multiple functional groups capable of complementary non-bonded contacts. Hexamethylenetetramine (**5**) in many ways is a model candidate for this purpose due to the presence of the four equivalent nitrogen atoms that are tetrahedrally arranged. In principle, since HMTA is able to participate in four contacts, use of this precursor with other Lewis acid components (e.g. hydrogen bond donors and metal centers) should allow the development of multidimensional molecular motifs.

HMTA is a white crystalline solid with a melting point of 280°C that was first reported some 130 years ago.<sup>61</sup> HMTA was the first organic molecule that was assessed by single-crystal X-ray crystallography and found to have nitrogen atoms with tetrahedral geometry.<sup>62</sup> It has been a versatile reagent in organic synthetic procedures, e.g. the Duff's reaction.<sup>63</sup> The initial synthesis of HMTA followed the condensation of ammonia and formaldehyde.<sup>64,65</sup>

**Scheme A**



Under strongly acidic conditions it decomposes to ammonium salts and formaldehyde.<sup>66</sup>

### Scheme B



Despite its importance in X-ray crystallography development, its potential as a supramolecular synthon has not been fully realized. Neutral HMTA behaves as an electron donor and cocrystalizes with a wide variety of organic compounds that possess labile protons for hydrogen bonding.<sup>67-69</sup> Cocrystals are also known in which one of the HMTA N atoms is protonated.<sup>70,71</sup> On very rare occasions hexamethylenetetramine-oxide cocrystals<sup>72,73</sup> and HMTA-halide<sup>74</sup> cocrystals have been reported. Taking advantage of the four equivalent nitrogen atoms on HMTA, there has been extensive reports that detail the ability of HMTA to act as a ligand in coordinating transition metals and forming diverse supramolecular architectures.<sup>75,76</sup> Even if the coordination of HMTA to metals in many instances is either monodentate or bidentate resulting in the formation of different metal organic frameworks with varying scaffolds, in almost all of these cocrystals HMTA provides a surface on which weak noncovalent intermolecular interactions take place to stabilize the complex. It is important to note that in both organic and organometallic crystals, we see a wide variety of crystal packing patterns. Suffice to say that despite all the nitrogen atoms on HMTA being chemically equivalent, not all are involved in coordination. There are many bicoordination and very few tetracoordination compounds. Another striking feature is that in most HMTA cocrystals, there exists a high incidence of weak HMTA...HMTA

interactions. This is not very surprising because these interactions were first observed in the single X-ray crystal structure of pure HMTA.<sup>63</sup> Unfortunately, these weak interactions have not been well reported in the literature although C-H...N interactions are crucial in many crystal growth processes.<sup>77,78</sup>

The overall objective of this research was to explore the supramolecular tendencies of HMTA. This was first accomplished by exploring the Cambridge Structure Database<sup>79</sup> (CSD) for the trends and features present in HMTA structures. Secondly, molecular modeling strategies using simple molecules like acetic acid and methanol as models for proton donors were performed to help explain the supramolecular behavior of HMTA. And lastly, a diverse collection of compounds derived from both organic and metal containing HMTA compounds were synthesized. The goal of this work is to clarify the role of HMTA in molecular assemblies and determine the supramolecular usefulness in constructing predictable molecular arrays.

## Section 2: Cambridge Structural Database Assessment of Hexamethylenetetramine Structures

### *2.1. HMTA and purely organic crystalline structures*

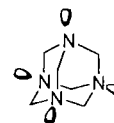
Hexamethylenetetramine (HMTA) may be characterized by tetrahedral geometry by virtue of four chemically equivalent N atoms affixed at the corners of a rigid tetrahedral framework. In spite of having an attractive spatial arrangement of donor moieties for applications in crystal engineering, we were somewhat surprised to discover that a search of the Cambridge Structural Database (CSD),<sup>79</sup> an extensive collection of small molecule organic and organometallic crystal structures, for HMTA cocrystalline compounds revealed relatively few structures that involve all four HMTA nitrogen atoms in intermolecular contacts. Of the 42 reported structures (Table 2) that contain neutral HMTA cocrystals, only seven adopt motifs that involve all four nitrogen atoms. Inspection of these structures and components reveals no clear trend that would suggest a preferred functional group or molecular framework for constructing tetracoordinated systems. The inclusion of alkyl halides, phenols, and carboxylic acids in this group provide a diverse set of components that do not readily offer a logical explanation for their tetracoordination behavior. Even so, the entire collection of 42 structures in this study shows a preference for alcohol components (21 structures) and crystal organization with dicoordinated HMTA molecules (20 structures).

A parallel search for protonated HMTA molecular salts with N<sup>+</sup>-H donor groups uncovered an additional 17 (Table 3) structures of which none exhibited



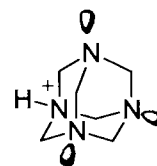
tri- or tetracoordination via  $N\cdots H-Z$  or  $N^+-H\cdots Z$  intermolecular contacts. The structures of these organic salts also consist of a chemically broad selection of building blocks that seem to favor carboxylate containing components (7 structures) and monocoordination of HMTA (12 structures).

**Table 2.** Cocrystalline components of HMTA and number of HMTA N atom contacts.



HMTA Contacts				
0	1	2	3	4
 PIZDUX	 YOLQOF	 MUDSIN	 HIFZIF	 BOQBEO
 PIZFAF	 VIJTIP	 HMTATU	 MIPVEW	 HUSWIB
		 HMTHQU	 HMTMCR	 CHI3
		 RSHMTA	 RAWCOH	 HEXAIF
		 RAWDAU	 RAWDIC	 IHERIW
		 QIHCUF	 ROKQIR	 CHBr3
		 RAWCUN	 QIHCIT	 MIPVIQ
		 QIHCOZ	 FEQXIJ	 RAWDEY
		 FEQXEF	 BINDIL	 H2O
		 MIPVOW	 BUQQAF	 RSHMTA
		 DIRVOP		 Ni <sub>3.12</sub>
		 RSHMTA		 HMTNTI
				 CBr <sub>4</sub>
				 HARWEC

**Table 3.** Cocrystalline components of HMTA<sup>+</sup>-H and number of HMTA<sup>+</sup>-H N atom contacts.



HMTA Contacts	
1	2
<p>MILLIC</p>	<p><math>\text{ClO}_4^-</math></p> <p>HAMYEA</p>
<p><math>\text{Cl}^-</math></p> <p>FETRUR</p>	<p>DEKDAY</p>
<p><math>\text{NO}_3^-</math></p> <p>HUQRAM</p>	<p><math>\text{I}_3^-</math></p> <p>YIPYUR</p>
<p><math>\text{NCS}^-</math></p> <p>GIGXOJ</p>	<p>MEVXIU</p>
<p>HUSVEW</p>	<p>MIPVAI</p>
<p>YOLQIZ</p>	<p>FIFFIK</p>
	<p>WISNER</p>
	<p>GUTSIX</p>
	<p>TIPWAQ</p>
	<p>BERPUK</p>

## **2.2. HMTA-Metal Organic Frameworks**

This research also investigated the role of metal centers on the coordination environment of HMTA. Data mining of the CSD for structures containing transition metals and HMTA uncovered 94 such examples that contained 159 HMTA fragments connected by covalent or non-bonded interactions (hydrogen bonds). Closer examination of this data revealed several notable trends as presented in Figures 6-8. A plot showing the correlation of the number of structures with HMTA connectivity reveals a high tendency of HMTA to exist in tetracoordination environments whereas relatively few of these structures participate with a coordination of zero or one i.e. HMTA not covalently bonded to a transition metal. Since this study surveyed metal-HMTA complexes for both electrostatic non-bonded contacts and covalent bonds to HMTA, we wondered about the contribution of each type of connection to the patterns observed in Figure 6. Sorting the data to only include metal-HMTA contacts results in Figure 7 and shows a drastically different pattern. In these cases, few structures exist with three or four metal centers covalently bonded to a HMTA. The vast majority of metal/HMTA complexes presented in Figure 7 show that HMTA in most cases is either di-, monocoordinated, or lack metal participation at all. In these same systems, the role of non-bonded contacts to HTMA shows a somewhat even distribution of structures with one to four HMTA connections (Figure 8). Inspection of this data also shows a somewhat weak penchant for forming compounds with no HMTA contacts. There are several patterns that emerge from this study. When considering all contacts to HMTA (covalent and

non-bonded interactions), the HMTA moieties prefer tetracoordination. These four contacts rarely consist of only metal or nonmetal groups, but rather a blend of the two. The metal centers seem to have a greater proportion of HTMA contacts that likely originate from the strength of the HMTA-M bond.

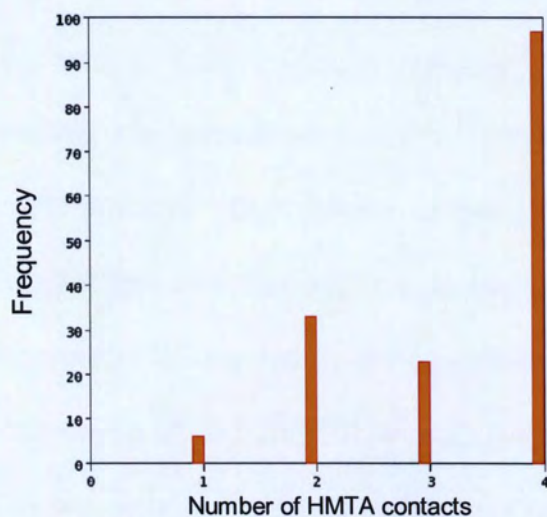


**Figure 6.** Plot of metal containing HMTA structures showing the number of HMTA contacts (covalent and noncovalent interactions) vs. occurrence of HMTA connections.

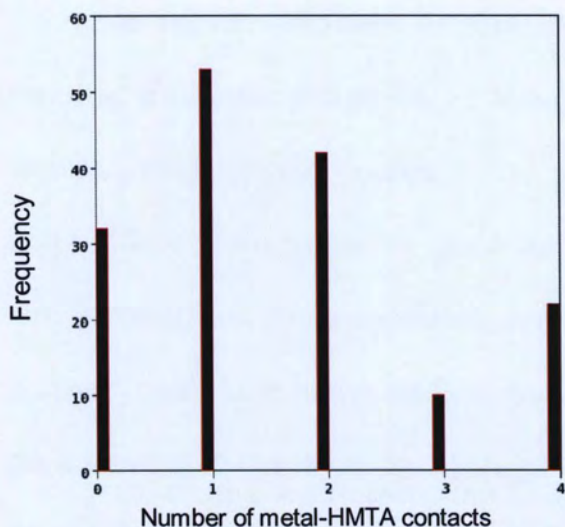


**Figure 7.** Plot of metal containing HMTA structures showing the number of metal-HMTA contacts vs. occurrence of HMTA connections.

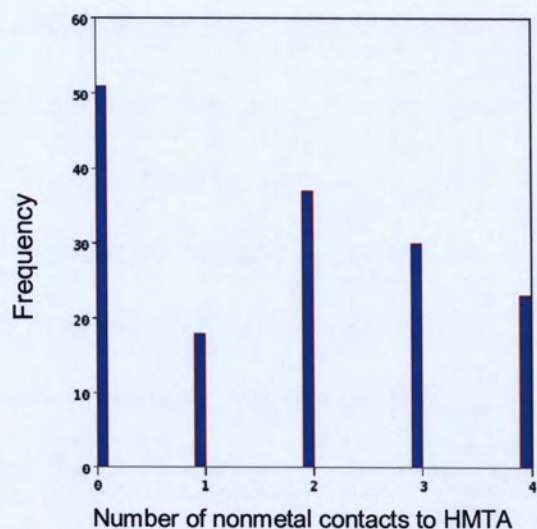


**Figure 8.** Plot of metal containing HMTA structures showing the number of donor...HMTA contacts vs. occurrence of HMTA connections.

### **2.3. Structure correlation of HMTA and number of proton donors**

To further probe the supramolecular behavior of HMTA, the CSD was evaluated to understand the correlation between HMTA...donor distance to the degree of HMTA coordination. Our search of the CSD consisted of organic structures containing alcohol and carboxylic acid moieties with N...O and N...H distances less than van der Waals radii + 0.1 angstroms. This search retrieved 39 structures (11 carboxylic acids) with 97 N...H-O fragments. A comparison of the number of HMTA contacts to the N...O distance (Figure 9) shows that as the number of HMTA contacts increases the hydrogen bond distance also increases. This observation is in agreement with our molecular modeling calculations (Section 3) that showed the hydrogen bond affinity of the HMTA N atoms decrease with an increase in number of attached groups. This suggests that there is a greater probability of forming tetracoordinated HMTA species using weak hydrogen bond donors. This view is supported by further inspection of Figure 9. The cluster of data points associated with the carboxylic acid structures (blue) show a notable decrease in N...O distances (and coordination number) compared to the alcohol counterparts (orange). The reason for this may be attributed to the stronger hydrogen bond donor character of carboxylic acids as compared to alcohols. Although this study is based on a logical strategy for understanding such structural behavior, a database with a larger sampling of related structures is needed to assess the validity of these findings.



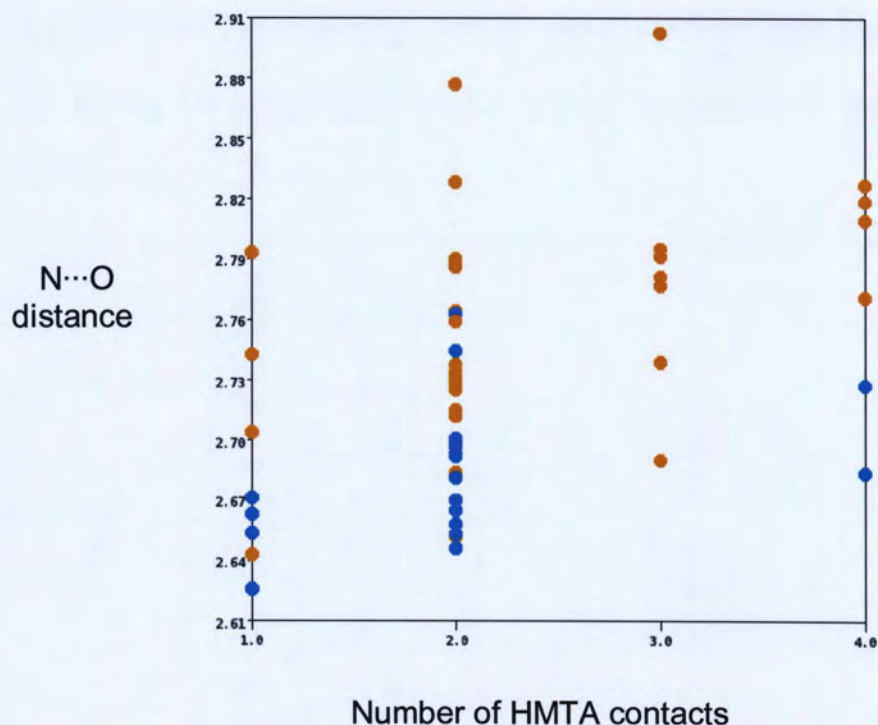


**Figure 9.** Graph of the number of HMTA contacts vs. N...O distance (blue represent carboxylic acids and orange alcohols).

Since it is known that HMTA degrades to formaldehyde and ammonia under acidic conditions,<sup>90,91</sup> we set forth to investigate the initial stages of this reaction profile using the preceding database of 36 organic alcohols and carboxylic acid containing structures. Figure 10 shows the variation of the C-N distance of HMTA to coordination environment. The first trend that emerges from this study is the trend of greater coordination of HMTA results in smaller variations in C-N distance. Comparing the spread of data points at HMTA contacts = 1 and 4 reveals a standard deviation of 0.0124 and 0.00259, respectively and shows less deviation of C-N distances at higher coordination. More importantly, the data seems to suggest that the consequence of carboxylic acids (blue data points) hydrogen bonded to HMTA is a longer C-N bond than



with alcohols (orange data points). This observation follows the inherent increase in acidity (and hydrogen donor ability) of carboxylic acids as compared to alcohols.

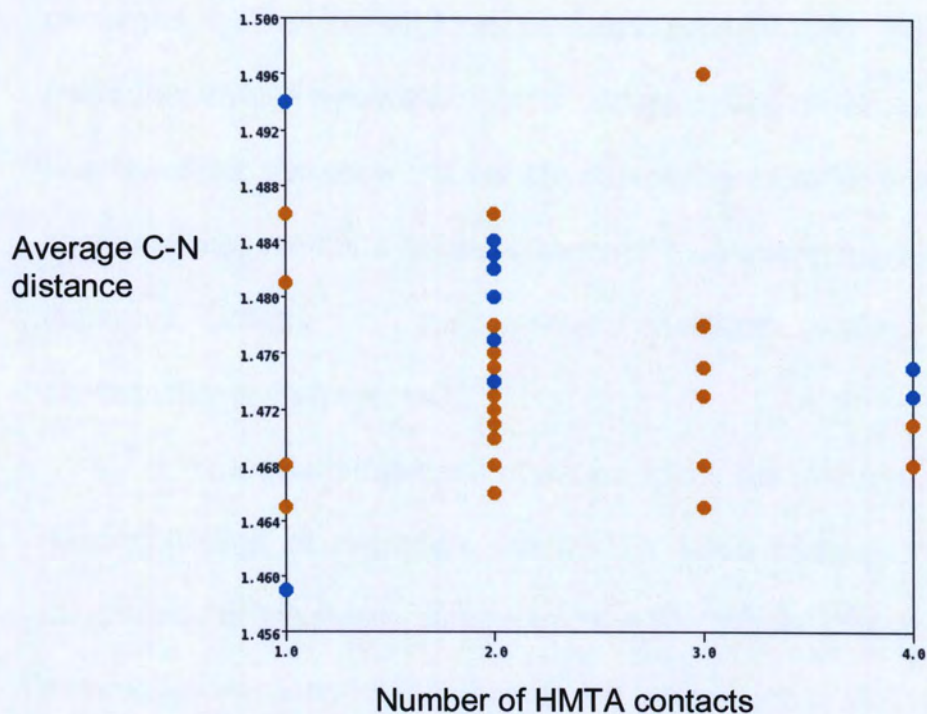


**Figure 10.** Graph of number of HMTA contacts vs. C-N bond distance (blue represent carboxylic acids and orange alcohols).

### **Section 3: HMTA Molecular Modeling**

Molecular modeling calculations are becoming increasingly popular due to advances and user-friendly platforms available with current software packages. The combination of computational and X-ray crystallographic methods provides a powerful tool for understanding molecular structure behavior. Numerous reports show the benefit of bringing together both experimental and computational methods to assess specific structural parameters and provide important insight to fundamental chemical features responsible for conformational preferences.<sup>80-83</sup>

The extant database of crystal structures that contain HMTA reveals a large collection of examples with HMTA either hydrogen bonded to organic compounds or covalently bonded to transition metals. Since the supramolecular assemblies involving HMTA often do not utilize each N atom in bonding or follow a predictable pattern, we set out to study the structural trends of HMTA using the Spartan04 computational package.<sup>84</sup> The hydrogen bond ability of HMTA was investigated by successive addition of donor molecules (i.e., methanol and acetic acid) with subsequent point charge assessment of each free N atom. We wish to clarify such questions as i) does the construction of hydrogen bonds to HMTA influence the hydrogen bond ability of the remaining N atoms and ii) do strong and weak contacts to HMTA influence the number of interactions to HMTA equally?

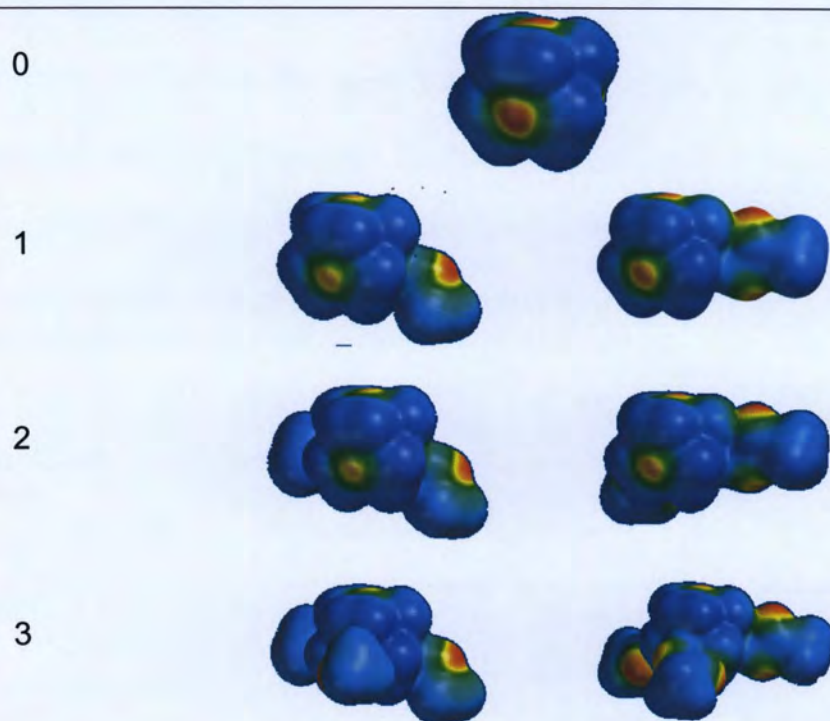


**Figure 11.** Electrostatic potential maps of HMTA and methanol/acetic acid complexes.

Semi-empirical calculations using an AM1 model were used to investigate coordination and hydrogen bond behavior of HMTA. AM1 model has been used to study hydrogen bonding in simple molecules.<sup>85,86</sup> The advantage of employing AM1 methods is the relative fast calculation times as compared to *ab initio* methods, well-suited for large organic systems, robust over a large range of chemical functionality and most importantly, they seem to do well with hydrogen bond energies for which other methods are impractical. Models of HMTA were assembled with either methanol or acetic acid and the hydrogen bond distances (O $\cdots$ N) were constrained to 2.82 Å and 2.68 Å respectively, while angle (N $\cdots$ H-O) was constrained to 180°. Both equilibrium geometry optimization at ground state and single point energy calculations were performed at the AM1



level. Electrostatic potential maps shown in Figure 11 were inspected and the values tabulated in Table 4 for each N atom not involved in hydrogen bonding (i.e., the spatial region of molecules that are susceptible to electrophilic attack - the more negative the value the higher the susceptibility).

**Table 4.** Electrostatic potential values showing HMTA and methanol/acetic acid complexes. Single point energy calculation at AM1 levels.

Hydrogen bond donor	Number of connections	Electrostatic Potential	
		AM1	PM3
None	0	-65	-56
MeOH	1	-61	-51
	2	-57	-47
	3	-54	-43
AcOH	1	-64	-56
	2	-58	-48
	3	-55	-45

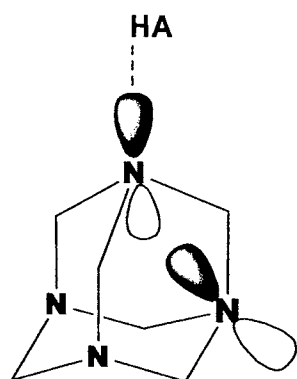


**Figure 12.** Cartoon representation of the anomeric effect showing the close proximity of  $sp^3$  N orbitals.

Inspection of Table 4 reveals a trend of decreasing electrostatic potential (values become less negative) with the successive addition of hydrogen bond groups. With the addition of each donor group to HMTA, the calculations

show the hydrogen bond ability of each free N atom diminishes. This result may be explained using the anomeric effect where the  $sp^3$  lobes of the N atoms participate in through space interactions (Figure 12).<sup>87</sup> Since the formation of hydrogen bonds displace the electron density of the acceptor group, the back lobe of the  $sp^3$  N atom becomes more electrophilic. Also, increasing the hydrogen bond strength of this interaction enhances the electrophilic character of the back lobe, thus influencing the other neighboring HMTA N atoms via through space interactions. This information provides a reasonable explanation why few tri- or tetracoordinated HMTA cocrystalline structures have been reported. Furthermore, our calculations show that protonating HMTA to give HMTA<sup>+</sup>-H affords an electrostatic potential of +28.9. Although hexamethylenetetraminium cations readily form N<sup>+</sup>-H...acceptor interactions as shown via crystallography studies, the three remaining N atoms do not often form additional intermolecular contacts. This can be attributed to the fact that N<sup>+</sup>-H is a strong proton donor forming a short and strong N<sup>+</sup>-H...acceptor interaction that also influences the hydrogen bond ability of the free HMTA N atoms via an anomeric effect. This phenomenon is also experimentally observed in crystal structures as indicated by the general trend of decreasing the number of HMTA contacts results in shorter N...O distances (Figure 9). In fact, this might explain why no tri- and tetracoordinated hexamethylenetetraminium species have been reported to date.

It is important to note that these calculations serve as an initial effort to understand the trends observed in the crystal structures of HMTA. Since these calculations were performed on isolated molecules (gas phase) with

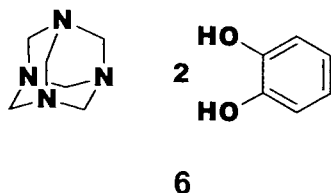
approximations that exclude the influences of sterically encumbered systems and crystal forces, additional calculations are likely needed that explore models of greater complexity, and methods that account for all forces responsible for the observed supramolecular trends.

## Section 4: Co Crystallization of HMTA and Organic Compounds

Reagents: Chemicals were purchased from the Aldrich Chemical Company, Acros Chemicals, Eastman Organic Company, ALFA Inorganics and Fisher Chemicals and used without further purification.

Instruments: Melting points were determined using a Mel-Temp apparatus and are uncorrected. Infrared spectra were obtained using a Nicolet Avatar 360 FT-IR, Bio-Rad Excalibur series FTS 30000MX FT-IR spectrometer as either a KBr pellet or nujol mull. IR transmittance maxima are reported in wavenumbers ( $\text{cm}^{-1}$ ) with spectra provided as supplementary material in the appendix (pp. 128-134).  $^1\text{H}$  NMR and proton decoupled  $^{13}\text{C}$  NMR spectra were collected using a 400 MHz Bruker Avance FT-NMR Spectrometer. All chemical shifts are reported in parts per million (ppm) relative to TMS or the residual solvent peak. The coupling constants ( $J$ ) are reported in hertz (Hz) and the following abbreviations are used in assigning signal multiplicity:  $s$  = singlet,  $d$  = doublet,  $t$  = triplet,  $dd$  = doublet of doublets, and  $dt$  = doublet of triplets. Crystal structures were determined using a Bruker single-crystal P4 X-ray Diffractometer.

### 4.1.1. Bis(1,2-dihydroxybenzene)hexamethylenetetramine<sup>88</sup>



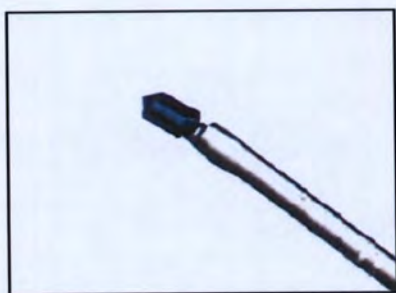
We present the crystal structure of bis(1,2-dihydroxybenzene) hexamethylenetetramine in detailed chronological sequence. The procedures and operations discussed for intensity data collection, refinement and structure solution are meant to serve as a reference for the other crystal structure determinations in this thesis.

#### **4.1.2. Crystal growth, selection, and mounting**

Crystals of bis(1,2-dihydroxybenzene)hexamethylenetetramine were obtained by slow evaporation of a 10mL 1:2 methanolic solution of hexamethylenetetramine (0.250 g, 1.79 mmoles) and 1,2-dihydroxybenzene (0.393 g, 3.60 mmoles). A recrystallization dish covered with a watchglass was used to grow crystals. Colorless crystals with block morphology were harvested after a few days. The crystals exhibited the following analytical data: mp 422-425K;  $^1\text{H}$  NMR (acetone- $d_6$ ):  $\delta$  = 4.63 (s, 12H, HMTA- $\text{CH}_2$ ), 6.62 (dd,  $J$  = 5.8 and 3.5 Hz, 4H, H-2, 5) 6.78 (dd,  $J$  = 5.8 and 3.5 Hz, 4H, H-3, 4);  $^{13}\text{C}$  NMR (acetone- $d_6$ )  $\delta$  = 145.6 (C7-C10), 119.4 (C3, 4), 115.7 (C2, 5), 74.4 (C1, 6); IR (KBr) 2995.15 (broad, -OH), 1464.15(C=C), 1101.64 (C-O), 1003.56 (C-N)  $\text{cm}^{-1}$ . Crystal quality of **6** was assessed by polarized light microscopy and a crystal with dimensions 0.41 x 0.41 x 0.20 mm was mounted on a glass fiber and affixed to a brass pin then onto the goniometer head as shown in Figure 13A and B.



A)



(B)



**Figure 13.** Representative examples of a (A) crystal mounted on a glass fiber and (B) goniometer head for diffraction studies.

#### 4.1.3. Intensity data collection

The crystal was transferred to a Huber XYZ-goniometer head (Model 1004) (Figure 13B) and optically centered using a Bruker P4 diffractometer equipped with a MoK $\alpha$  source (50 KV, 30 mA). A hemisphere search from  $\theta = 4$  to  $12^\circ$  for reflections  $> 30,000$  counts resulted in 6 reflections well dispersed in reciprocal space. Refinement of this low angle data by least-squares methods gave an orientation matrix and unit cell parameters with the following corresponding standard deviations,  $a = 23.75(2)\text{\AA}$ ,  $b = 6.844(6)\text{\AA}$ ,  $c = 13.22(2)\text{\AA}$ ,  $\alpha = 90.08(9)^\circ$ ,  $\beta = 123.12(6)^\circ$ ,  $\gamma = 89.95(6)^\circ$ . Iterative refinement of the data obtained between  $4^\circ \leq \theta \leq 12^\circ$  was followed by least-squares analysis. The resulting orientation matrix used for data collection gave the following unit cell parameters:  $a = 23.794(2)\text{\AA}$ ,  $b = 6.8422(5)\text{\AA}$ ,  $c = 13.244(1)\text{\AA}$ ,  $\alpha = 90^\circ$ ,  $\beta = 123.135(6)^\circ$ ,  $\gamma = 90^\circ$ . The  $\theta$ - $2\theta$  scan mode was used for data collection, with  $2.0^\circ \leq \theta \leq 25.4^\circ$ . 1921 reflections were collected of the type  $-1 \leq h \leq 28$ ,  $-1 \leq k \leq 8$ ,  $-14$

$\leq I \leq 13$ . During the data collection, variable scan speeds ( $5\text{-}15^\circ\cdot\text{min}^{-1}$ ) and a symmetrical scan range ( $-0.5$  to  $0.5^\circ$ ) were employed. Standard reflections, (10, 2, -3), (2, 2, -4), and (1, 3, 4) were monitored after every 97 reflections to assess crystal degradation, alignment, and instrument fluctuations. For reflections (10, 2, -3), (2, 2, -4), and (1, 3, 4) the variation in intensity was  $\leq 3\%$ .

#### 4.1.4. Intensity Data Reduction

Data was reduced using the XSCANS software package. The analytical scattering factors of Cromer and Waber<sup>89</sup> were used; real and imaginary components of anomalous scattering for nonhydrogen atoms were included in the calculations. The data were reduced ( $I \rightarrow |F_o|$ ) by applying Lorentz-Polarization ( $Lp$ ) corrections. The structure factor had the form  $|F_d| = (I/Lp)^{1/2}$  where  $Lp$  is defined as follows:

$$Lp = \frac{1 + \cos^2 2\theta}{2 \sin 2\theta}$$

Data were sorted and equivalent reflections averaged using the XPREP<sup>90</sup> program. The agreement factors,  $R_{\text{int}}$ , for the equivalent reflections was calculated using:

$$R_{\text{int}} = \frac{\sum |F_o^2 - F_o^2(\text{mean})|}{\sum |F_o^2|}$$

572 reflections for which  $I/\sigma(I) \leq 2$  were rejected as unobserved. Structure factors were computed and assigned standard deviations ( $\sigma(F_o)$ ) calculated by the method of finite differences:

$$\rho_c = \frac{1}{V \sum (F_c) \exp(-2\pi i)} \quad \text{and} \quad \rho_o = \frac{1}{V \sum (F_o) \exp(-2\pi i)}$$

#### 4.1.5. Structure Solution and Refinement

The structure of **1** was solved using the X-Seed<sup>91</sup> platform with the SHELXL97<sup>92</sup> module; the coordinates of all nonhydrogen atoms were located on an E-map from the first trial solution. Least-squares full-matrix refinement of the scale factor, positional, and isotropic displacement parameters for all nonhydrogen atoms led to  $R = 0.094$  and  $R_w = 0.119$ . The atoms were then assigned anisotropic displacement parameters and refinement converged to  $R = 0.051$  and  $R_w = 0.102$ . Where  $R$  and  $wR$  are defined as follows:

$$R = \frac{\sum ||F_o| - |F_c||}{\sum |F_o|}$$

$$wR = \sqrt{\frac{\sum \omega (|F_o|^2 - |F_c|^2)^2}{\sum \omega (F_o^2)^2}}$$

The function minimized in the least-squares procedure was  $\omega[|F_o| - |F_c|]^2$  where  $\omega$  is a constant weighting scheme<sup>93</sup>. At convergence, the largest parameter shift was 0.001 times the corresponding estimated standard deviation. The residual values were 0.051 and 0.0119. At the end of the analysis, a difference Fourier map was calculated, which revealed random residual density from 0.15 to -0.25 e·Å<sup>3</sup>. The details of this data collection and structure determination procedure, atomic coordinates, atomic displacement parameters, bond geometries, and hydrogen bond parameters are summarized in Tables 5 -

11. These tables, including data from other structures investigated, are located in the appendix section of this thesis.

#### **4.1.6. Crystal structure assessment**

The asymmetric unit of **6** comprises a molecule of 1,2-dihydroxybenzene and half molecule of HMTA positioned on a two fold rotational axis. The bond angles/lengths and the torsion angles for the complex are shown in Tables 5 and 6, and are consistent with typical bond geometries. Both hydroxyl groups participate in hydrogen bonding (Figure 14). Hydroxyl group O2 forms an intramolecular interaction, whereas O1 forms an intermolecular hydrogen bond connecting neighboring HMTA molecules.

The remaining N atoms on HMTA also interact with the neighboring dihydroxybenzene via hydrogen bonds. These collections of non-bonded contacts involve all four HMTA N atoms and form molecular strands that propagate along the *c*-axis (Figure 15). The projection of the unit cell and the 3D packing pattern are shown in Figures 16 and 17. The influence of HMTA–HMTA contacts are ruled out since the shortest distance between these groups is 4.48 Å which is significantly beyond the sum of their van der Waals radii.



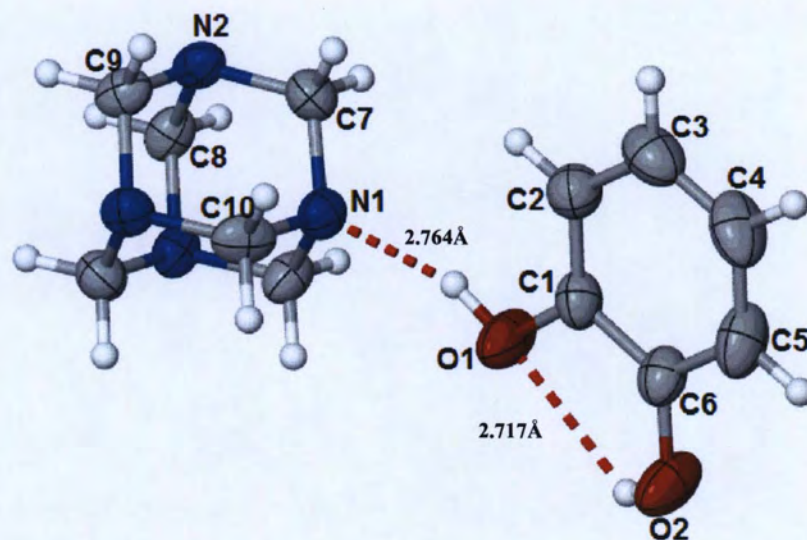


**Figure 14.** Crystal structure of the HMTA and 1,2-dihydroxybenzene showing atom labeling scheme and atomic displacement ellipsoids at the 50% probability level. Dashed lines indicate hydrogen bonding.

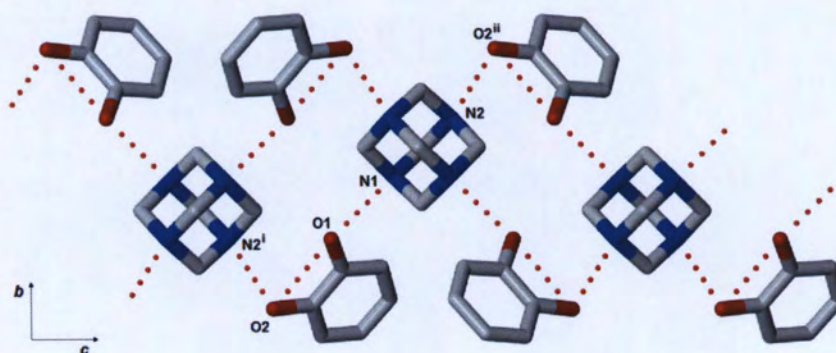


**Figure 15.** Packing pattern of **6** showing the catemeric O-H...N interactions as dashed lines. H atoms have been omitted for clarity.

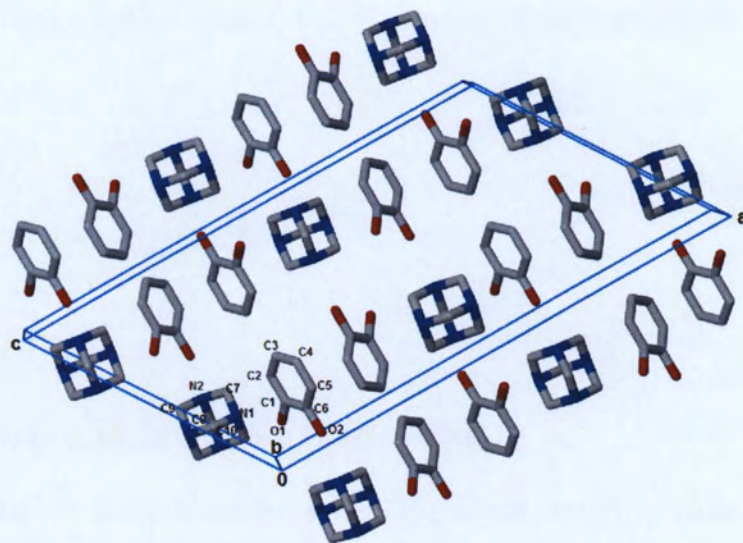


**Figure 16.** Projection of the unit cell contents of **6**.

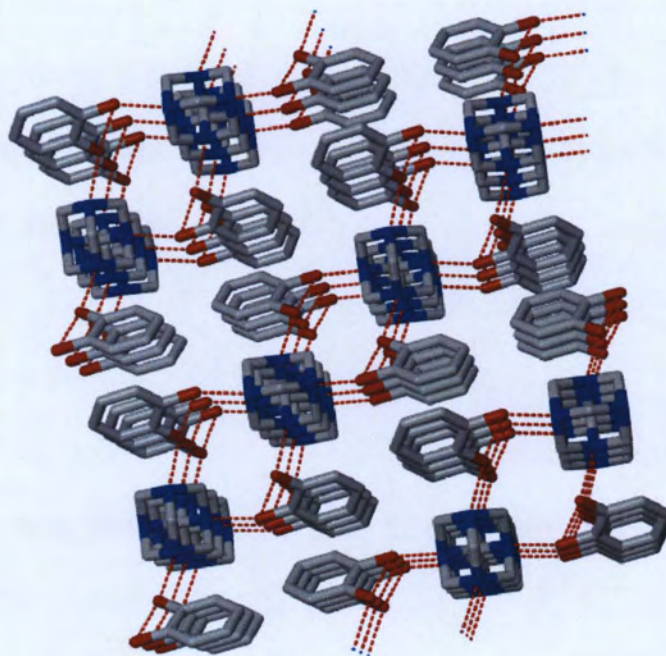
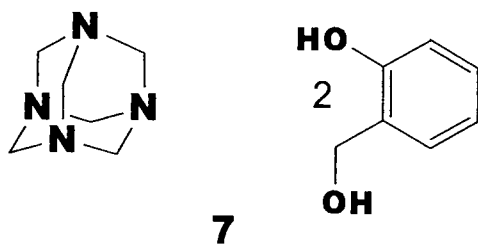


**Figure 17.** 3D molecular packing pattern of **6** showing inter- and intramolecular H-bonding patterns.



#### 4.2.1. Bis(2-hydroxybenzylalcohol) hexamethylenetetramine



#### 4.2.2. Crystal growth, selection, and mounting

Crystals of bis(2-hydroxybenzylalcohol)hexamethylenetetramine **7** were obtained by slow evaporation of a 15mL methanolic solution of hexamethylenetetramine (0.250 g, 1.78 mmoles) and 2-hydroxybenzylalcohol (0.442 g, 3.55 mmoles). A recrystallization dish covered with a watch glass was used to grow crystals. Colorless crystals with needle like morphology were harvested after a few days. The crystals exhibited the following analytical data: mp 342-344K; <sup>1</sup>H NMR (DMSO-d<sub>6</sub>/D<sub>2</sub>O): δ = 4.60 (s, 2H, Ar-CH<sub>2</sub>), 4.75 (s, 12H, HMTA-CH<sub>2</sub>), 6.88 (*d*, *J* = 8.05 Hz, 1H, Ar-H), 6.94 (*dt*, *J* = 7.44 and 7.48 Hz, 1H, Ar-H), 7.23 (*dt*, *J* = 7.48 and 7.96 Hz, 1H, Ar-H), 7.31 (*d*, *J* = 7.48Hz, 1H, Ar-H); <sup>13</sup>C NMR (DMSO-d<sub>6</sub>/D<sub>2</sub>O): δ = 56.0 (C3) (2-hydroxybenzylalcohol), 73.35 (HMTA-CH<sub>2</sub>), 130.62 (2), 130.53 (C7) 128.33 (C6) 121.77 (C5), 116.77 (C4), 60.61 (C1); IR (nujol). 2934.50 (*broad*), 1451.62 (C=C), 1107.5 (C-O), 1000.98 (C-N) cm<sup>-1</sup>. Crystal quality of **7** was assessed by polarized light microscopy.

X-ray data collection, data reduction, structure solution and refinement processes were performed as described for structure **6** (Sections 4.1.3 - 4.1.5) with details of the data collection and structure determination procedure, atomic

coordinates, atomic displacements parameters, bond geometries and hydrogen bond parameters summarized in Tables 12 - 18.

#### **4.2.3. Crystal structure assessment**

The asymmetric unit of **7** consists of a molecule of 2-hydroxybenzylalcohol and one-half molecule of HMTA positioned on a mirror symmetry plane (Figure 18). Both hydroxyl groups on 2-hydroxybenzylalcohol participate in hydrogen bonding (Table 17). The phenolic hydroxyl group of one molecule participates in a catemeric motif by O-H...O contacts to neighboring benzyl hydroxyl group of the adjacent molecule (Figure 19). This generates a continuous array of 2-hydroxybenzylalcohol molecules along the *a*-axis linked to each other via hydrogen bonds. These motifs are further connected by 2-hydroxybenzyl...HMTA interactions along the *b*-axis. Each HMTA forms two contacts to give 'ladder' like motifs. The arrangement of molecules in the unit cell is provided in Figure 20. As shown in Figure 21, the 3D packing pattern reveals that the 2-hydroxybenzylalcohol molecules between the 'ladder' like motifs arranged with 3.54 Å between aryl rings, suggesting the presence of  $\pi$ -stacking and C-H... $\pi$  interactions. There are no HMTA-HMTA interactions as the shortest distance between them is 3.925 Å which exceeds the distance of any meaningful contact (Figure 21).



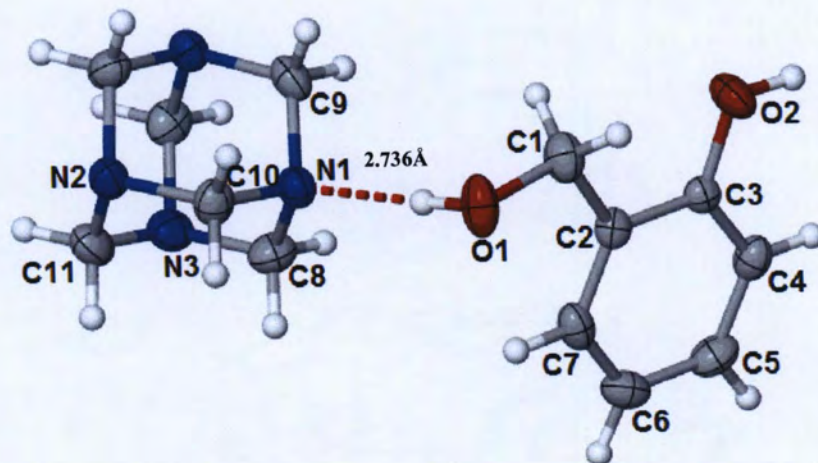


**Figure 18.** The structure of the components molecules of **7** showing atom labeling scheme and atomic displacement ellipsoids at the 50% probability level.

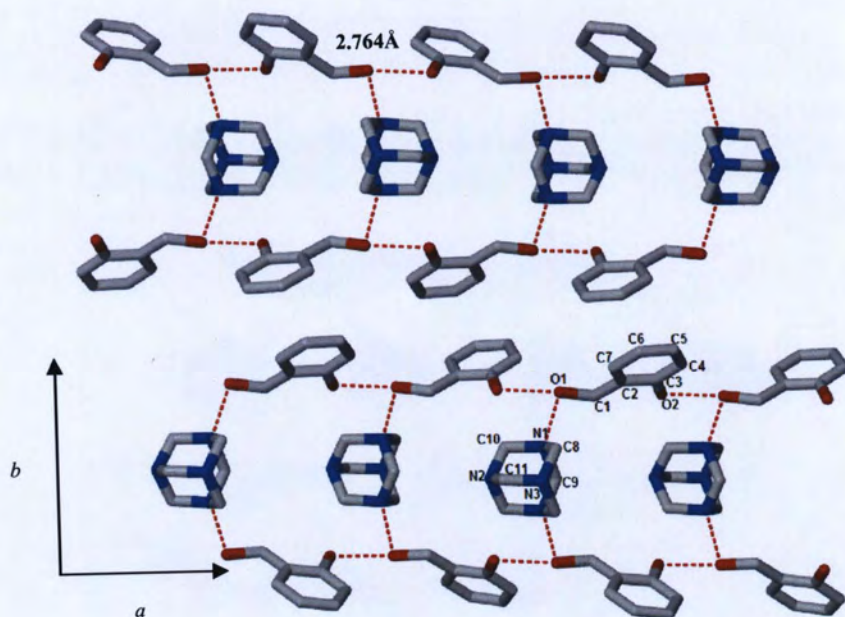


**Figure 19.** View of the packing pattern of **7** showing heteromeric catemeric O-H...N and O...H-O interactions as dashed lines. H atoms have been omitted for clarity.

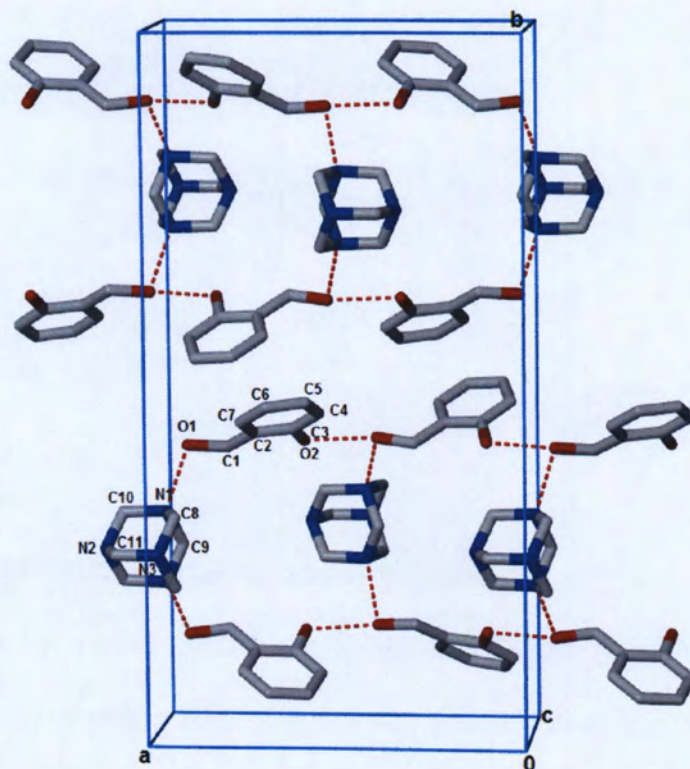


**Figure 20.** Projection of **7** showing the unit cell and hydrogen bond network. Hydrogen atoms have been omitted for clarity.

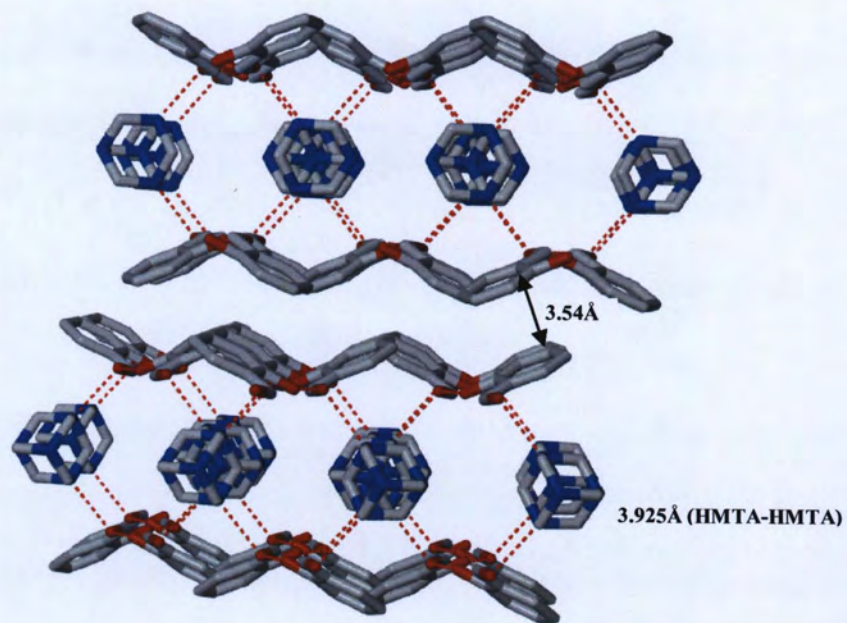
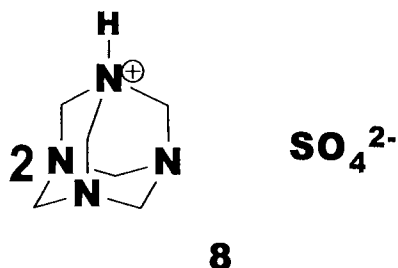


**Figure 21.** Crystal packing diagram of **7** showing both hydrogen bond and  $\pi$ - $\pi$  stacking. Dashed lines indicate hydrogen bonds.



#### 4.3.1. Bis(hexamethylenetetramminium) sulfate



#### 4.3.2. Crystal growth, selection, and mounting

Bis(hexamethylenetetramminium) sulfate (**8**) was prepared by dissolution of hexamethylenetetramine (0.125 g, 0.893 mmoles) and sodium sulfate (0.25 g, 1.761 mmoles) in 15mL of water. The resulting clear homogenous solution was adjusted to pH 6 with 0.005M sulfuric acid and allowed to recrystallize via room-temperature slow evaporation. Colorless plate-shaped crystals were collected after 7 days and assessed for quality by polarized light microscopy. The crystals exhibited the following analytical data: mp > 523K;  $^1\text{H}$  NMR (DMSO- $d_6$ /D $_2$ O):  $\delta$  = 4.62 (s, HMTA-NH), 4.69 (s, 12H, HMTA-CH $_2$ );  $^{13}\text{C}$  NMR (DMSO- $d_6$ /D $_2$ O):  $\delta$  = 73.34 (HMTA-CH $_2$ ); IR (nujol): 36.08.15 (N $^+$ -H ), 1236.29 (broad, S=O and C-N)  $\text{cm}^{-1}$ .

Intensity data collection, data reduction, structure solution and refinement processes were performed as described previously for compound **6** (Sections 4.1.3 - 4.1.5) with details of the data collection and structure determination procedure, atomic coordinates, atomic displacements parameters, bond geometries and hydrogen bond parameters summarized in Tables 19 – 25.

### 4.3.3. Crystal structure assessment

The asymmetric unit of **8** consists of two molecules of HMTA<sup>+</sup>-H and a molecule of sulfate (SO<sub>4</sub><sup>2-</sup>). Unlike the previous cases in which the HMTA moiety acts as a proton acceptor, **8** behaves as a proton donor and participates in N-H···O contacts with neighboring sulfate molecules (Figure 22 and Table 25). The HMTA···sulfate interactions generate discrete trimers that are held together by weak HMTA-HMTA (N···H-C) interactions as shown in Figures 23 and 24. These interactions form a 3D molecular scaffold connected via both strong and weak intermolecular contacts.

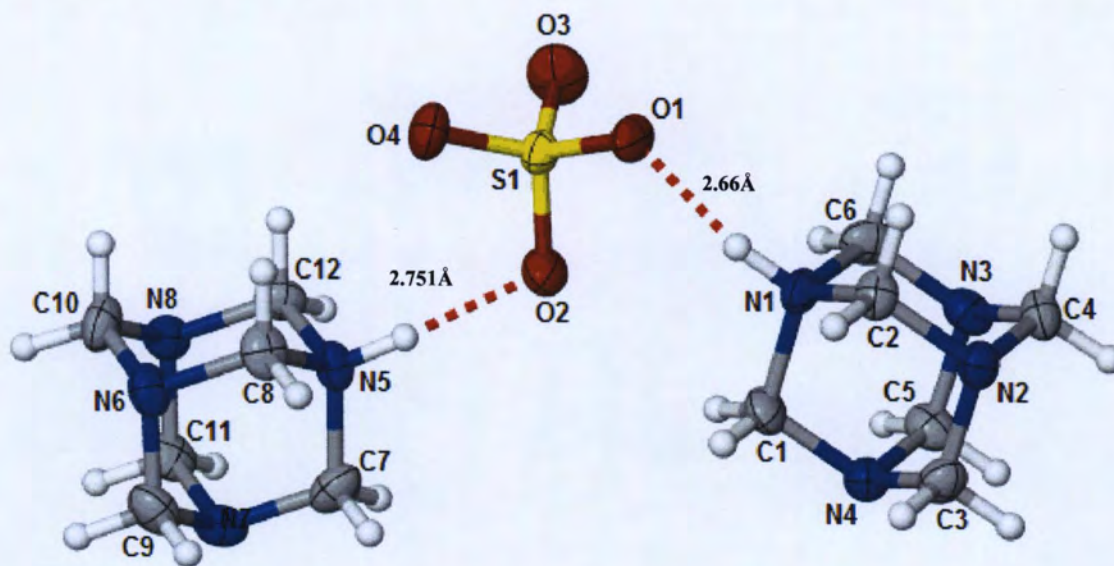


**Figure 22.** Crystal structure of **8** showing the asymmetric unit, labeling scheme, and atomic displacement ellipsoids at the 50% probability level.



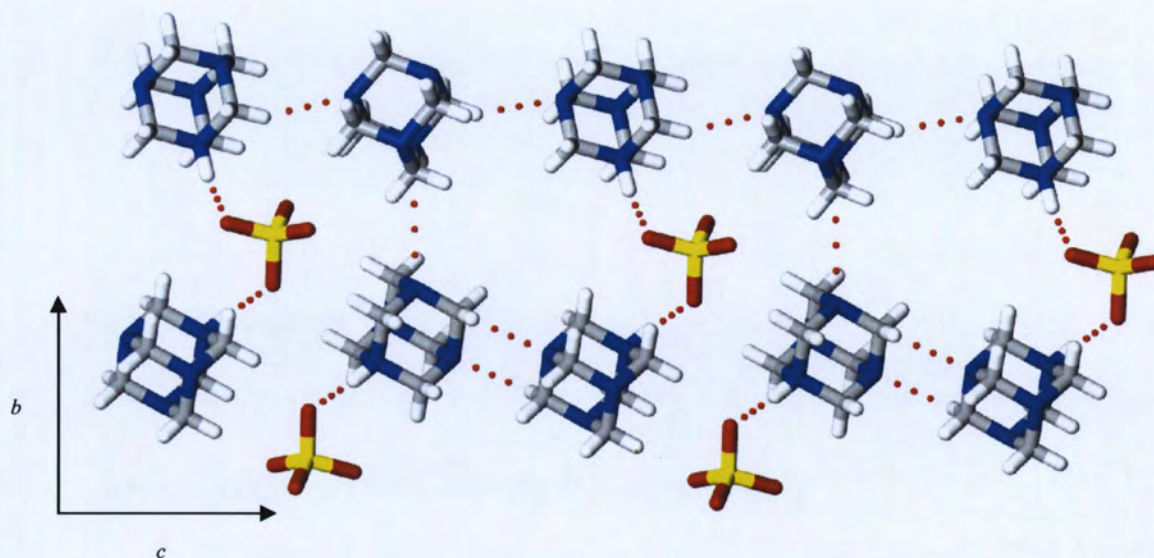


**Figure 23.** View of the packing pattern of **8** showing catemeric N-H...O and N...H-C contacts in the *bc* plane. Hydrogen bonds are shown as dashed lines.

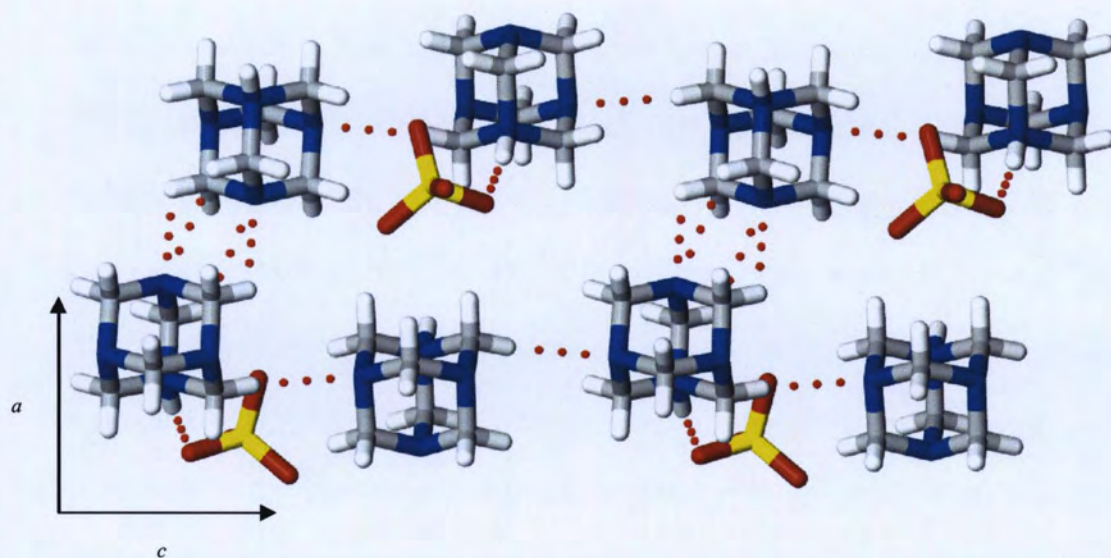
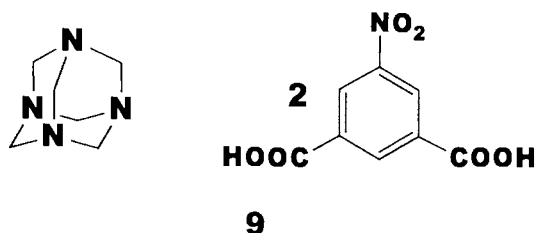


**Figure 24.** View of the packing pattern of **8** showing catemeric N-H...O and N...H-C in the *ac* plane. Hydrogen bonds are represented as dashed lines.

#### 4.4.1. Bis(5-nitroisophthalic acid)hexamethylenetetramine dihydrate



#### 4.4.2. Crystal growth, selection, and mounting

Crystals of hexamethylenetetramine and 5-nitroisophthalic acid (**9**) were grown by slow evaporation of a 10mL 1:4 water/methanol solution of hexamethylenetetramine (0.05 g, 0.357 mmoles) and 5-nitroisophthalic acid (0.15 g, 0.711 mmoles). A recrystallization dish covered with a watch glass was used to grow crystals. Colorless crystals with needle like morphology were harvested after one week. The crystals exhibited the following analytical data: mp 481-483K; <sup>1</sup>H NMR (DMSO-d<sub>6</sub>): δ = 4.38 (s, 12H, HMTA-CH<sub>2</sub>), 8.749 (s), 8.752 (s) (5-Nitroisophthalic acid); <sup>13</sup>C NMR (DMSO-d<sub>6</sub>): δ = 72.50 (HMTA-CH<sub>2</sub>), 165.26 (C1, C8, C15, C22), 148.09 (C4, 18), 135.10 (C7, C21), 134.37 (C2, C6, C16, C22), 126.79 (C3, C5, C17, C19) (5-nitroisophthalic acid); IR (nujol): 3434.66 (OH), 1703.9 (C=O), 1545.18 and 1257.09 (N=O), 1462.92 (C=C), 1200 (C-O), 1027.58 (C-N) cm<sup>-1</sup>. Crystal quality of **9** was assessed by polarized light microscopy and an appropriate crystal was mounted on a glass fiber and affixed to a brass pin then onto the goniometer head.

X-ray data collection, data reduction, structure solution and refinement processes were performed as described for structure **6** (Sections 4.1.3 - 4.1.5)

with details of the data collection and structure determination procedure, atomic coordinates, atomic displacements parameters, bond geometries and hydrogen bond parameters summarized in Tables 26 - 32.

#### **4.4.3. Crystal structure assessment**

The asymmetric unit of **9** consists of a molecule of HMTA, two molecules of 5-nitroisophthalic acid, and two water molecules. Each of these components link via hydrogen bonding (Figure 25). The two symmetry independent 5-nitroisophthalic acids are linked by O-H...O contacts that are further connected to adjacent HMTA and water moieties each (Figure 26). These intermolecular interactions generate a zigzag pattern arrangement of acids along the *c*-axis. These noncovalent interactions generate supramolecular patterns in which only two HMTA nitrogen atoms are involved in hydrogen bonding. A perspective of the unit cell contents and some symmetry generated atoms are shown in Figure 27. Close inspection of the crystal structure (Figure 28) reveals the presence of HMTA-HMTA (C-H...N, 3.353 Å) interactions; even so, all aromatic-aromatic stacking (5.638 Å) and HMTA–nitro contact (C-H...O-N, 3.351 Å) distances are too long for any meaningful interactions between them.



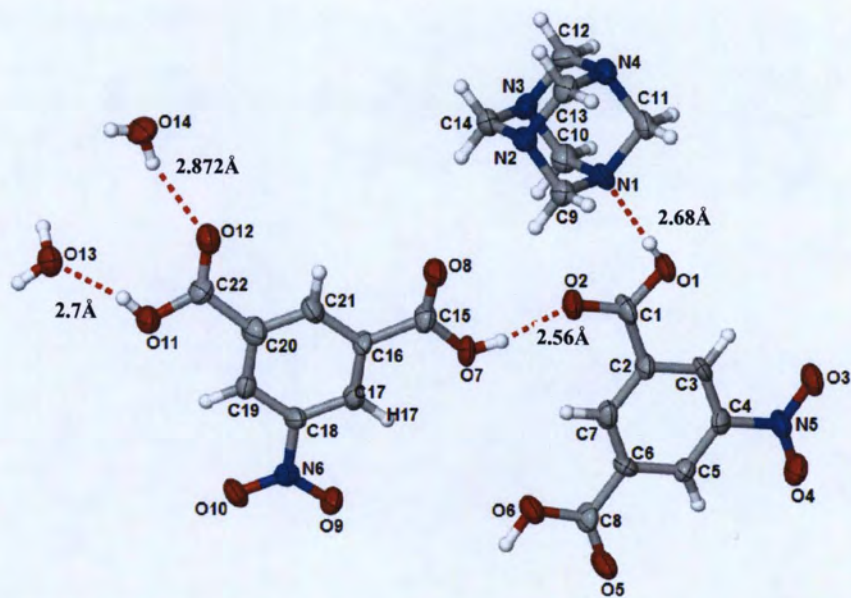


**Figure 25.** Crystal structure **9** showing the asymmetric unit, labeling scheme, and atomic displacement ellipsoids at the 50% probability. Hydrogen bonds are represented as dashed lines.

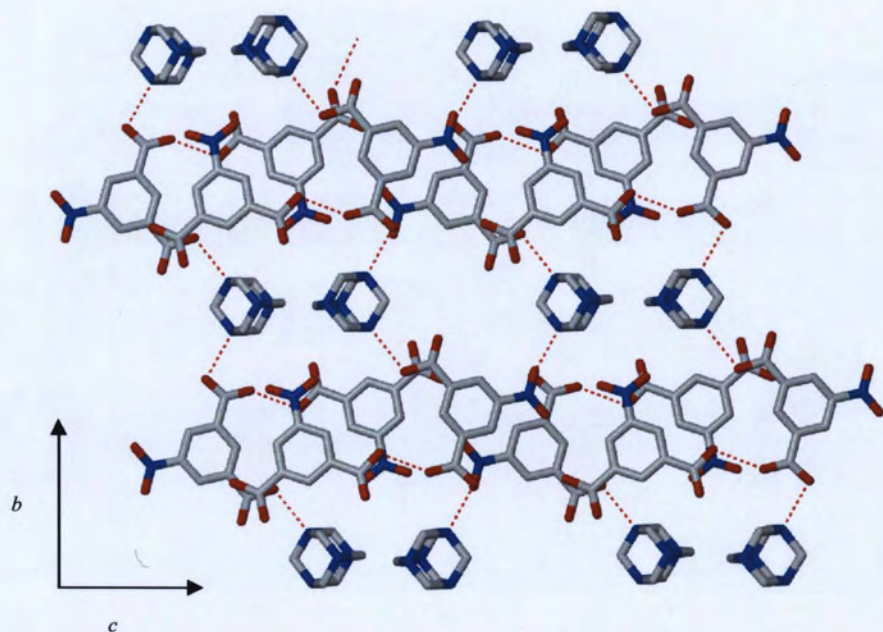


**Figure 26.** View of the crystal packing of **9** showing catemeric N-H...O interactions as dashed lines. H atoms have been omitted for clarity.



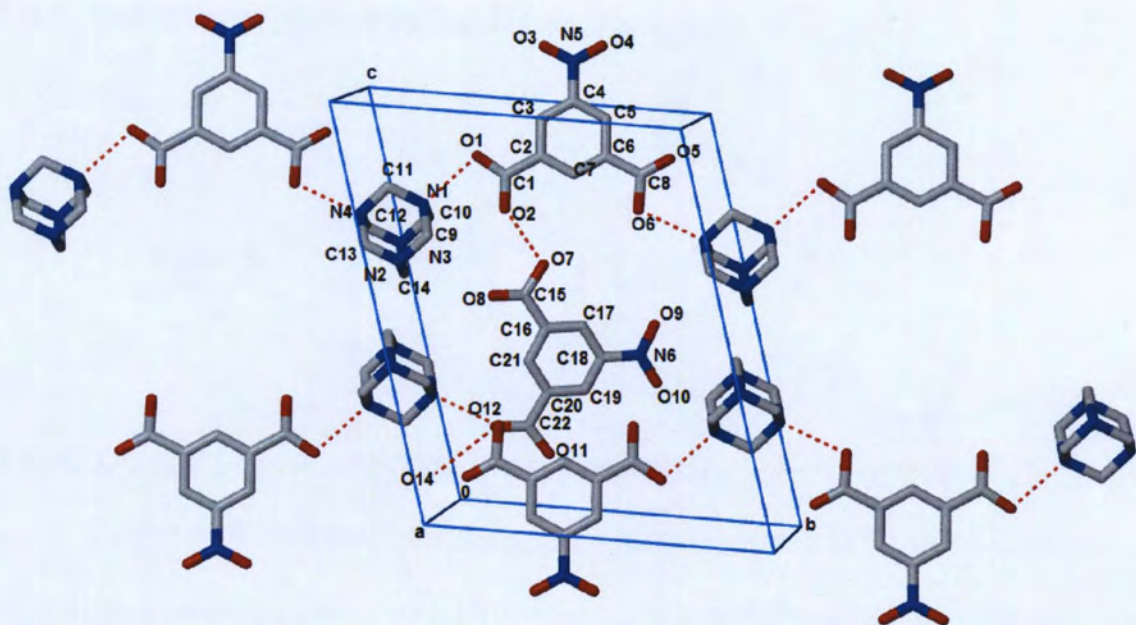


**Figure 27.** Projection of the unit cell contents of **9** showing the constructions of molecular strands. Hydrogen atoms have been omitted for clarity. H bonds are shown by dashed lines.

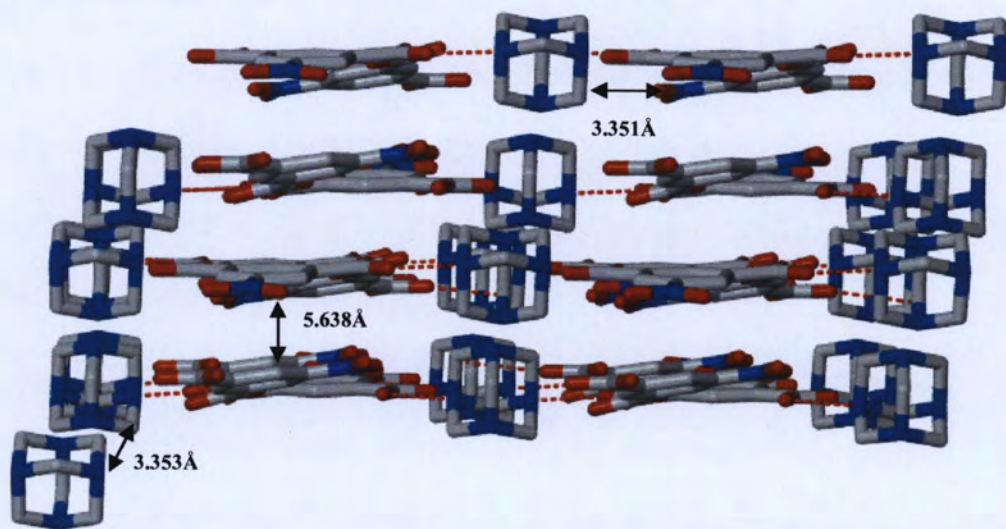
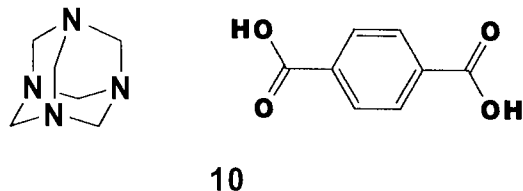


**Figure 28.** Crystal projection of **9** showing hydrogen bond scheme and close HMTA-HMTA interactions.

#### 4.5.1. Hexamethylenetetramine terephthalic acid



#### 4.5.2. Crystal growth, selection, and mounting

Crystals of hexamethylenetetramine terephthalic acid **10** were obtained by slow evaporation of a 15 mL 2:1 water/methanol solution of hexamethylenetetramine (0.0250 g, 1.78 mmoles) and terephthalic acid (0.0592 g, 0.357 mmoles). Colorless crystals with block like morphology were harvested after one week whose quality was assessed by polarized light microscopy. The crystals exhibited the following analytical data: mp > 523K;  $^1\text{H}$  NMR (DMSO- $d_6$ ):  $\delta$  = 4.29 (s, 12H, HMTA- $\text{CH}_2$ ), 7.97 (s, 4H, Ar-H);  $^{13}\text{C}$  NMR (DMSO- $d_6$ /D $_2$ O):  $\delta$  = 73.11 (HMTA- $\text{CH}_2$ ),  $\delta$  = 130.03 (C1, C8), 137.56 (C2, C5), 169.89 (C3, C4, C6, C7) (terephthalic acid); IR (nujol): 2847.36 (broad, OH), 1685.76 (C=O), 1456.3 (C=C), 1241.4 (C-O), 1006.8 (C-N)  $\text{cm}^{-1}$ .

X-ray data collection, data reduction, structure solution and refinement processes were performed as described for structure **6** (Sections 4.1.3 - 4.1.5) with details of the data collection and structure determination procedure, atomic coordinates, atomic displacements parameters, bond geometries and hydrogen bond parameters summarized in Tables 33 - 39.

#### 4.5.3. Crystal structure assessment

The asymmetric unit of **10** comprises three molecules of HMTA and three molecules of terephthalic acid, one of the terephthalic moieties is disordered over two positions (Figure 29). The HMTA and terephthalic acids are linked to each other via hydrogen bonding. These weak intermolecular interactions generate an array of molecules that extend along the *b*-axis in an alternating fashion between HMTA and terephthalic acid (Figure 30). Inspection of the 2D network along the *ac* plane reveals undulating patterns that are stuck on top of each other (Figure 31). We also note that the spaces between disordered terephthalic acids strands along the *ac* plane are occupied by two ordered terephthalic acid strands. This collection of non-bonded contacts involve only two HMTA N atoms and forms molecular strands that propagate along the *b* axis. A projection of the unit cell is shown in Figure 32. HMTA...HMTA contacts and  $\pi$ -stacking interactions are ruled out as the shortest distance between them are 4.17 Å and 12 Å, respectively, which is beyond van der Waals forces of radii for any meaningful interaction.



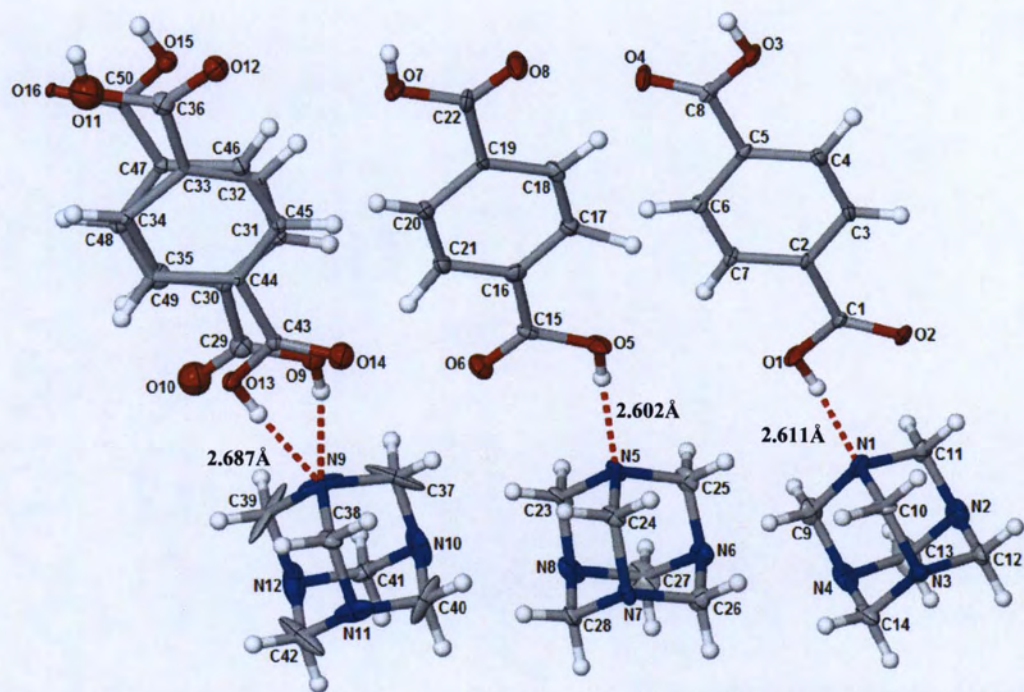


**Figure 29.** The crystal structure **10** showing the asymmetric unit, labeling scheme, and atomic displacement ellipsoids at the 50% probability level. Dashed lines represent hydrogen bonds.

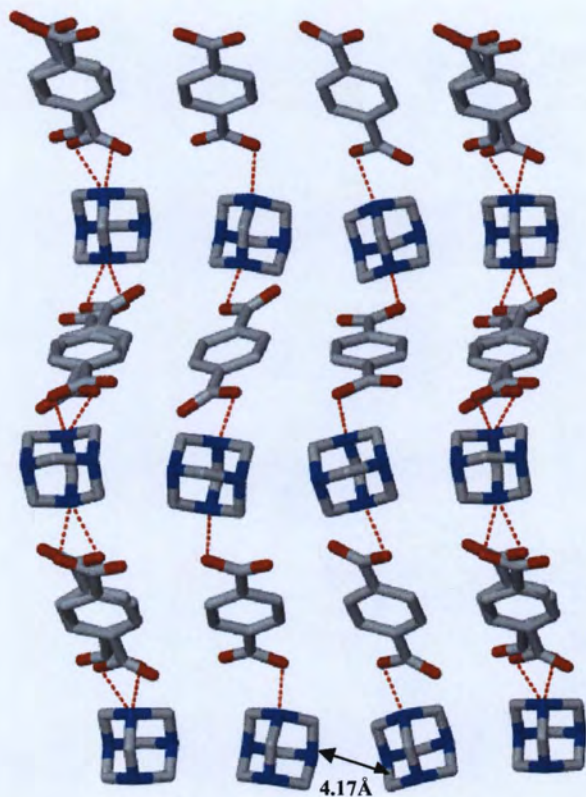


**Figure 30.** View of the crystal packing of **10** showing the catemeric N···H-O motif in the *ab* plane. Hydrogen bond interactions are shown as dashed lines.

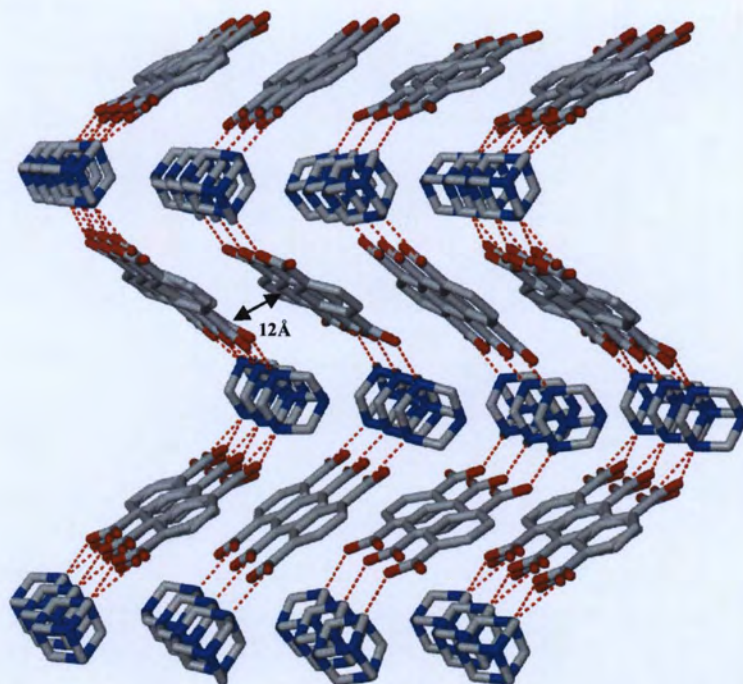


**Figure 31.** View of the packing pattern of **10** showing the catemeric N···H-O contacts in the *ac* plane. Hydrogen bond interactions are shown as dashed lines.



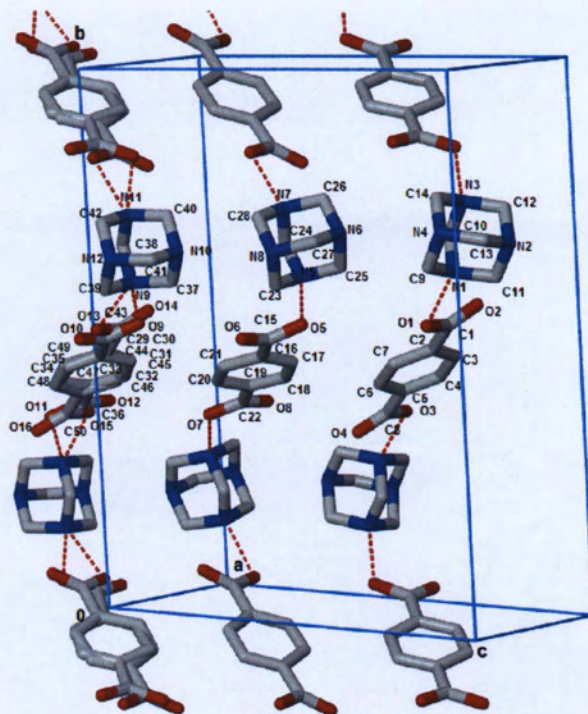
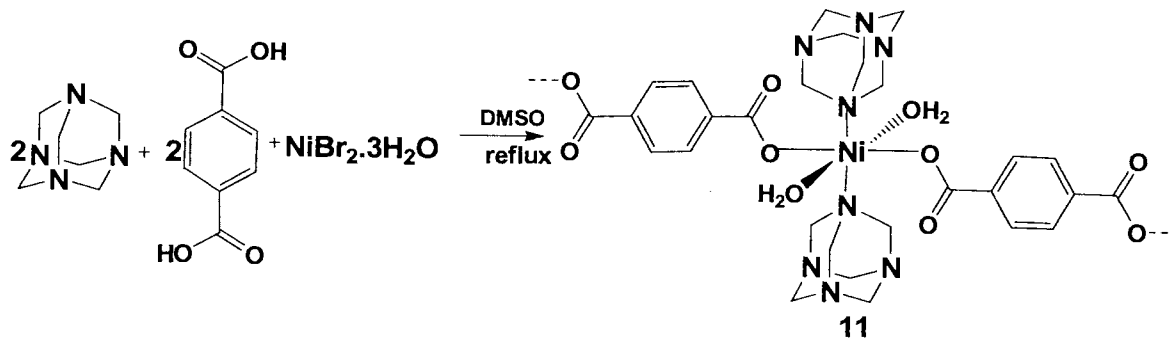


**Figure 32.** Projection of the unit cell contents of **10** showing of the molecular strands, H atoms and other atoms have been omitted for clarity. H bonds are shown by dotted line.

## Section 5: Metal Organic Frameworks of HMTA

### 5.1.1. Bis( $\mu_2$ -terephthalato)-(hexamethylenetetramino)-diaqua-dinickel(II) dihydrate



### 5.1.2. Crystal growth, selection, and mounting

Crystals of catena-[bis( $\mu_2$ -terephthalato)-(hexamethylenetetramino)-diaqua-dinickel (II) dihydrate] (11) were prepared by dissolution of hexamethylenetetramine (0.25 g, 1.79 mmoles), nickel (II) bromide trihydrate (0.081 g, 0.273 mmoles), and terephthalic acid (0.25 g, 1.506 mmoles) in 15 mL DMSO. The mixture was heated at 60°C for thirty minutes with continuous stirring in a roundbottom flask until all solids dissolved. The clear green solution was filtered and allowed to crystallize at room temperature by slow evaporation. Green transparent crystals were harvested after two weeks with rod morphology. Crystal quality was assessed by polarized light microscopy and they exhibited a mp > 523K; IR (nujol): 3444.48 (OH), 1557.06 (C=O), 1228.41, 1250 (C-O) (C=C), 1000.06 (C-N)  $\text{cm}^{-1}$ . X-ray diffraction data were collected at 208K.

Intensity data collection, data reduction, structure solution and refinement processes were performed as described previously for compound **6** (Sections 4.1.3 - 4.1.5) with details of the data collection and structure determination procedure, atomic coordinates, atomic displacements parameters, bond geometries and hydrogen bond parameters summarized in Tables 40–46.

### **5.1.3. Crystal structure assessment**

The asymmetric unit of **11** consists of a nickel atom, HMTA, one coordinated water, two DMSO molecules and a half part of the terephthalate. The Ni atom is positioned on a crystallographic inversion center (Figure 33). These components assemble to generate a distorted octahedron around the nickel atom. The nickel atoms are connected by the bidentate terephthalate moieties, while as HMTA molecules are stabilized by weak HMTA···HMTA interactions generating a 2-D network (Figure 34). A further view of this network along the *c*-axis reveals that adjacent molecular sheets are connected to each other via a series of O-H···O bonds involving coordinated water and DMSO molecules (Figure 35). Additional DMSO···DMSO (C-H···O) contacts exist and provide further crystal stabilization (Figure 35).



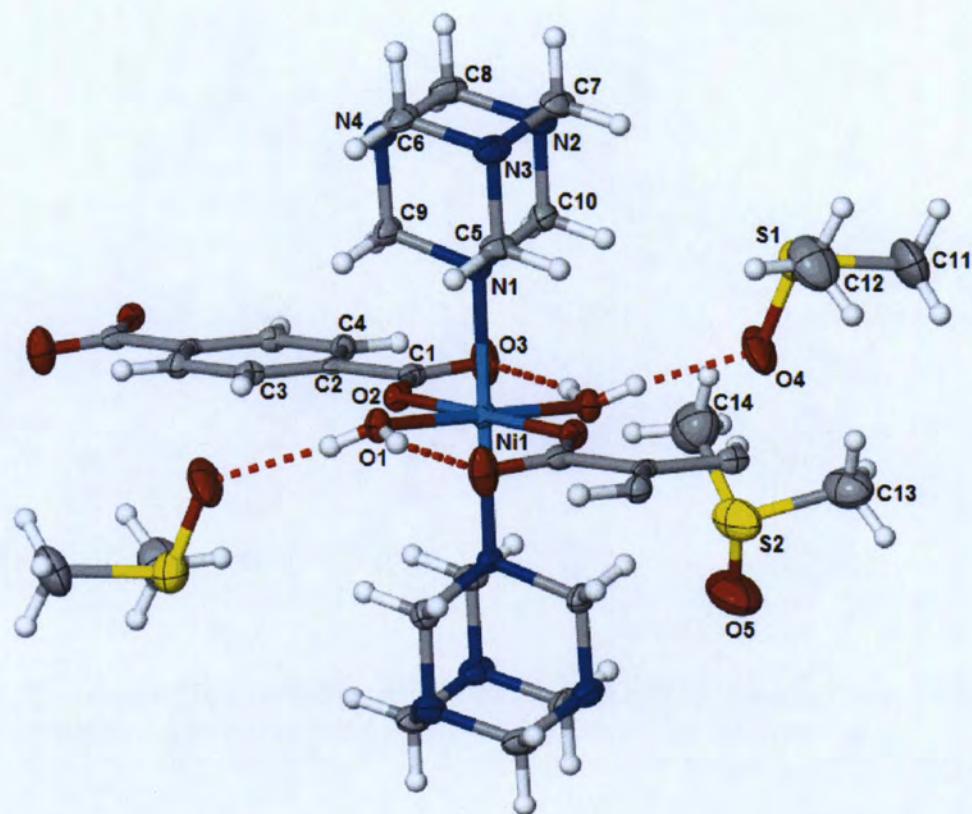


**Figure 33.** The structure of the component molecules of **11** showing the atom labeling scheme and the displacement ellipsoids at the 50% probability level.

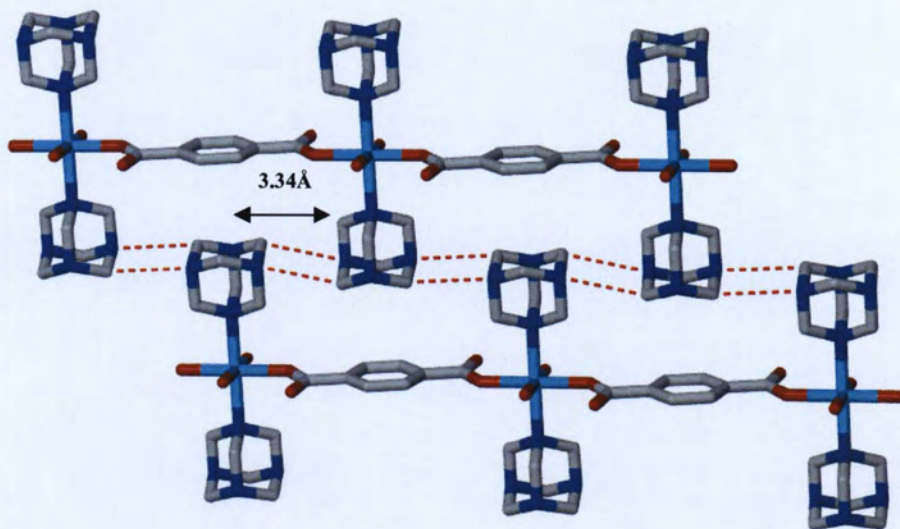


**Figure 34.** View of the packing pattern of **11** showing the propagation of HMTA... HMTA interactions along the *c*-axis.

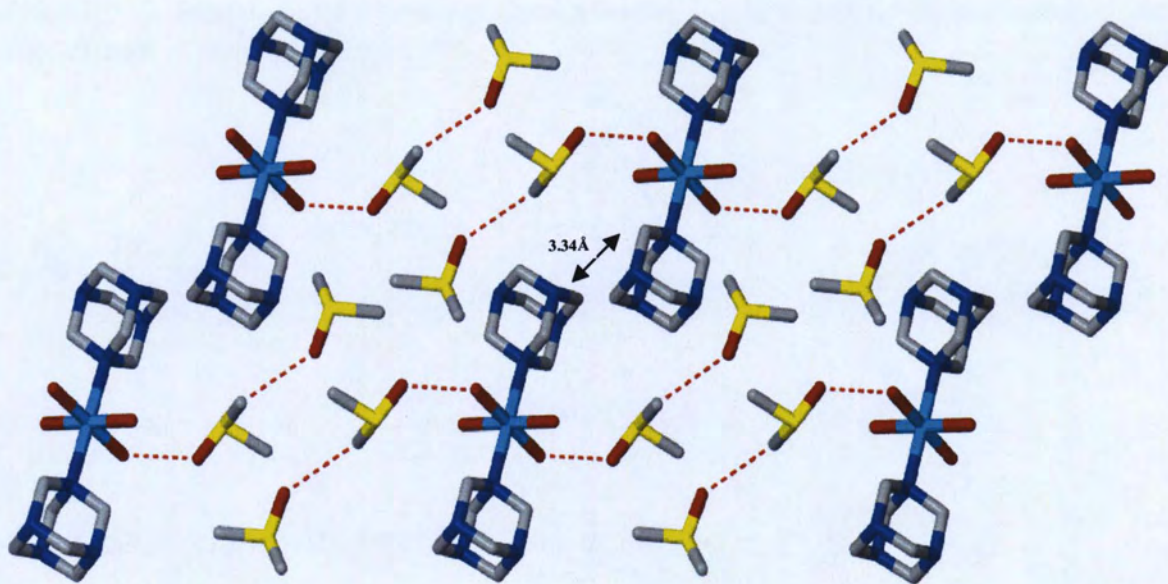
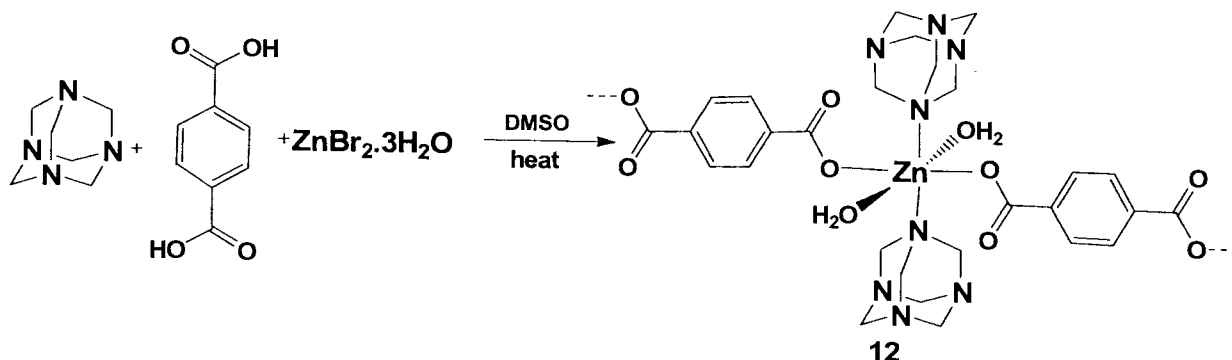


**Figure 35.** View of the packing pattern of **11** showing catemeric O-H...O and C-H...O interactions looking down the *a* axis are shown as dashed lines.

### 5.2.1. Bis( $\mu_2$ -terephthalato)-(hexamethylenetetramino)diaqua-zinc (ii) dihydrate



### 5.2.2. Crystal growth, selection, and mounting

Preparation of [bis( $\mu_2$ -terephthalato)-(hexamethylenetetramino)-diaqua-zinc (II) dihydrate] crystals (12) was prepared by dissolution of hexamethylenetetramine (0.25 g, 1.8 mmoles), zinc (II) bromide trihydrate (0.34 g, 1.23 mmoles) and terephthalic acid (0.25 g, 1.301 mmoles) in 15 mL DMSO. The mixture was heated at 60°C for thirty minutes with continuous stirring in a round bottom flask until all the solids dissolved. A clear homogenous solution was formed which was filtered and allowed to crystallize by slow evaporation at room temperature. Colorless crystals with rod morphology were harvested after three weeks. Crystal quality was assessed by polarized light microscopy and exhibited the following analytical data: mp > 523K; IR (nujol): 2879.95 (*broad*, OH), 1547.66 (C=O), 1239.9 (C-O), 1025.9 (C-N) $\text{cm}^{-1}$ .

Intensity data collection, data reduction, structure solution and refinement processes were performed as described previously for compound 6



(Sections 4.1.3 - 4.1.5) with details of the data collection and structure determination procedure, atomic coordinates, atomic displacements parameters, bond geometries and hydrogen bond parameters summarized in Tables 47–53.

### **5.2.3. Crystal structure assessment**

The asymmetric unit of **12** contains two Zn atoms, one and a half terephthalate, one HMTA, two coordinated water, and two uncoordinated water molecules. Zn2 and one of the terephthalate anions are positioned on an inversion center and uncoordinated water molecule O10 is positioned on a mirror plane (Figure 36). The two Zn atoms exist in different coordination environments with Zn1 being trigonal bipyramidal with two HMTA, two terephthalate groups, and a coordinated water molecule, and Zn2 octahedrally coordinated with two HMTA, two terephthalate, and two coordinated water molecules. The Zn atoms are connected by Zn-N bonds with bridging HMTA molecules to give an undulating pattern. This is further joined to bidentate terephthalate groups (Figure 37). Further inspection of Figure 37 reveals weak water-water interactions that participates in O-H...O hydrogen bonds with these undulating patterns. These hydrogen bonds, along with HMTA-HMTA contacts, assemble adjacent coordination polymer motifs to give 3-D networks (Figures 38 and 39).

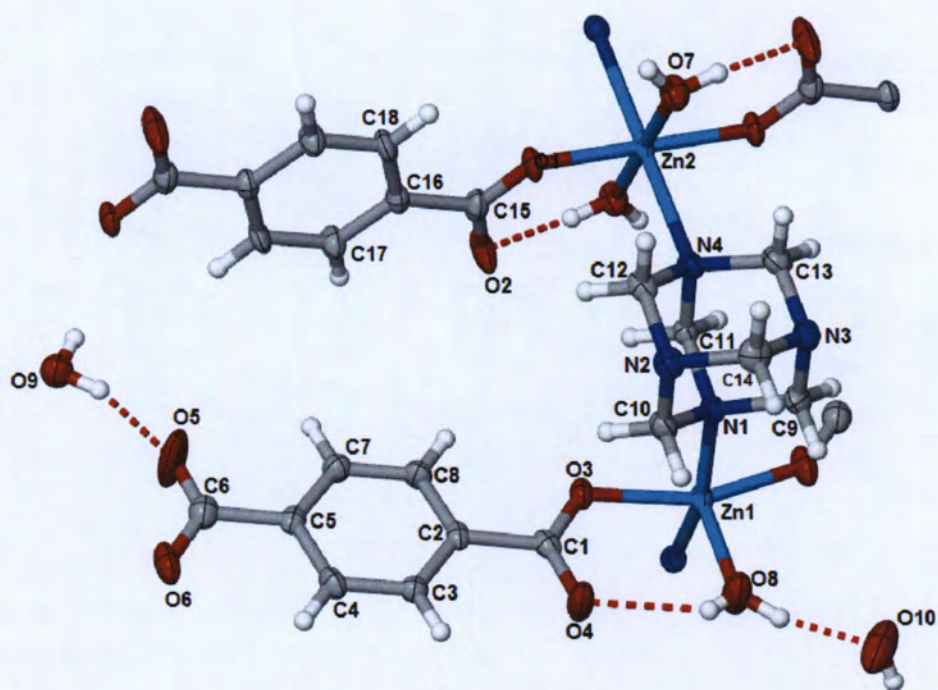


**Figure 36.** The structure of the component molecules of **12** showing the atom labeling scheme, and displacement ellipsoids at the 50% probability level.

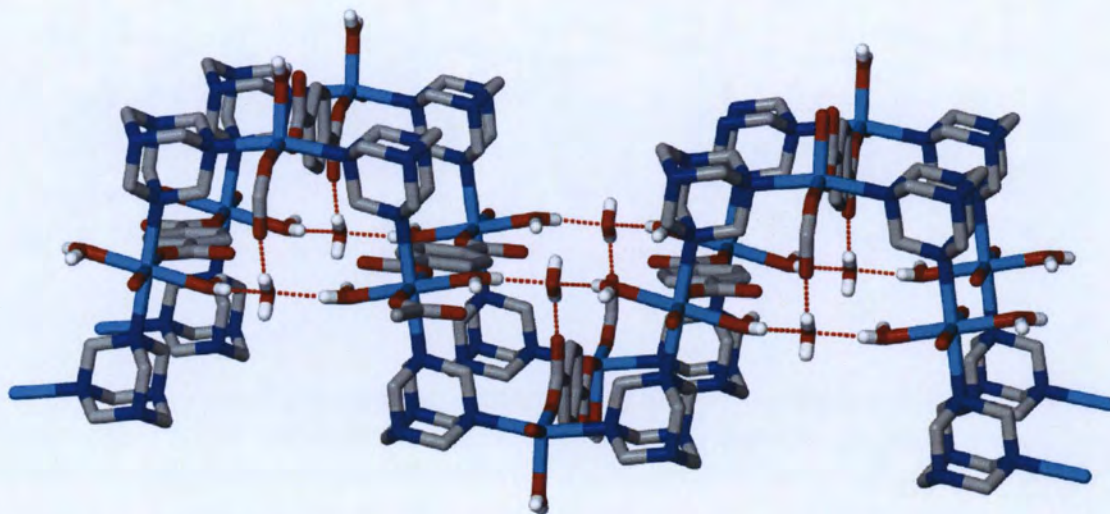


**Figure 37.** View of the packing pattern of **12** looking down the *c*-axis showing the Zn coordination environment and weak catemeric water-terephthalate and water-water (O-H...O) interactions.



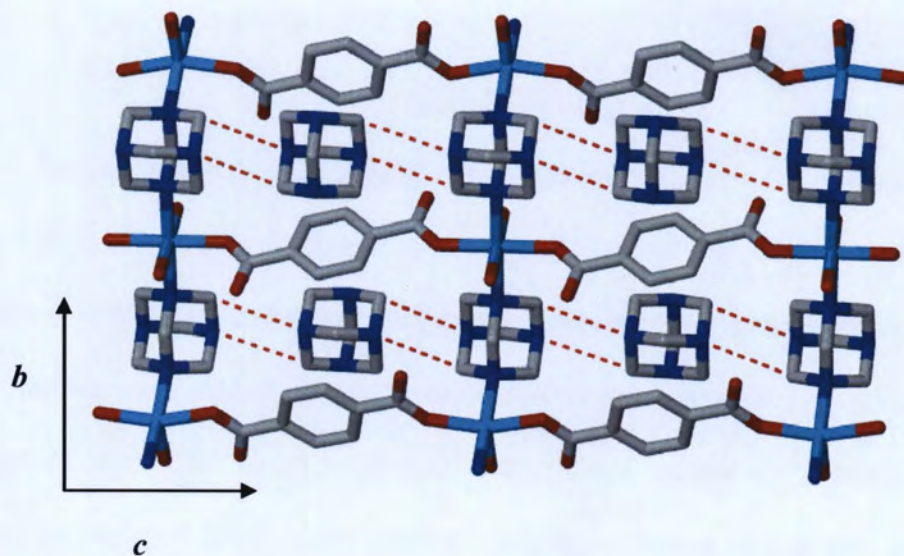


**Figure 38.** View of the packing pattern of **12** showing catemeric C-H...N interactions as dashed lines looking down the *a*-axis.

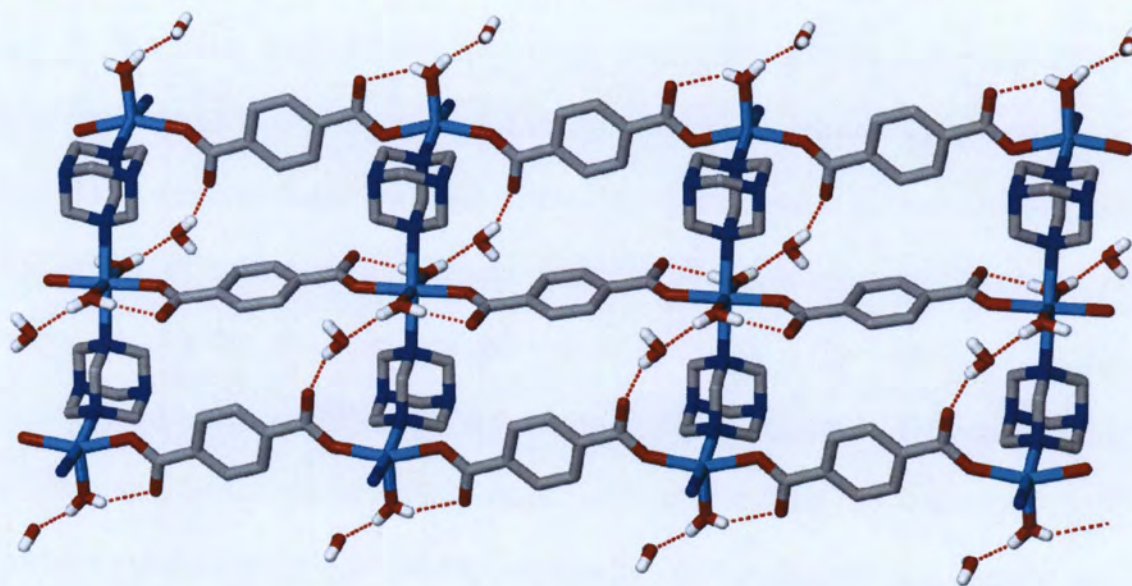


**Figure 39.** View of the packing pattern of **12** showing catemeric water-terephthalate and water-water (O-H...O) interactions in the *ab* plane. Intermolecular interactions are shown as dashed lines.

## CONCLUSION

To investigate the supramolecular behavior of HMTA, seven diverse compounds that possess the common chemical feature of HMTA were prepared. Of these, four were purely organic-based, one was a hexamethylenetetraminium salt, and two consisted of metal-coordinated frameworks. An inspection of the crystal structure of each of these compounds revealed a wide sampling of molecular associations and crystal motifs. These structural patterns were compared to the trends observed from studies of the Cambridge Structural Database (CSD) and molecular modeling calculations of HMTA.

The four HMTA organic-based cocrystalline materials consisted of components with either carboxylic acid or alcoholic proton donor groups. As expected, each of these systems readily cocrystalize due to the complementary interaction of the lone pair of electrons on the HMTA N atom and OH (alcohol or carboxyl moiety) group of the second component. This mode of molecular association agreed with our search of the CSD for neutral HMTA multimolecular structures. Of the 42 structures retrieved from the CSD, 26 consisted of either alcohol or carboxyl containing components. Although the small set of compounds prepared and structures determined in this thesis preclude us from formulating specific criteria for predicting the organization of HMTA structures, the ease with which these cocrystals form clearly demonstrate and complement the high population of alcohol and carboxyl containing components we observed in the CSD search. One logical approach to constructing predictable HMTA

molecular assemblies is to use strong hydrogen bond donors such as carboxylic acids. This tactic has been applied by us and others and often leads to an acid/base reaction to form a molecular salt or possibly the degradation of HMTA to produce ammonia and formaldehyde<sup>66</sup>. Although structures of the former (i.e., hexamethyleaminium cations) are not plentiful in the literature, the coordination behavior of the HMTA<sup>+</sup>-H does not exceed two. In comparison, weaker cocrystalizing agents such as alcohols form a wide range of connections to HTMA (0-4), suggesting that strong hydrogen bond donors adversely affect the coordination ability of HTMA.

Surprisingly, despite amines and amides being relatively strong proton donors, our search of the CSD retrieved very few structures that contain either of these species. Further assessment of our four organic cocrystalline systems indicate the predominance of mono- and dicoordinated HMTA. This observation parallels our CSD study that showed most structures tend to only form one or two contacts to HMTA. This lack of coordination behavior of HMTA led us to study this phenomena using *ab initio* calculations. Data gleaned from electrostatic potential calculations supported the trends observed from our studies and CSD searches and suggested a cooperative through-space electronic affect of the HMTA N atoms. It is proposed that the formation of hydrogen bonds displace the electron density of the HMTA N lone pair. The back lobe of the  $sp^3$  N orbital likely becomes more electrophilic, that in turn, affects the electronic character of nearby N atoms of HMTA via an intramolecular through space interaction. This phenomenon drastically reduces the hydrogen bond ability of the uncoordinated



N atoms. This idea of a cooperative electronic effect was supported by our crystallographic and CSD studies that showed increasing the strength of hydrogen bonds results in fewer connections to HMTA (Figure 9).

Extending our CSD studies to include HMTA<sup>+</sup>-H salts reinforced the notion that HMTA participates in an anomeric effect as explained above. The addition of a proton to HMTA reduces the electron density on the back *sp*<sup>3</sup> lobe of the corresponding nitrogen atom. This in turn decreases the electron density of the other three nitrogen HTMA atoms and thus reducing the donor ability of these groups. A CSD search for HMTA<sup>+</sup>-H revealed 17 such crystal structures with none exhibiting tri- or tetracoordination. The protonation of HMTA to give an ammonium cation produces a drastic shift of electron density. Several indications of this is the elongation of the C-N HMTA bonds as shown in the structure of **8** and the lack of reported tri- and tetracoordinated HMTA<sup>+</sup>-H salts (Table 3).

We then shifted our attention to the study of crystal structures of metal organic frameworks (MOFs). Two HMTA materials consisting of either zinc or nickel centers were synthesized, crystal structures determined, and structural trends assessed. Although these structures possessed many similar chemical features the crystal structures showed markedly different patterns in coordination environment and molecular packing. This diversity of MOFs generated was also observed in the CSD where we uncovered 92 structures with varying packing patterns. Another notable feature of metal-containing HTMA structures was the existence of weak HMTA⋯HMTA interactions that provided additional crystal stabilization.

Although the versatility of HMTA as a supramolecular building-block has been demonstrated through the synthesis and crystal chemistry of seven samples, motif prediction remains a difficult task that requires further study. The underlying reason for this lack of crystal engineering is due to an incomplete list of all known molecular contacts that contribute to crystal packing. One of the goals of this thesis was to exploit the favorable structural features of HTMA for the construction of 3D supramolecular networks. Although we were successful at synthesizing a tetracoordinated HTMA hydrogen bonded complex, the overall objective of molecular assemblies with tetracoordinated HMTAs is still in its infancy. Some structures suggest that generation of such frameworks is possible especially when moderately strong proton donor moieties like alcohols are used. This is counterintuitive to current practices in the field that seek to develop new molecular associations and motifs based on strong intermolecular interactions. This approach proved ineffective in our pursuit to generate highly ordered HMTA motifs.

Apart from the reasons outlined above, the incompatibility of component solubility's can serve as a significant limiting factor in the generation of HTMA complexes or salts. Although designing components with complementary features for specific supramolecular interactions is the first step in the generation of predictable motifs, studies of cocrystalline systems are often fraught with problems owing to the difference in physical properties of the components. Solvent-free crystallization methods seem like a logical answer to this problem;

however, the list available solvent-free procedures tend to be complicated and somewhat unreliable.

The ultimate goal of crystal engineering practitioners centers on full prediction of crystal structures starting with only the knowledge of chemical connectivity and composition. Though the development of this Holy Grail has been a long standing objective, recent advances in the field continue to make steady progress towards this goal. In many instances, progress has only been realized by small incremental successes that when viewed as isolated discoveries seem insignificant. The collection of such findings though provide significant impact on this area of science and thus the contributions presented in this thesis will hopefully add to the already growing body of data towards structure prediction. Discoveries in this field continue to make real-life connections with applications in such areas as catalysis,<sup>94</sup> gas storage,<sup>95-97</sup> host guest chemistry,<sup>98</sup> and nanotechnology<sup>99</sup>

---

## REFERENCES

1. Desiraju, G. R. *Current Science*, **2001**, *81*, 1038-1042.
2. Lehn, J. M. *Supramolecular Chemistry Concepts and Perspectives*. VCH: New York, 1995.
3. Atwood, J. L.; Steed, J. W. *Encyclopedia of Supramolecular Chemistry*, Marcel Dekker: New York, 2004, vols. 1-2.
4. Schneider, H-J.; Ystsimirski, A. K. *Principles and Methods in Supramolecular Chemistry*, Wiley; New York, 2000.
5. Subramania, S.; Zaworotko, M. J. *Coord. Chem. Rev.* **1994**, *137*, 357-401.
6. Mizushima, S.; Shimanouchi, T.; Tsuboi, M.; Souda, R. *J. Am. Chem. Soc.* **1952**, *74*, 270-271.
7. Tanaka, N.; Kitano, H.; Ise, N. *Macromolecules*, **1991**, *24*, 3017-3019.
8. Taylor, R.; Kennard, O. *J. Am. Chem. Soc.* **1982**, *104*, 5063-5070.
9. Latimer, W. M.; Rodebush, W. H. *J. Am. Chem. Soc.* **1920**, *42*, 1419-1433.
10. Pauling, L. *The Nature of the Chemical and the Structure of Molecules and Crystals. An Introduction to Modern Structural Chemistry*, 2<sup>nd</sup> ed.; University Press: London, 1940.
11. Huyskens, P. L.; Luck, W. A. P. In *Intermolecular Forces- An Introduction to Modern Methods and Results*; Zeegers-Huyskens, T. Ed.; Springer-Verlag: Berlin, 1991.
12. Pimentel, G. C.; McClellan, A. L. *The Hydrogen Bond*, Freeman: San Francisco, 1960.
13. Atkins, W. P. *General Chemistry; Scientific American Book*, New York, 1989.
14. Etter, M. C. *Acc. Chem. Res.* **1990**, *23*, 120-126.
15. Aakeroy, C. B.; Seddon, K. R. *Chem. Soc. Rev.* **1993**, 397-407.
16. Kawase, T.; Kurata, H. *Chem. Rev.* **2006**, *106*, 5250-5273.
17. Hunter, C. A.; Sanders, J. K. M. *J. Am. Chem. Soc.* **1990**, *112*, 5525-5534.
18. Burley, S. K.; Petsko, G. A., *Adv. Protein Chem.* **1988**, *39*, 125-192.

- 
19. Saenger, W. *Principles of Nucleic Acid Structures*; Springer-Verlag: New York, 1984; pp. 132-140.
  20. Sokolov, A. N.; Frisciv, T.; Blais, S.; Ripmeester, J. A.; MacGillivray, L. R. *Cryst. Growth Des.* **2006**, *6*, 2427-2428.
  21. Sygula, A.; Fronczek, F. R.; Sygula, R.; Rabideau, P. W. *J. Am. Chem. Soc.* **2007**, *129*, 3842-3843.
  22. G. M. J. Schmidt *Pure Appl. Chem.* **1971**, *27*, 647-678.
  23. (a) Jagarlapudi, S. P. R. A.; Desiraju, G. R. *Chem. Phys. Lett.* **1985**, *117*, 160-164. (b) Desiraju, G. R. *Angew. Chem.* **1995**, *34*, 2311-2327. (c) Nangia, A.; Desiraju, G. R. *Top. Curr. Chem.* **1998**, *198*, 57-95.
  24. Price, S. L.; Stone, A. J.; Lucas, J.; Rowland, R. S.; Thornley, A. E. *J. Am. Chem. Soc.* **1994**, *116*, 4910-4918.
  25. Bosch, E.; Barnes, C. L. *Cryst. Growth. Des.* **2002**, *2*, 299-302.
  26. Chopra, D.; Cameron, T. S.; Ferrara, J. D.; Guru Row, T. N. *J. Phys. Chem. A* **2006**, *110*, 10465-10477.
  27. Matsumoto, A.; Tanaka, T.; Tsubouchi, T.; Tashiro, K.; Saragai, S.; Nakamoto, S. *J. Am. Chem. Soc.* **2002**, *124*, 8891-8902.
  28. Zaman, M. B.; Udachin, K. A.; Ripmeester, J. A. *Cryst. Growth. Des.* **2004**, *4*, 585-589.
  29. Kumar, K. D.; Ballabh, A.; Jose, D. A.; Dastdar, P.; Das, A. *Cryst. Growth Des.* **2005**, *5*, 651-660.
  30. Thalladi, V. R.; Weiss, H-C.; Blaser, D.; Boese, R.; Nangia, A.; Desiraju, G. *J. Am. Chem. Soc.* **1998**, *120*, 8702-8710.
  31. Brammer, L.; Bruton, E. A.; Sherwood, P. *Cryst. Growth, Des.* **2001**, *1*, 277-290.
  32. Buckton, K. S.; Azrak, R. G. *J. Chem. Phys.* **1970**, *52*, 5652-5655.
  33. Griffith, R. G.; Roberts, J. D. *Tetrahedron Lett.* **1974**, *15*, 3499-3502.
  34. Hobza, P.; Mulder, F.; Sandorfy, C. *J. Am. Chem. Soc.* **1981**, *103*, 1360-1366.

- 
35. Curtis, L. A.; Frurip, D. J.; Blander, M. J. *J. Am. Chem. Soc.* **1978**, *100*, 79-86.
  36. Moorthy, N. J.; Venkatakrishnan, P.; Singh, A. S. *J. CrystEngComm.* **2003**, *5*, 507-513.
  37. Desiraju, G. R.; Steiner, T. *The Weak Hydrogen Bond in Structural Chemistry and Biology*, Oxford University Press: Oxford, 1999.
  38. Malone, J. F.; Murray, C. M.; Charlton, M. H.; Docherty, R.; Lavery, A. J. *J. Chem. Soc. Faraday Trans.* **1997**, *93*, 3429-3436.
  39. Chowdhury, S. K.; Joshi, V. S.; Puranik, V. G.; Samuel, G. A.; Tavale, S. S.; Sarkar, A. *Organometallics*, **1994**, *13*, 4092-4096.
  40. Munshi, P.; Guru Row, T. N. *J. Phys. Chem. A*, **2005**, *109*, 659-672.
  41. Vögtle, F. *Supramolecular Chemistry: An Introduction*. John Wiley and Sons: New York, 2000; pp. 291-336.
  42. Kawahata, M.; Yamaguchi, K.; Ishikawa, T.; *Cryst. Growth Des.* **2005**, *5*, 373-377.
  43. MacDonald, J. C.; Whitesides, G. M. *Chem. Rev.* **1994**, *94*, 2383-2420.
  44. Etter, M. C.; Bernstein, J.; MacDonald, J. C. *J. Chem. Soc. Perkin Trans. 2.* **1990**, 695-698.
  45. See, R. F.; Kruse, R. A.; Strub, W. M. *Inorg. Chem.* **1998**, *37*, 5369-537.
  46. MacDonald, J. C.; Dorrestein, P. C.; Pilley, M. M.; Foote, M. M.; Lundburg, J. L.; Henning, R. W.; Schultz, A. J.; Manson, J. L. *J. Am. Chem. Soc.* **2000**, *122*, 11692-11702.
  47. G. M. J. Schmidt, in *Solid-State Photochemistry*, ed. D. Ginsburg, VCH, Weinheim, 1976, p. 2ff.
  48. Ermer, O. *J. Am. Chem. Soc.* **1988**, *110*, 3747-3754.
  49. Desiraju, G. R. *The Design of Organic Solids*, Elsevier: Amsterdam, 1989.
  50. Albrecht, M.; Lutz, M.; Spek, A. L.; Van Koten, G. *Nature*, **2000**, *406*, 970-973.
  51. Shimizu, L. S.; Hughes, A. D.; Smith, M. D.; Davis, M. J.; Zhang, P. B.; zur Loye, H-C.; Shimizu, K. D. *J. Am. Chem. Soc.* **2003**, *125*, 14972-14973.



- 
52. Ranganathan, D.; Lakshmi, C.; Haridas, V.; Gopikumar, M. *Pure App. Chem.* **2000**, 365-272.
53. (a) Desiraju, G. R. *Science* **1997**, 278, 404-405. (b) Bernstein, J. *Polymorphism in Molecular Crystals*, Clarendon: Oxford, 2002, pp. 151-187.
54. Tiekink, E. R. T.; Vittal, J. J. *Frontiers in Crystal Engineering*, John Wiley & Sons Ltd: 2006, p. 28.
55. Munakata, M.; Yamamoto, M.; Wu, L. P.; Kuroda-Sowa, T.; Maekawa, M. *J. Am. Chem. Soc.* **1996**, 118, 3117-3124.
56. Burrows, A. D.; Chan, C-W.; Chowdry, M. M.; McGrady, J. E.; Mingos, M. D. *P. Chem. Soc. Rev.* **1995**, 329-339.
57. Beatty, A. M.; Helfrich, B. A.; Hogan, G. A.; Reed, B. A. *Cryst. Growth Des.* **2006**, 6, 122-126.
58. Thylen, L.; Qiu, M.; Anand, S. *ChemPhysChem.* **2004**, 5, 1268-1283.
59. Batten, S. R.; Murray, K. S. *Coord. Chem. Rev.* **2003**, 246, 103-130.
60. Shin, D. M.; Lee, I. S.; Chung, Y. K. *Eur. J. Inorg. Chem.* **2003**, 2311-2317.
61. Smolin, E. M.; Rapoport, L. *The Chemistry of Heterocyclic Compounds Triazines*, Interscience: New York, 1959, p. 545.
62. Dickinson, R. G.; Raymond, A. L. *J. Am. Chem. Soc.* **1923**, 45, 22-29.
63. Duff, J. C. *J. Chem. Soc.* **1945**, 276-277.
64. Kawamata, S.; Kodera, H. *Anatomical Science International.* **2004**, 79, 152-157.
65. Higashino, N. *Formaldehyde*, Encyclopedia Chemica, Kyoritsu Shuppan: Tokyo, 1961, vol. 8, pp. 804-805.
66. Haas, P. A.; Pitt, W. W.; Robinson, S. M. Jr.; Ryon, A. D. *Ind. Eng. Chem. Prod. Res. Dev.* **1983**, 22, 461-466.
67. Gardon, M.; Schonleber, A.; Chapuls, G.; Hostettler, M.; Bonin, M. *Acta Crystallogr.* **2001**, C57, 936-938.
68. Ghosh, K.; Datta, M.; Frohlich, R.; Ganguly, N. C. *J. Mol. Struct.* **2005**, 737, 201-206.

- 
69. Vishweshwar, P.; Thaimattam, R.; Jaskolski, M.; Desiraju, G. R. *Chem. Comm.* **2002**, 1830-1831.
70. Bowes, K. F.; Ferguson, G.; Lough, A. J.; Glidewell, C. *Acta Crystallogr.* **2003**, B59, 100-117.
71. Fun, H-K.; Usman, A.; Chantrapromma, S.; Osman, J.; Ong, L-H.; Tilley, D. R.; Ishibashi, Y. *Solid State Comm.*, **2003**, 127, 677-682.
72. Yu, P-Y.; Mak, T. C. W. *Acta Crystallogr.* **1978**, B34, 3053-3056.
73. Trotter, J.; Mak, T. C. W. *Acta Crystallogr.* **1979**, B35, 2367-2369.
74. Walsh, R. B.; Padgett, C. W.; Metrangolo, P.; Reanatl, G.; Hanks, T. W.; Pennington, W. T. *Cryst. Growth Des.* **2001**, 1, 165-175.
75. Banerjee, S.; Drew, M. G. B.; Ghosh, A. *Polyhedron*, **2003**, 22, 2933-2941.
76. Zheng, S-L.; Tong, M-L.; Fu, R-W.; Chen, X-M.; Ng, S-W. *Inorg. Chem.* **2001**, 40, 3562-3569.
77. Berkovitch-Yellin, Z.; Leiserowitz, L. *Acta Crystallogr.* **1984**, B40, 159-165.
78. Bowen, R.J.; Fernandes, M. A.; Gitari, P. W.; Layh, M. *Acta Crystallogr.* **2004**, C60, 258-260.
79. Allen, F.H. *Acta Crystallogr.* **2002**, B58, 380-388
80. Johnston, A.; Florence, A. J.; Shankland, N.; Kennedy, A. R.; Shankland, K.; Price, S. L. *Cryst. Growth Des.* **2007**, 7, 705-712.
81. Hurley, L. A.; Jones, A. G.; Hammond, R. B. *Cryst. Growth Des.* **2004**, 4, 711-715.
82. Hammond, R. B.; Pencheva, K.; Roberts, K. J. *Cryst. Growth Des.* **2007**, 7, 875-884.
83. Li, T.; Liu, S.; Feng, S.; Aubrey, C. E. *J. Am. Chem. Soc.* **2005**, 127, 1364-1365.
84. *Spartan04*, Wave function, Inc., Irvine, CA.
85. Dado, G. P.; Gellman, S. H. *J. Am. Chem. Soc.* **1992**, 114, 3138-3139.
86. Càrdenas-Jirón, G. I.; Masunov, A.; Dannenberg, J. J. *J. Phy. Chem. A.* **1999**, 103, 7042-7046.

- 
87. Alder, R. W.; Carniero, T. M. G.; Mowlam, R. W.; Orpen, G. A.; Petillo, P. A.; Vachon, D. J.; Weisman, G. R.; White, J. M. *J. Chem. Soc. Perkin Trans. 2.* **1999**, 3, 589-599.
- 88 Daka, P.; Wheeler, K. A. *Acta. Crystallogr.* **2006**, E62, 5477-5479.
89. Cromer, D. T.; Waber, J. T. *Acta. Cryst.* **1965**, 18, 104-9.
90. Sheldrick, G. M. *SHELXTL DOS/Windows/Version 5.10* Bruker Analytical X-ray Instrumentation Inc Madison WI 1997.
91. Barbour, L. J. *J. Supramol. Chem.* **2001**, 1, 189-191.
92. Sheldrick, G. M. *SHELXL-97; Program for Refining of Crystal Structures*, University of Gottingen: Germany, 1997.
93. Woolfson M. M. *An Introduction to X-ray Crystallography*, Cambridge University Press: Cambridge, 1970, pp. 147-149.
94. Grimshaw, R. W. *The Chemistry and Physics of Clays and other Ceramic Materials*, 4<sup>th</sup> ed.; Wiley-Interscience: New York, 1971.
95. Rowsell, J. L. C.; Yaghi, O. M. *Angew. Chem. Int. Ed.* **2005**, 44, 4670-4679.
96. Millward, A. R.; Yaghi, O. M. *J. Am. Chem. Soc.* **2005**, 127, 17998-17999.
97. Nassimbeni, L. R. *Acc. Chem. Res.* **2003**, 36, 631-637.
98. Ohmori, O.; Kawano, M.; Fujita, M. *J. Am. Chem. Soc.* **2004**, 126, 16292-16293.
99. Gogotsi, Y. *Cryst. Growth. Des.* **2001**, 1, 179-181.

## APPENDIX

**Table 5.** Crystal data and structure refinement for bis(1,2-dihydroxybenzene) hexamethylenetetramine (6)

Formula weight	360.41 gmol <sup>-1</sup>
Temperature	298(2) K
Empirical formula	C <sub>18</sub> H <sub>24</sub> N <sub>4</sub> O <sub>4</sub>
Wavelength	0.71073 Å
Crystal system	Monoclinic
Space group	C2/c
Unit cell dimensions	$a = 23.794(2) \text{ \AA}$ $\alpha = 90^\circ$ $b = 6.8422(5) \text{ \AA}$ $\beta = 123.135(6)^\circ$ $c = 13.244(1) \text{ \AA}$ $\gamma = 90^\circ$
Volume	1805.5(3) Å <sup>3</sup>
Z	4
Density (calculated)	1.326 mg/m <sup>3</sup>
Absorption coefficient	0.095 mm <sup>-1</sup>
F(000)	768
Crystal size	0.41 x 0.41 x 0.20 mm <sup>3</sup>
Theta range for data collection	2.0 to 25.4°
Index ranges	$1 \leq h \leq 28, -1 \leq k \leq 8, -14 \leq l \leq 13$
Reflections collected	1921
Independent reflections	1626 [R(int) = 0.022]
Completeness to theta = 25.4	99.2 %
Absorption correction	None
Refinement method	Full-matrix least-squares on F <sup>2</sup>
Data / restraints / parameters	1626 / 0 / 127
Goodness-of-fit on F <sup>2</sup>	1.04
Final R indices [ >2sigma(I)]	R1 = 0.051, wR2 = 0.102
R indices (all data)	R1 = 0.094, wR2 = 0.119

**Table 6.** Atomic coordinates ( $\times 10^4$ ) and equivalent isotropic displacement parameters ( $\text{\AA}^2 \times 10^3$ ) for bis(1,2-dihydroxybenzene)hexamethylenetetramine. U (eq) is defined as one third of the trace of the orthogonalized U<sub>ij</sub> tensor.

	x	y	z	U(eq)
O(1)	890(1)	7382(3)	1361(2)	62(1)
O(2)	1133(1)	4389(3)	301(2)	64(1)
N(1)	457(1)	10108(3)	2332(2)	39(1)
N(2)	409(1)	12620(3)	3590(2)	39(1)
C(1)	1376(1)	6071(4)	2089(2)	41(1)
C(2)	1746(1)	6174(4)	3328(2)	47(1)
C(3)	2240(1)	4820(4)	4012(2)	56(1)
C(4)	2361(1)	3361(4)	3459(2)	61(1)
C(5)	1989(1)	3225(4)	2220(2)	56(1)

C(6)	1496(1)	4572(4)	1527(2)	43(1)
C(7)	845(1)	11372(4)	3404(2)	44(1)
C(8)	0	13817(5)	2500	41(1)
C(9)	-44(1)	11370(3)	3727(2)	42(1)
C(10)	8920(5)	2500	2500	45(1)

**Table 7.** Hydrogen coordinates ( $\times 10^4$ ) and isotropic displacement parameters ( $\text{\AA}^2 \times 10^3$ ) for bis(1,2-dihydroxybenzene) hexamethylenetetramine (**6**)

	x	y	z	U(eq)
H(2)	1662	7169	3707	56
H(3)	2489	4903	4849	67
H(4)	2696	2450	3919	74
H(5)	2072	2215	1849	67
H(7A)	1115	10560	4111	53
H(7B)	1146	12188	3309	53
H(8A)	-293	14652	2606	49
H(8B)	293	14652	2394	49
H(9A)	-335	12183	3849	50
H(9B)	219	10558	4437	50
H(10A)	-263	8085	1802	54
H(10B)	263	8085	3198	54
H(1O)	839(15)	8270(40)	1820(30)	86(10)
H(2O)	902(15)	5300(50)	-30(30)	77(11)

**Table 8.** Anisotropic displacement parameters ( $\text{\AA}^2 \times 10^3$ ) for bis(1,2-dihydroxybenzene) hexamethylenetetramine (**6**). The anisotropic displacement factor exponent takes the form:  $-2p^2 [h^2 a^{*2}U^{11} + \dots + 2hk a^* b^* U^{12}]$

	U <sup>11</sup>	U <sup>22</sup>	U <sup>33</sup>	U <sup>23</sup>	U <sup>13</sup>	U <sup>12</sup>
O(1)	70(1)	65(1)	41(1)	5(1)	24(1)	36(1)
O(2)	91(2)	55(1)	49(1)	8(1)	39(1)	32(1)
N(1)	42(1)	36(1)	40(1)	2(1)	23(1)	7(1)
N(2)	47(1)	34(1)	40(1)	-7(1)	27(1)	-10(1)
C(1)	39(1)	43(1)	46(1)	8(1)	26(1)	9(1)
C(2)	47(2)	50(2)	45(1)	1(1)	26(1)	1(1)
C(3)	44(2)	70(2)	46(2)	15(1)	21(1)	2(2)
C(4)	51(2)	71(2)	64(2)	32(2)	33(2)	23(2)
C(5)	68(2)	49(2)	70(2)	17(1)	50(2)	22(1)
C(6)	49(1)	46(2)	46(1)	10(1)	32(1)	10(1)
C(7)	38(1)	46(2)	44(1)	1(1)	20(1)	0(1)
C(8)	55(2)	28(2)	52(2)	0	36(2)	0
C(9)	54(1)	38(1)	39(1)	-3(1)	29(1)	-8(1)

C(10)	58(2)	24(2)	43(2)	0	21(2)	0
-------	-------	-------	-------	---	-------	---

**Table 9.** Bond lengths [Å] and angles [°] for bis(1,2-dihydroxybenzene) hexamethylenetetramine (**6**)

O(1)-C(1)	1.361(3)	O(1)-C(1)-C(6)	116.8(2)
O(1)-H(1O)	0.91(3)	C(2)-C(1)-C(6)	119.6(2)
O(2)-C(6)	1.365(3)	C(1)-C(2)-C(3)	120.6(3)
O(2)-H(2O)	0.79(3)	C(1)-C(2)-H(2)	119.7
N(1)-C(10)	1.470(3)	C(3)-C(2)-H(2)	119.7
N(1)-C(9)1	1.473(3)	C(4)-C(3)-C(2)	119.7(2)
N(1)-C(7)	1.478(3)	C(4)-C(3)-H(3)	120.1
N(2)-C(9)	1.462(3)	C(2)-C(3)-H(3)	120.1
N(2)-C(7)	1.464(3)	C(3)-C(4)-C(5)	120.3(2)
N(2)-C(8)	1.472(2)	C(3)-C(4)-H(4)	119.9
C(1)-C(2)	1.376(3)	C(5)-C(4)-H(4)	119.9
C(1)-C(6)	1.386(3)	C(6)-C(5)-C(4)	120.5(3)
C(2)-C(3)	1.376(3)	C(6)-C(5)-H(5)	119.7
C(2)-H(2)	0.9300	C(4)-C(5)-H(5)	119.7
C(3)-C(4)	1.360(4)	O(2)-C(6)-C(5)	119.1(2)
C(3)-H(3)	0.9300	O(2)-C(6)-C(1)	121.6(2)
C(4)-C(5)	1.377(4)	C(5)-C(6)-C(1)	119.3(2)
C(4)-H(4)	0.9300	N(2)-C(7)-N(1)	112.12(17)
C(5)-C(6)	1.375(3)	N(2)-C(7)-H(7A)	109.2
C(5)-H(5)	0.9300	N(1)-C(7)-H(7A)	109.2
C(7)-H(7A)	0.9700	N(2)-C(7)-H(7B)	109.2
C(7)-H(7B)	0.9700	N(1)-C(7)-H(7B)	109.2
C(8)-N(2)#1	1.472(2)	H(7A)-C(7)-H(7B)	107.9
C(8)-H(8A)	0.9700	N(2)#1-C(8)-N(2)	112.4(2)
C(8)-H(8B)	0.9700	N(2)#1-C(8)-H(8A)	109.1
C(9)-N(1)#1	1.473(3)	N(2)-C(8)-H(8A)	109.1
C(9)-H(9A)	0.9700	N(2)#1-C(8)-H(8B)	109.1
C(9)-H(9B)	0.9700	N(2)-C(8)-H(8B)	109.1
C(10)-N(1)#1	1.470(3)	H(8A)-C(8)-H(8B)	107.9
C(10)-H(10A)	0.9700	N(2)-C(9)-N(1)#1	112.35(7)
C(10)-H(10B)	0.9700	N(2)-C(9)-H(9A)	109.1
C(1)-O(1)-H(1O)	109.7(18)	N(1)#1-C(9)-H(9A)	109.1
C(6)-O(2)-H(2O)	112(2)	N(2)-C(9)-H(9B)	109.1
C(10)-N(1)-C(9)#1	107.64(16)	N(1)#1-C(9)-H(9B)	109.1
C(10)-N(1)-C(7)	107.58(16)	H(9A)-C(9)-H(9B)	107.9
C(9)#1-N(1)-C(7)	108.21(17)	N(1)#1-C(10)-N(1)	112.8(3)
C(9)-N(2)-C(7)	108.47(18)	N(1)#1-C(10)-H(10A)	109.0
C(9)-N(2)-C(8)	108.04(16)	N(1)-C(10)-H(10A)	109.0
C(7)-N(2)-C(8)	107.97(15)	N(1)#1-C(10)-H(10B)	109.0
O(1)-C(1)-C(2)	123.6(2)	N(1)-C(10)-H(10B)	109.0
		H(10A)-C(10)-H(10B)	107

Symmetry transformations used to generate equivalent atoms: #1 -x, y, -z+1/2



**Table 10.** Torsion angles [°] for bis(1,2-dihydroxybenzene) hexamethylenetetramine (6)

O(1)-C(1)-C(2)-C(3)	-178.7(2)
C(6)-C(1)-C(2)-C(3)	0.9(4)
C(1)-C(2)-C(3)-C(4)	-0.3(4)
C(2)-C(3)-C(4)-C(5)	-0.5(4)
C(3)-C(4)-C(5)-C(6)	0.6(4)
C(4)-C(5)-C(6)-O(2)	-179.5(2)
C(4)-C(5)-C(6)-C(1)	0.0(4)
O(1)-C(1)-C(6)-O(2)	-1.6(4)
C(2)-C(1)-C(6)-O(2)	178.8(2)
O(1)-C(1)-C(6)-C(5)	178.9(2)
C(2)-C(1)-C(6)-C(5)	-0.8(4)
C(9)-N(2)-C(7)-N(1)	58.6(2)
C(8)-N(2)-C(7)-N(1)	-58.2(2)
C(10)-N(1)-C(7)-N(2)	-58.0(2)
C(9)#1-N(1)-C(7)-N(2)	58.0(2)
C(9)-N(2)-C(8)-N(2)#1	-58.50(13)
C(7)-N(2)-C(8)-N(2)#1	58.63(13)
C(7)-N(2)-C(9)-N(1)#1	-58.7(2)
C(8)-N(2)-C(9)-N(1)#1	58.1(2)
C(9)#1-N(1)-C(10)-N(1)#1	-58.19(13)
C(7)-N(1)-C(10)-N(1)#1	58.22(13)

**Table 11.** Hydrogen bonds for bis(1,2-dihydroxybenzene) hexamethylenetetramine (6) [Å and °]

D-H...A	d(D-H)	d(H...A)	d(D...A)	<(DHA)
O(1)-H(1) ...N(1)	0.91(3)	1.89(3)	2.764(3)	162(3)
O(2)-H(2) ...O(1)	0.79(3)	2.34(3)	2.717(3)	111(2)
O(2)-H(2) ...N(2)#2	0.79(3)	2.10(3)	2.832(3)	155(3)

Symmetry transformations used to generate equivalent atoms:  
 #1 -x,y,-z+1/2 #2 x,-y+2,z-1/2

**Table 12.** Crystal data and structure refinement for bis(2-hydroxybenzylalcohol) hexamethylenetetramine, (7).

Empirical formula	C <sub>10</sub> H <sub>14</sub> N <sub>2</sub> O <sub>2</sub>
Formula weight	194.23 g.mol <sup>-1</sup>

Temperature	298(2) K	
Wavelength	0.71073 Å	
Crystal system	Orthorhombic	
Space group	<i>Pnma</i>	
Unit cell dimensions	$a = 12.6831(13)$ Å	$\alpha = 90.0^\circ$
	$b = 23.960(2)$ Å	$\beta = 90.0^\circ$
	$c = 6.5009(7)$ Å	$\gamma = 90.0^\circ$
Volume	1975.6(3) Å <sup>3</sup>	
Z	8	
Density (calculated)	1.306 mg/m <sup>3</sup>	
Absorption coefficient	0.092 mm <sup>-1</sup>	
F(000)	832	
Theta range for data collection	3.21 to 27.49°	
Index ranges	$-11 \leq h \leq 1, -31 \leq k \leq 1, -1 \leq l \leq 8$	
Reflections collected	2317	
Independent reflections	1708 [R(int) = 0.0255]	
Completeness to theta = 27.49°	73.3 %	
Absorption correction	None	
Refinement method	Full-matrix least-squares on $F^2$	
Data / restraints / parameters	1708 / 0 / 141	
Goodness-of-fit on $F^2$	1.062	
Final R indices [ $I > 2\sigma(I)$ ]	$R = 0.0518, wR2 = 0.0968$	
R indices (all data)	$R = 0.1089, wR2 = 0.1216$	
Largest diff. peak and hole	0.218 and -0.306 e.Å <sup>-3</sup>	

**Table 13.** Atomic coordinates ( $\times 10^4$ ) and equivalent isotropic displacement parameters ( $\text{Å}^2 \times 10^3$ ) for bis(2-hydroxybenzylalcohol) hexamethylenetetramine, (7).  $U(\text{eq})$  is defined as one third of the trace of the orthogonalized  $U_{ij}$  tensor.

	x	y	z	U(eq)
O(1)	9559(2)	3873(1)	10755(3)	39(1)
O(2)	6469(2)	3883(1)	12678(3)	39(1)
N(1)	10000(2)	3012(1)	8127(3)	31(1)
N(2)	11585(3)	2500	7080(5)	33(1)
N(3)	10021(3)	2500	4868(5)	37(1)
C(1)	8511(2)	3826(1)	11530(5)	36(1)
C(2)	7709(2)	4084(1)	10126(4)	25(1)
C(3)	6672(2)	4123(1)	10820(4)	25(1)
C(4)	5915(2)	4385(1)	9647(4)	32(1)
C(5)	6184(3)	4604(1)	7744(5)	36(1)
C(6)	7197(3)	4555(1)	7010(5)	36(1)
C(7)	7949(2)	4301(1)	8213(4)	31(1)
C(8)	9638(3)	2996(1)	5964(4)	38(1)

C(9)	9617(3)	2500	9137(6)	35(1)
C(10)	11163(2)	2992(1)	8128(5)	34(1)
C(11)	11178(4)	2500	4958(6)	41(1)

**Table 14.** Hydrogen coordinates ( $\times 10^4$ ) and isotropic displacement parameters ( $\text{\AA}^2 \times 10^3$ ) for bis(2-hydroxybenzylalcohol) hexamethylenetetramine, (7).

	x	y	z	U(eq)
H(1A)	8474	4007	12863	44
H(1B)	8343	3435	11723	44
H(1)	9630(30)	3594(14)	9800(50)	67(12)
H(2)	5770(30)	3918(17)	13070(60)	100(16)
H(4)	5227	4415	10128	38
H(5)	5676	4785	6958	43
H(6)	7371	4692	5716	43
H(7)	8637	4274	7725	37
H(8A)	8873	2998	5937	45
H(8B)	9883	3328	5259	45
H(9A)	8852	2500	9125	42
H(9B)	9845	2500	10561	42
H(10A)	11432	3325	7459	41
H(10B)	11412	2994	9538	41
H(11A)	11442	2827	4246	49
H(11B)	11442	2173	4246	49

**Table 15.** Anisotropic displacement parameters ( $\text{\AA}^2 \times 10^3$ ) for bis(2-hydroxybenzylalcohol) hexamethylenetetramine, (7). The anisotropic displacement factor exponent takes the form:  $-2p^2 [h^2 a^* U_{11} + \dots + 2hk a^* b^* U_{12}]$

	U <sub>11</sub>	U <sub>22</sub>	U <sub>33</sub>	U <sub>23</sub>	U <sub>13</sub>	U <sub>12</sub>
O(1)	20(1)	53(1)	46(1)	-21(1)	-2(1)	2(1)
O(2)	29(2)	57(1)	31(1)	8(1)	6(1)	2(1)
N(1)	26(2)	34(1)	32(1)	0(1)	3(1)	1(1)
N(2)	33(2)	29(2)	37(2)	0	7(2)	0
N(3)	47(3)	38(2)	27(2)	0	0(2)	0
C(1)	27(2)	45(2)	38(2)	-6(2)	1(2)	4(2)
C(2)	23(2)	27(1)	27(1)	-4(1)	-3(1)	0(1)
C(3)	25(2)	23(1)	26(1)	-2(1)	-1(1)	-2(1)

C(4)	24(2)	28(1)	43(2)	-3(1)	-1(2)	1(2)
C(5)	38(2)	29(2)	40(2)	4(1)	-14(2)	1(2)
C(6)	43(2)	34(2)	31(2)	4(1)	0(2)	-7(2)
C(7)	26(2)	35(2)	34(2)	-8(2)	5(2)	-3(2)
C(8)	42(2)	34(2)	37(2)	5(2)	-5(2)	1(2)
C(9)	28(3)	47(3)	29(2)	0	5(2)	0
C(10)	33(2)	29(2)	41(2)	-5(1)	3(2)	-1(2)
C(11)	51(4)	38(3)	33(2)	0	12(2)	0

**Table 16.** Bond lengths [Å] and angles [°] for bis(2-hydroxybenzylalcohol) hexamethylenetetramine, (7).

O(1)-C(1)	1.426(3)	C(3)-C(4)	1.378(4)
O(1)-H(1)	0.91(3)	C(4)-C(5)	1.386(4)
O(2)-C(3)	1.362(3)	C(4)-H(4)	0.9300
O(2)-H(2)	0.93(4)	C(5)-C(6)	1.375(4)
N(1)-C(9)	1.473(3)	C(5)-H(5)	0.9300
N(1)-C(10)	1.475(4)	C(6)-C(7)	1.376(4)
N(1)-C(8)	1.480(3)	C(6)-H(6)	0.9300
N(2)-C(10)#1	1.463(3)	C(7)-H(7)	0.9300
N(2)-C(10)	1.463(3)	C(8)-H(8A)	0.9700
N(2)-C(11)	1.472(5)	C(8)-H(8B)	0.9700
N(3)-C(8)	1.468(3)	C(9)-N(1)#1	1.473(3)
N(3)-C(8)#1	1.468(3)	C(9)-H(9A)	0.9700
N(3)-C(11)	1.468(6)	C(9)-H(9B)	0.9700
C(1)-C(2)	1.499(4)	C(10)-H(10A)	0.9700
C(1)-H(1A)	0.9700	C(10)-H(10B)	0.9700
C(1)-H(1B)	0.9700	C(11)-H(11A)	0.9700
C(2)-C(7)	1.382(4)	C(11)-H(11B)	0.9700
C(2)-C(3)	1.395(4)		
O(1)-C(1)-C(2)	112.6(2)	N(1)#1-C(9)-H(9B)	109.1
O(1)-C(1)-H(1A)	109.1	N(1)-C(10)-H(10A)	109.0
O(1)-C(1)-H(1B)	109.1	N(1)-C(10)-H(10B)	109.0
O(2)-C(3)-C(2)	115.9(2)	N(2)-C(10)-N(1)	113.0(2)
O(2)-C(3)-C(4)	123.5(3)	N(2)-C(10)-H(10A)	109.0
N(1)-C(8)-H(8A)	109.1	N(2)-C(10)-H(10B)	109.0
N(1)-C(8)-H(8B)	109.1	N(2)-C(11)-H(11A)	109.0
N(1)-C(9)-N(1)#1	112.6(3)	N(2)-C(11)-H(11B)	109.0
N(1)-C(9)-H(9A)	109.1		
N(1)#1-C(9)-H(9A)	109.1		
N(1)-C(9)-H(9B)	109.1		
N(3)-C(8)-N(1)	112.3(2)		
N(3)-C(8)-H(8A)	109.1		
N(3)-C(8)-H(8B)	109.1	N(3)-C(11)-H(11A)	109.0
N(3)-C(11)-N(2)	112.8(3)	N(3)-C(11)-H(11B)	109.0

C(1)-O(1)-H(1)	106(2)	C(5)-C(6)-C(7)	119.2(3)
C(2)-C(1)-H(1A)	109.1	C(5)-C(6)-H(6)	120.4
C(2)-C(7)-H(7)	119.2	C(6)-C(5)-H(5)	119.7
C(2)-C(1)-H(1B)	109.1	C(6)-C(5)-C(4)	120.5(3)
C(3)-O(2)-H(2)	113(2)	C(6)-C(5)-H(5)	119.7
C(3)-C(4)-C(5)	119.7(3)	C(6)-C(7)-C(2)	121.7(3)
C(3)-C(4)-H(4)	120.2	C(7)-C(2)-C(3)	118.3(3)
C(3)-C(2)-C(1)	118.1(2)	C(7)-C(6)-H(6)	120.4
C(4)-C(3)-C(2)	120.6(3)	C(8)-N(3)-C(8)#1	108.0(3)
C(4)-C(5)-H(5)	119.7	C(8)-N(3)-C(11)	108.2(2)
C(5)-C(4)-H(4)	120.2	C(8)#1-N(3)-C(11)	108.2(2)
C(9)-N(1)-C(8)	107.4(2)	H(8A)-C(8)-H(8B)	107.9
C(9)-N(1)-C(10)	107.7(3)	H(1A)-C(1)-H(1B)	107.8
C(10)#1-N(2)-C(10)	107.4(3)	H(9A)-C(9)-H(9B)	107.8
C(10)-N(1)-C(8)	108.1(2)	H(10A)-C(10)-H(10B)	107.8
C(10)#1-N(2)-C(11)	107.9(2)	H(11A)-C(11)-H(11B)	107.8

**Table 17.** Hydrogen bonds for bis(2-hydroxybenzylalcohol) hexamethylenetetramine, (7) [Å and °]

D-H...A	d(D-H)	d(H...A)	d(D...A)	<(DHA)
O (1)-H(1) ...N(1)	0.91(3)	1.83(4)	2.736(3)	170(3)
O (2)-H(2) ...O(1)#2	0.93(4)	1.71(4)	2.628(3)	166(4)

Symmetry transformations used to generate equivalent atoms:  
 #1  $x, -y+1/2, z$  #2  $x-1/2, y, -z+5/2$

**Table 18.** Torsion angles [°] for bis(2-hydroxybenzylalcohol) hexamethylenetetramine (7).

O(1)-C(1)-C(2)-C(7)	5.0(4)
O(1)-C(1)-C(2)-C(3)	-172.7(2)
O(2)-C(3)-C(4)-C(5)	-178.1(3)
C(1)-C(2)-C(7)-C(6)	-177.1(3)
C(1)-C(2)-C(3)-O(2)	-4.7(4)
C(1)-C(2)-C(3)-C(4)	176.1(2)
C(2)-C(3)-C(4)-C(5)	1.1(4)
C(3)-C(2)-C(7)-C(6)	0.6(4)
C(3)-C(4)-C(5)-C(6)	0.8(4)
C(4)-C(5)-C(6)-C(7)	-1.9(4)
C(5)-C(6)-C(7)-C(2)	1.2(4)
C(7)-C(2)-C(3)-O(2)	177.5(2)
C(7)-C(2)-C(3)-C(4)	-1.7(4)
C(8)-N(1)-C(9)-N(1)#1	58.7(4)
C(8)-N(1)-C(10)-N(2)	-57.4(3)
C(8)#1-N(3)-C(8)-N(1)	58.9(4)
C(8)-N(3)-C(11)-N(2)	58.4(2)
C(8)#1-N(3)-C(11)-N(2)	-58.4(2)
C(9)-N(1)-C(8)-N(3)	-58.6(3)
C(9)-N(1)-C(10)-N(2)	58.3(3)
C(10)-N(1)-C(9)-N(1)#1	-57.5(4)
C(10)-N(1)-C(8)-N(3)	57.4(3)
C(10)#1-N(2)-C(11)-N(3)	57.9(2)
C(10)#1-N(2)-C(10)-N(1)	-58.7(4)
C(10)-N(2)-C(11)-N(3)	-57.9(2)
C(11)-N(2)-C(10)-N(1)	57.5(3)
C(11)-N(3)-C(8)-N(1)	-57.9(3)

Symmetry transformations used to generate equivalent atoms:  
#1  $x, -y+1/2, z$

**Table 19.** Crystal data and structure refinement for hexamethylenetetramminium sulfate (8)

Empirical formula	$C_{12} H_{26} N_8 O_4 S$	
Formula weight	$378.47 \text{ g mol}^{-1}$	
Temperature	298(2) K	
Wavelength	0.71073 Å	
Crystal system	Monoclinic	
Space group	$P2_1/c$	
Unit cell dimensions	$a = 12.060(3) \text{ Å}$	$\alpha = 90^\circ$
	$b = 12.021(2) \text{ Å}$	$\beta = 108.727(11)^\circ$
	$c = 12.428(2) \text{ Å}$	$\gamma = 90^\circ$



Volume	1706.4(6) Å <sup>3</sup>
Z	4
Density (calculated)	1.473 mg/m <sup>3</sup>
Absorption coefficient	0.228 mm <sup>-1</sup>
F(000)	808
Crystal size	0.72 x 0.40 x 0.36 mm <sup>3</sup>
Theta range for data collection	2.42 to 27.49°
Index ranges	-1 ≤ h ≤ 7, -1 ≤ k ≤ 15, -16 ≤ l ≤ 15
Reflections collected	3168
Independent reflections	2364 [R(int) = 0.0136]
Completeness to theta = 27.49°	60.2 %
Max. and min. transmission	0.9224 and 0.8530
Refinement method	Full-matrix least-squares on F <sup>2</sup>
Data / restraints / parameters	2364 / 0 / 230
Goodness-of-fit on F <sup>2</sup>	1.008
Final R indices [ >2sigma(I)]	R1 = 0.0369, wR2 = 0.0895
R indices (all data)	R1 = 0.0524, wR2 = 0.0976
Largest diff. peak and hole	0.158 and -0.270 e.Å <sup>-3</sup>

**Table 20.** Atomic coordinates (x 10<sup>4</sup>) and equivalent isotropic displacement parameters (Å<sup>2</sup> x 10<sup>3</sup>) for Hexamethylenetetramminium sulfate (**8**). U(eq) is defined as one third of the trace of the orthogonalized U<sub>ij</sub> tensor.

	x	y	z	U(eq)
S(1)	2647(1)	6073(1)	343(1)	28(1)
O(1)	1328(2)	6019(1)	-74(1)	37(1)
O(2)	3060(2)	5741(1)	-632(1)	40(1)
O(3)	3101(2)	5302(2)	1299(1)	52(1)
O(4)	3018(2)	7222(1)	686(1)	44(1)
N(1)	377(2)	4776(2)	-1910(1)	31(1)
N(2)	-1420(2)	4162(1)	-3334(1)	30(1)
N(3)	12(2)	2786(2)	-2241(2)	32(1)
N(4)	478(2)	3958(2)	-3672(1)	32(1)
N(5)	4707(2)	7217(2)	-873(2)	30(1)
N(6)	5382(2)	9131(2)	-823(2)	33(1)
N(7)	6079(2)	7703(2)	-1868(2)	36(1)
N(8)	6721(2)	7667(2)	223(1)	32(1)
C(1)	980(3)	4804(2)	-2809(2)	35(1)
C(2)	-919(3)	5004(2)	-2471(2)	31(1)
C(3)	-803(3)	4175(2)	-4185(2)	35(1)
C(4)	-1252(3)	3047(2)	-2783(2)	33(1)
C(5)	609(3)	2850(2)	-3114(2)	36(1)

C(6)	522(3)	3622(2)	-1376(2)	37(1)
C(7)	5084(3)	7000(2)	-1910(2)	40(1)
C(8)	4376(3)	8449(2)	-864(2)	36(1)
C(9)	5731(3)	8885(2)	-1831(2)	41(1)
C(10)	6362(3)	8846(2)	215(2)	40(1)
C(11)	7049(3)	7454(2)	-813(2)	37(1)
C(12)	5732(3)	6963(2)	192(2)	34(1)

**Table 21.** Bond lengths [Å] and angles [°] for hexamethylenetetramminium sulfate (**8**).

S(1)-O(3)	1.4667(16)	N(5)-C(7)	1.520(3)
S(1)-O(4)	1.4727(16)	N(5)-C(12)	1.523(3)
S(1)-O(2)	1.5032(19)	N(5)-C(8)	1.534(3)
S(1)-O(1)	1.508(2)	N(5)-H(2)	0.92(3)
N(1)-C(1)	1.517(3)	N(6)-C(8)	1.452(3)
N(1)-C(2)	1.517(3)	N(6)-C(9)	1.474(3)
N(1)-C(6)	1.524(3)	N(6)-C(10)	1.483(3)
N(1)-H(1)	0.9100	N(7)-C(7)	1.455(4)
N(2)-C(2)	1.458(3)	N(7)-C(11)	1.481(3)
N(2)-C(3)	1.477(3)	N(7)-C(9)	1.486(3)
N(2)-C(4)	1.489(3)	N(8)-C(12)	1.453(3)
N(3)-C(6)	1.456(3)	N(8)-C(10)	1.481(3)
N(3)-C(5)	1.484(3)	N(8)-C(11)	1.485(3)
N(3)-C(4)	1.488(4)	C(1)-H(1A)	0.9700
N(4)-C(1)	1.462(3)	C(1)-H(1B)	0.9700
N(4)-C(5)	1.486(3)	C(2)-H(2A)	0.9700
N(4)-C(3)	1.492(4)		
C(2)-H(2B)	0.9700	C(8)-H(8A)	0.9700
C(3)-H(3A)	0.9700	C(8)-H(8B)	0.9700
C(3)-H(3B)	0.9700	C(9)-H(9A)	0.9700
C(4)-H(4A)	0.9700	C(9)-H(9B)	0.9700
C(4)-H(4B)	0.9700	C(10)-H(10A)	0.9700
C(5)-H(5A)	0.9700	C(10)-H(10B)	0.9700
C(5)-H(5B)	0.9700	C(11)-H(11A)	0.9700
C(6)-H(6A)	0.9700	C(11)-H(11B)	0.9700
C(6)-H(6B)	0.9700	C(12)-H(12A)	0.9700
C(7)-H(7A)	0.9700	C(12)-H(12B)	0.9700
C(7)-H(7B)	0.9700		
O(3)-S(1)-O(4)	110.98(10)	O(2)-S(1)-O(1)	107.33(10)
O(3)-S(1)-O(2)	110.57(12)	C(1)-N(1)-C(2)	108.90(18)
O(4)-S(1)-O(2)	109.53(11)	C(1)-N(1)-C(6)	109.01(19)
O(3)-S(1)-O(1)	109.22(12)	C(2)-N(1)-C(6)	108.8(2)
O(4)-S(1)-O(1)	109.12(11)	C(1)-N(1)-H(1)	110.0

C(2)-N(1)-H(1)	110.0	N(2)-C(4)-H(4A)	109.3
C(6)-N(1)-H(1)	110.0	N(3)-C(4)-H(4B)	109.3
C(2)-N(2)-C(3)	109.5(2)	N(2)-C(4)-H(4B)	109.3
C(2)-N(2)-C(4)	108.89(16)	H(4A)-C(4)-H(4B)	108.0
C(3)-N(2)-C(4)	108.2(2)	N(3)-C(5)-N(4)	112.6(2)
C(6)-N(3)-C(5)	108.3(2)	N(3)-C(5)-H(5A)	109.1
C(6)-N(3)-C(4)	108.50(19)	N(4)-C(5)-H(5A)	109.1
C(5)-N(3)-C(4)	109.0(2)	N(3)-C(5)-H(5B)	109.1
C(1)-N(4)-C(5)	108.89(17)	N(4)-C(5)-H(5B)	109.1
C(1)-N(4)-C(3)	108.7(2)	H(5A)-C(5)-H(5B)	107.8
C(5)-N(4)-C(3)	107.2(2)	N(3)-C(6)-N(1)	110.16(16)
C(7)-N(5)-C(12)	108.8(2)	N(3)-C(6)-H(6A)	109.6
C(7)-N(5)-C(8)	108.73(19)	N(1)-C(6)-H(6A)	109.6
C(12)-N(5)-C(8)	109.10(18)	N(3)-C(6)-H(6B)	109.6
C(7)-N(5)-H(2)	114.2(16)	N(1)-C(6)-H(6B)	109.6
C(12)-N(5)-H(2)	108.1(16)	H(6A)-C(6)-H(6B)	108.1
C(8)-N(5)-H(2)	107.8(18)	N(7)-C(7)-N(5)	109.73(19)
C(8)-N(6)-C(9)	108.7(2)	N(7)-C(7)-H(7A)	109.7
C(8)-N(6)-C(10)	108.8(2)	N(5)-C(7)-H(7A)	109.7
C(9)-N(6)-C(10)	109.1(2)	N(7)-C(7)-H(7B)	109.7
C(7)-N(7)-C(11)	108.77(19)	N(5)-C(7)-H(7B)	109.7
C(7)-N(7)-C(9)	108.6(2)	H(7A)-C(7)-H(7B)	108.2
C(11)-N(7)-C(9)	108.45(19)	N(6)-C(8)-N(5)	109.2(2)
C(12)-N(8)-C(10)	108.7(2)	N(6)-C(8)-H(8A)	109.8
C(12)-N(8)-C(11)	108.79(19)	N(5)-C(8)-H(8A)	109.8
C(10)-N(8)-C(11)	108.50(19)	N(6)-C(8)-H(8B)	109.8
N(4)-C(1)-N(1)	110.0(2)	N(5)-C(8)-H(8B)	109.8
N(4)-C(1)-H(1A)	109.7	H(8A)-C(8)-H(8B)	108.3
N(1)-C(1)-H(1A)	109.7	N(6)-C(9)-N(7)	112.24(18)
N(4)-C(1)-H(1B)	109.7	N(6)-C(9)-H(9A)	109.2
N(1)-C(1)-H(1B)	109.7	N(7)-C(9)-H(9A)	109.2
H(1A)-C(1)-H(1B)	108.2	N(6)-C(9)-H(9B)	109.2
N(2)-C(2)-N(1)	109.6(2)	N(7)-C(9)-H(9B)	109.2
N(2)-C(2)-H(2A)	109.7	H(9A)-C(9)-H(9B)	107.9
N(1)-C(2)-H(2A)	109.7	N(8)-C(10)-N(6)	112.14(17)
N(2)-C(2)-H(2B)	109.7	N(8)-C(10)-H(10A)	109.2
N(1)-C(2)-H(2B)	109.7	N(6)-C(10)-H(10A)	109.2
H(2A)-C(2)-H(2B)	108.2	N(8)-C(10)-H(10B)	109.2
N(2)-C(3)-N(4)	112.52(18)	N(6)-C(10)-H(10B)	109.2
N(2)-C(3)-H(3A)	109.1	H(10A)-C(10)-H(10B)	107.9
N(4)-C(3)-H(3A)	109.1	N(7)-C(11)-N(8)	112.3(2)
N(2)-C(3)-H(3B)	109.1	N(7)-C(11)-H(11A)	109.2
N(4)-C(3)-H(3B)	109.1	N(8)-C(11)-H(11A)	109.2
H(3A)-C(3)-H(3B)	107.8	N(7)-C(11)-H(11B)	109.2
N(3)-C(4)-N(2)	111.5(2)	N(8)-C(11)-H(11B)	109.2
N(3)-C(4)-H(4A)	109.3	H(11A)-C(11)-H(11B)	107.9

N(8)-C(12)-N(5)	109.66(18)	N(8)-C(12)-H(12B)	109.7
N(8)-C(12)-H(12A)	109.7	N(5)-C(12)-H(12B)	109.7
N(5)-C(12)-H(12A)	109.7	H(12A)-C(12)-H(12B)	108.2

**Table 22.** Anisotropic displacement parameters ( $\text{\AA}^2 \times 10^3$ ) for hexamethylenetetramminium sulfate (**8**), the anisotropic displacement factor exponent takes the form:  $-2p^2[h^2 a^*2U^{11} + \dots + 2 h k a^* b^* U^{12}]$

	U <sup>11</sup>	U <sup>22</sup>	U <sup>33</sup>	U <sup>23</sup>	U <sup>13</sup>	U <sup>12</sup>
S(1)	25(1)	29(1)	27(1)	-1(1)	4(1)	-3(1)
O(1)	16(2)	59(1)	36(1)	-13(1)	8(1)	-8(1)
O(2)	34(2)	47(1)	45(1)	-11(1)	21(1)	-8(1)
O(3)	53(2)	50(1)	46(1)	18(1)	6(1)	5(1)
O(4)	45(2)	36(1)	46(1)	-11(1)	10(1)	-14(1)
N(1)	22(2)	38(1)	31(1)	-10(1)	7(1)	-6(1)
N(2)	23(2)	32(1)	31(1)	-1(1)	4(1)	-2(1)
N(3)	28(2)	32(1)	40(1)	6(1)	17(1)	6(1)
N(4)	33(2)	32(1)	30(1)	-1(1)	11(1)	-1(1)
N(5)	22(2)	28(1)	38(1)	2(1)	7(1)	-3(1)
N(6)	23(2)	31(1)	47(1)	0(1)	11(1)	0(1)
N(7)	37(2)	43(1)	31(1)	6(1)	14(1)	5(1)
N(8)	20(2)	44(1)	30(1)	2(1)	5(1)	1(1)
C(1)	26(3)	40(1)	42(1)	-4(1)	16(1)	-7(1)
C(2)	26(3)	27(1)	39(1)	-4(1)	10(1)	3(1)
C(3)	37(3)	37(1)	27(1)	2(1)	5(1)	0(1)
C(4)	29(3)	30(1)	43(1)	-2(1)	14(1)	-4(1)
C(5)	35(3)	33(1)	44(1)	2(1)	20(1)	6(1)
C(6)	32(3)	50(1)	27(1)	8(1)	5(1)	8(1)
C(7)	47(3)	38(1)	28(1)	-4(1)	1(1)	3(2)
C(8)	23(3)	34(1)	49(1)	3(1)	9(1)	5(1)
C(9)	40(3)	40(1)	44(1)	14(1)	16(1)	0(1)
C(10)	31(3)	41(1)	43(1)	-12(1)	5(1)	-10(1)
C(11)	24(3)	46(1)	43(1)	4(1)	14(1)	4(1)
C(12)	33(3)	41(1)	27(1)	7(1)	9(1)	7(1)

**Table 23.** Hydrogen coordinates ( $\times 10^4$ ) and isotropic displacement parameters ( $\text{\AA}^2 \times 10^3$ ) for Hexamethylenetetramminium sulfate (**8**).

	x	y	z	U(eq)
H(1)	694	5297	-1367	37
H(1A)	884	5534	-3161	42
H(1B)	1811	4668	-2458	42
H(2A)	-1315	4991	-1904	37
H(2B)	-1025	5736	-2818	37
H(3A)	-916	4894	-4559	42
H(3B)	-1142	3614	-4758	42
H(4A)	-1642	3028	-2212	40
H(4B)	-1607	2484	-3348	40
H(5A)	288	2285	-3687	43
H(5B)	1435	2693	-2759	43
H(6A)	1347	3465	-1014	45
H(6B)	139	3596	-798	45
H(7A)	5298	6224	-1927	48
H(7B)	4439	7157	-2595	48
H(8A)	3729	8622	-1542	43
H(8B)	4132	8602	-207	43
H(9A)	6382	9361	-1827	49
H(9B)	5083	9052	-2511	49
H(10A)	7026	9321	263	48
H(10B)	6125	8988	878	48
H(11A)	7721	7909	-788	44
H(11B)	7274	6680	-822	44
H(12A)	5504	7097	862	41
H(12B)	5952	6187	192	41
H(2)	4080(30)	6800(20)	-850(20)	39(9)

**Table 24.** Torsion angles [ $^{\circ}$ ] for hexamethylenetetramminium sulfate (**8**).

C(6)-N(3)-C(5)-N(4)	-60.0(3)	C(5)-N(3)-C(6)-N(1)	59.0(3)
C(4)-N(3)-C(5)-N(4)	57.8(3)	C(4)-N(3)-C(6)-N(1)	-59.2(3)
C(1)-N(4)-C(5)-N(3)	59.7(3)	C(1)-N(1)-C(6)-N(3)	-59.4(3)
C(3)-N(4)-C(5)-N(3)	-57.7(2)	C(2)-N(1)-C(6)-N(3)	59.3(3)
C(3)-N(2)-C(2)-N(1)	-58.6(2)	N(5)-C(7)-N(7)-C(11)	59.0(3)
C(4)-N(2)-C(2)-N(1)	59.6(3)	N(5)-C(7)-N(7)-C(9)	-58.8(2)
C(1)-N(1)-C(2)-N(2)	59.6(2)	N(6)-C(9)-N(7)-C(7)	60.6(3)
C(6)-N(1)-C(2)-N(2)	-59.1(2)	N(6)-C(9)-N(7)-C(11)	-57.4(3)
C(2)-N(2)-C(3)-N(4)	58.9(2)	C(12)-N(8)-C(10)-N(6)	-60.9(3)
C(4)-N(2)-C(3)-N(4)	-59.6(2)	C(11)-N(8)-C(10)-N(6)	57.3(3)
C(1)-N(4)-C(3)-N(2)	-58.6(2)	C(8)-N(6)-C(10)-N(8)	61.1(3)
C(5)-N(4)-C(3)-N(2)	59.0(2)	C(9)-N(6)-C(10)-N(8)	-57.3(3)
C(8)-N(6)-C(9)-N(7)	-61.3(3)	C(6)-N(3)-C(4)-N(2)	60.5(2)
C(10)-N(6)-C(9)-N(7)	57.3(3)	C(5)-N(3)-C(4)-N(2)	-57.3(2)
C(5)-N(4)-C(1)-N(1)	-58.1(3)	C(2)-N(2)-C(4)-N(3)	-60.9(3)
C(3)-N(4)-C(1)-N(1)	58.4(2)	C(3)-N(2)-C(4)-N(3)	58.1(2)
C(2)-N(1)-C(1)-N(4)	-60.0(2)	C(9)-N(6)-C(8)-N(5)	59.7(2)
C(6)-N(1)-C(1)-N(4)	58.6(3)	C(10)-N(6)-C(8)-N(5)	-59.0(2)
C(10)-N(8)-C(12)-N(5)	59.0(2)	C(7)-N(5)-C(8)-N(6)	-59.6(3)
C(11)-N(8)-C(12)-N(5)	-59.0(3)	C(12)-N(5)-C(8)-N(6)	59.0(3)
C(7)-N(5)-C(12)-N(8)	59.5(2)	C(7)-N(7)-C(11)-N(8)	-60.1(3)
C(8)-N(5)-C(12)-N(8)	-59.0(3)	C(9)-N(7)-C(11)-N(8)	57.8(3)
C(12)-N(5)-C(7)-N(7)	-59.4(2)	C(12)-N(8)-C(11)-N(7)	60.1(3)
C(8)-N(5)-C(7)-N(7)	59.3(3)	C(10)-N(8)-C(11)-N(7)	-58.0(3)

**Table 25.** Hydrogen bonds for hexamethylenetetramminium sulfate (**8**) [ $\text{\AA}$  and  $^{\circ}$ ].

D-H...A	d(D-H)	d(H...A)	d(D...A)	$\angle(\text{DHA})$
N(5)-H(2) ...O(2)	0.92(3)	1.85(3)	2.751(3)	167(3)
N(1)-H(1) ...O(1)	0.91	1.77	2.660(2)	165.2

**Table 26.** Crystal data and structure refinement for bis (5-nitroisophthalic acid) hexamethylenetetramine (**9**).

Empirical formula	$\text{C}_{21} \text{H}_{24} \text{N}_6 \text{O}_{14}$
Formula weight	$321.27 \text{g mol}^{-1}$
Temperature	153(2) K



Wavelength	0.71073 Å	
Crystal system	Triclinic	
Space group	<i>P</i> -1	
Unit cell dimensions	<i>a</i> = 6.5629(8) Å	$\alpha = 106.580(4)^\circ$
	<i>b</i> = 12.8399(12) Å	$\beta = 90.995(4)^\circ$
	<i>c</i> = 15.8571(17) Å	$\gamma = 99.475(7)^\circ$
Volume	1260.3(2) Å <sup>3</sup>	
Z	4	
Density (calculated)	1.693 mg/m <sup>3</sup>	
Absorption coefficient	0.132 mm <sup>-1</sup>	
F(000)	666	
Crystal size	0.20 x 0.06 x 0.04 mm <sup>3</sup>	
Theta range for data collection	3.24 to 25.04°	
Index ranges	-6 ≤ <i>h</i> ≤ 7, -15 ≤ <i>k</i> ≤ 13, -18 ≤ <i>l</i> ≤ 17	
Reflections collected	6482	
Independent reflections	4242 [R(int) = 0.0727]	
Completeness to theta = 25.04°	95.3 %	
Max & min. transmission	0.9947 and 0.9741	
Refinement method	Full-matrix least-squares on <i>F</i> <sup>2</sup>	
Data / restraints / parameters	4242 / 0 / 379	
Goodness-of-fit on <i>F</i> <sup>2</sup>	1.214	
Final R indices [ <i>I</i> > 2σ( <i>I</i> )]	<i>R</i> 1 = 0.1497, <i>wR</i> 2 = 0.3556	
R indices (all data)	<i>R</i> 1 = 0.2559, <i>wR</i> 2 = 0.4085	
Largest diff. peak and hole	1.019 and -0.465 e.Å <sup>-3</sup>	

**Table 27.** Atomic coordinates ( $\times 10^4$ ) and equivalent isotropic displacement parameters ( $\text{Å}^2 \times 10^3$ ) for bis(5-nitroisophthalic acid)hexamethylenetetramine (9). *U*(eq) is defined as one third of the trace of the orthogonalized *U*<sub>ij</sub> tensor

	<i>x</i>	<i>y</i>	<i>z</i>	<i>U</i> (eq)
O(1)	3146(11)	3147(5)	8669(4)	42(2)
O(2)	3360(11)	3632(6)	7432(4)	48(2)
O(3)	2070(12)	5711(6)	11417(4)	53(2)
O(4)	2166(12)	7453(7)	11534(4)	56(2)
O(5)	3007(13)	8795(6)	8948(4)	58(2)
O(6)	3104(11)	7547(6)	7649(4)	49(2)
O(7)	2871(10)	4353(6)	6104(4)	43(2)
O(8)	3548(12)	2735(6)	5291(4)	48(2)
O(9)	1576(12)	7120(6)	4792(4)	51(2)
O(10)	1347(12)	6781(6)	3368(4)	51(2)
O(11)	1951(11)	3180(6)	1428(4)	46(2)
O(12)	2142(12)	1803(6)	2023(4)	55(2)
O(13)	1901(11)	1899(6)	9833(4)	51(2)

O(14)	8335(12)	319(6)	9273(4)	56(2)
N(1)	3315(13)	1276(7)	7397(5)	42(2)
N(2)	4495(14)	306(7)	6000(5)	42(2)
N(3)	825(13)	29(7)	6253(5)	42(2)
N(4)	3283(14)	-692(6)	7027(5)	42(2)
N(5)	2236(13)	6502(8)	11108(5)	42(2)
N(6)	1601(13)	6500(7)	4035(6)	41(2)
C(1)	3169(16)	3855(9)	8250(6)	40(3)
C(2)	2971(16)	5000(8)	8771(6)	38(2)
C(3)	2651(15)	5218(8)	9673(6)	39(3)
C(4)	2568(15)	6284(8)	10166(6)	37(2)
C(5)	2703(14)	7149(8)	9807(6)	33(2)
C(6)	2955(15)	6917(8)	8885(6)	36(2)
C(7)	3048(15)	5867(9)	8398(6)	41(3)
C(8)	2986(16)	7839(9)	8517(6)	41(3)
C(9)	4853(16)	1350(8)	6708(6)	41(3)
C(10)	1173(18)	1054(9)	6967(7)	52(3)
C(11)	3657(18)	347(8)	7756(6)	45(3)
C(12)	1146(16)	-849(8)	6613(7)	43(3)
C(13)	4757(16)	-570(8)	6374(6)	42(3)
C(14)	2382(17)	105(9)	5605(6)	48(3)
C(15)	3081(15)	3617(9)	5349(6)	39(2)
C(16)	2664(14)	4003(8)	4568(5)	30(2)
C(17)	2318(14)	5054(8)	4667(6)	36(2)
C(18)	1932(16)	5387(7)	3918(6)	36(2)
C(19)	1925(14)	4671(8)	3092(6)	35(2)
C(20)	2246(15)	3593(8)	2987(6)	40(3)
C(21)	2683(15)	3268(8)	3721(6)	37(2)
C(22)	2107(16)	2761(9)	2089(6)	41(3)

---

**Table 28.** Bond lengths [Å] and angles [°] for bis(5-nitroisophthalic acid)hexamethylenetetramine (**9**).

O(1)-C(1)	1.269(11)	C(9)-H(32B)	0.9900
O(1)-H(1)	0.8400	C(10)-H(34A)	0.9900
O(2)-C(1)	1.260(11)	C(10)-H(34B)	0.9900
O(3)-N(5)	1.237(10)	C(11)-H(41A)	0.9900
O(4)-N(5)	1.223(10)	C(11)-H(41B)	0.9900
O(5)-C(8)	1.220(11)	C(12)-H(40A)	0.9900
O(6)-C(8)	1.327(11)	C(12)-H(40B)	0.9900
O(6)-H(6)	0.8400	C(13)-H(38A)	0.9900
O(7)-C(15)	1.323(11)	C(13)-H(38B)	0.9900
O(7)-H(7)	0.8400	C(14)-H(36A)	0.9900
O(8)-C(15)	1.201(11)	C(14)-H(36B)	0.9900
O(9)-N(6)	1.239(10)	C(15)-C(16)	1.495(13)
O(10)-N(6)	1.228(10)	C(16)-C(17)	1.372(13)
O(11)-C(22)	1.317(12)	C(16)-C(21)	1.406(13)
O(12)-C(22)	1.208(11)	C(17)-C(18)	1.404(13)
O(12)-H(12)	0.8400	C(17)-H(30)	0.9500
N(1)-C(10)	1.499(13)	C(18)-C(19)	1.369(12)
N(1)-C(11)	1.506(12)	C(19)-C(20)	1.397(13)
N(1)-C(9)	1.513(12)	C(19)-H(28)	0.9500
N(2)-C(13)	1.445(12)	C(20)-C(21)	1.385(13)
N(2)-C(9)	1.462(12)	C(20)-C(22)	1.508(14)
N(2)-C(14)	1.463(13)	C(21)-H(26)	0.9500
N(3)-C(12)	1.443(12)		
N(3)-C(10)	1.453(13)	C(1)-O(1)-H(1)	109.5
N(3)-C(14)	1.474(13)	C(8)-O(6)-H(6)	109.5
N(4)-C(13)	1.453(13)	C(15)-O(7)-H(7)	109.5
N(4)-C(11)	1.475(12)	C(22)-O(12)-H(12)	109.5
N(4)-C(12)	1.496(13)	C(10)-N(1)-C(11)	110.8(8)
N(5)-C(4)	1.467(12)	C(10)-N(1)-C(9)	108.4(7)
N(6)-C(18)	1.441(12)	C(11)-N(1)-C(9)	108.0(8)
C(1)-C(2)	1.495(14)	C(13)-N(2)-C(9)	108.4(7)
C(2)-C(7)	1.397(14)	C(13)-N(2)-C(14)	109.7(8)
C(2)-C(3)	1.403(13)	C(9)-N(2)-C(14)	109.3(8)
C(3)-C(4)	1.379(13)	C(12)-N(3)-C(10)	108.1(8)
C(3)-H(15)	0.9500	C(12)-N(3)-C(14)	107.8(8)
C(4)-C(5)	1.378(13)	C(10)-N(3)-C(14)	108.7(8)
C(5)-C(6)	1.423(13)	C(13)-N(4)-C(11)	107.4(8)
C(5)-H(13)	0.9500	C(13)-N(4)-C(12)	108.4(7)
C(6)-C(7)	1.361(14)	C(11)-N(4)-C(12)	108.7(7)
C(6)-C(8)	1.459(14)	O(4)-N(5)-O(3)	124.7(8)
C(7)-H(11)	0.9500	O(4)-N(5)-C(4)	117.8(8)
C(9)-H(32A)	0.9900	O(3)-N(5)-C(4)	117.5(9)

O(10)-N(6)-O(9)	123.4(8)	H(41A)-C(11)-H(41B)	108.3
O(10)-N(6)-C(18)	117.5(8)	N(3)-C(12)-N(4)	113.4(8)
O(9)-N(6)-C(18)	119.1(8)	N(3)-C(12)-H(40A)	108.9
O(2)-C(1)-O(1)	123.0(9)	N(4)-C(12)-H(40A)	108.9
O(2)-C(1)-C(2)	119.9(8)	N(3)-C(12)-H(40B)	108.9
O(1)-C(1)-C(2)	117.1(8)	N(4)-C(12)-H(40B)	108.9
C(7)-C(2)-C(3)	118.0(9)	H(40A)-C(12)-H(40B)	107.7
C(7)-C(2)-C(1)	123.0(8)	N(2)-C(13)-N(4)	112.8(8)
C(3)-C(2)-C(1)	119.0(8)	N(2)-C(13)-H(38A)	109.0
C(4)-C(3)-C(2)	119.2(9)	N(4)-C(13)-H(38A)	109.0
C(4)-C(3)-H(15)	120.4	N(2)-C(13)-H(38B)	109.0
C(2)-C(3)-H(15)	120.4	N(4)-C(13)-H(38B)	109.0
C(5)-C(4)-C(3)	123.0(9)	H(38A)-C(13)-H(38B)	107.8
C(5)-C(4)-N(5)	118.2(9)	N(2)-C(14)-N(3)	111.9(8)
C(3)-C(4)-N(5)	118.7(9)	N(2)-C(14)-H(36A)	109.2
C(4)-C(5)-C(6)	117.6(9)	N(3)-C(14)-H(36A)	109.2
C(4)-C(5)-H(13)	121.2	N(2)-C(14)-H(36B)	109.2
C(6)-C(5)-H(13)	121.2	N(3)-C(14)-H(36B)	109.2
C(7)-C(6)-C(5)	119.5(8)	H(36A)-C(14)-H(36B)	107.9
C(7)-C(6)-C(8)	124.1(9)	O(8)-C(15)-O(7)	124.1(9)
C(5)-C(6)-C(8)	116.3(9)	O(8)-C(15)-C(16)	123.4(8)
C(6)-C(7)-C(2)	122.5(9)	O(7)-C(15)-C(16)	112.4(9)
C(6)-C(7)-H(11)	118.7	C(17)-C(16)-C(21)	120.2(8)
C(2)-C(7)-H(11)	118.7	C(17)-C(16)-C(15)	121.4(8)
O(5)-C(8)-O(6)	122.1(9)	C(21)-C(16)-C(15)	118.4(8)
O(5)-C(8)-C(6)	125.0(9)	C(16)-C(17)-C(18)	119.7(8)
O(6)-C(8)-C(6)	112.8(9)	C(16)-C(17)-H(30)	120.1
N(2)-C(9)-N(1)	108.9(8)	C(18)-C(17)-H(30)	120.1
N(2)-C(9)-H(32A)	109.9	C(19)-C(18)-C(17)	120.3(9)
N(1)-C(9)-H(32A)	109.9	C(19)-C(18)-N(6)	120.8(8)
N(2)-C(9)-H(32B)	109.9	C(17)-C(18)-N(6)	118.9(8)
N(1)-C(9)-H(32B)	109.9	C(18)-C(19)-C(20)	120.3(8)
H(32A)-C(9)-H(32B)	108.3	C(18)-C(19)-H(28)	119.9
N(3)-C(10)-N(1)	110.8(8)	C(20)-C(19)-H(28)	119.9
N(3)-C(10)-H(34A)	109.5	C(21)-C(20)-C(19)	119.8(9)
N(1)-C(10)-H(34A)	109.5	C(21)-C(20)-C(22)	118.6(9)
N(3)-C(10)-H(34B)	109.5	C(19)-C(20)-C(22)	121.7(9)
N(1)-C(10)-H(34B)	109.5	C(20)-C(21)-C(16)	119.6(9)
H(34A)-C(10)-H(34B)	108.1	C(20)-C(21)-H(26)	120.2
N(4)-C(11)-N(1)	108.6(7)	C(16)-C(21)-H(26)	120.2
N(4)-C(11)-H(41A)	110.0	O(12)-C(22)-O(11)	125.7(9)
N(1)-C(11)-H(41A)	110.0	O(12)-C(22)-C(20)	120.2(9)
N(4)-C(11)-H(41B)	110.0	O(11)-C(22)-C(20)	114.1(9)
N(1)-C(11)-H(41B)	110.0		

**Table 29.** Anisotropic displacement parameters ( $\text{\AA}^2 \times 10^3$ ) for bis(5-nitroisophthalic acid)hexamethylenetetramine (**9**). The anisotropic displacement factor exponent takes the form:  $-2p^2[h^2 a^*2U_{11} + \dots + 2hk a^* b^* U_{12}]$ .

	U <sub>11</sub>	U <sub>22</sub>	U <sub>33</sub>	U <sub>23</sub>	U <sub>13</sub>	U <sub>12</sub>
O(1)	73(5)	37(4)	23(3)	14(3)	8(3)	17(3)
O(2)	78(6)	46(5)	24(4)	13(3)	3(3)	16(4)
O(3)	81(6)	57(5)	28(4)	20(4)	12(4)	19(4)
O(4)	85(6)	54(5)	25(4)	5(4)	3(4)	14(4)
O(5)	106(7)	43(5)	34(4)	19(4)	20(4)	23(4)
O(6)	76(6)	43(4)	35(4)	19(3)	12(4)	15(4)
O(7)	57(5)	51(5)	20(3)	11(3)	2(3)	8(4)
O(8)	82(6)	37(5)	26(4)	8(3)	8(3)	15(4)
O(9)	88(6)	39(4)	22(4)	2(3)	4(3)	13(4)
O(10)	77(6)	46(5)	38(4)	24(4)	11(4)	16(4)
O(11)	64(5)	42(4)	35(4)	20(3)	5(3)	8(4)
O(12)	87(6)	53(6)	25(4)	12(4)	5(4)	12(4)
O(13)	68(5)	53(5)	31(4)	12(3)	9(3)	10(4)
O(14)	80(6)	42(5)	42(4)	8(4)	12(4)	11(4)
N(1)	62(6)	38(5)	33(4)	21(4)	1(4)	9(4)
N(2)	64(6)	31(5)	32(4)	10(4)	6(4)	11(4)
N(3)	56(6)	36(5)	26(4)	2(4)	1(4)	0(4)
N(4)	71(6)	32(5)	24(4)	6(4)	9(4)	15(4)
N(5)	62(6)	44(6)	25(4)	14(5)	8(4)	16(5)
N(6)	48(6)	36(5)	37(5)	12(4)	-2(4)	-2(4)
C(1)	57(7)	45(7)	29(6)	22(5)	18(5)	20(5)
C(2)	58(7)	38(6)	19(5)	9(4)	6(4)	12(5)
C(3)	55(7)	37(6)	29(5)	22(5)	-2(5)	-1(5)
C(4)	42(6)	42(7)	28(5)	11(5)	-8(4)	8(5)
C(5)	42(6)	31(6)	26(5)	5(4)	2(4)	8(4)
C(6)	51(7)	25(6)	36(6)	16(5)	1(5)	1(5)
C(7)	45(7)	52(7)	27(5)	16(5)	2(4)	-1(5)
C(8)	52(7)	47(8)	24(5)	6(5)	12(5)	14(5)
C(9)	49(7)	39(6)	31(5)	9(5)	1(5)	2(5)
C(10)	69(8)	48(7)	38(6)	14(5)	4(6)	12(6)
C(11)	66(8)	48(7)	24(5)	17(5)	6(5)	11(6)
C(12)	52(7)	28(6)	44(6)	7(5)	3(5)	2(5)
C(13)	53(7)	41(7)	26(5)	2(5)	5(5)	9(5)
C(14)	66(8)	45(7)	34(6)	18(5)	-3(5)	0(6)
C(15)	46(7)	46(7)	23(5)	7(5)	6(4)	12(5)
C(16)	41(6)	30(6)	20(5)	3(4)	7(4)	14(4)
C(17)	38(6)	41(7)	26(5)	10(5)	5(4)	1(5)
C(18)	59(7)	24(6)	24(5)	6(4)	11(4)	2(5)
C(19)	36(6)	39(6)	26(5)	8(4)	-2(4)	0(5)

C(20)	45(7)	46(7)	31(5)	11(5)	12(5)	11(5)
C(21)	44(6)	36(6)	34(6)	18(5)	2(4)	9(5)
C(22)	54(7)	27(6)	38(6)	1(5)	8(5)	8(5)

**Table 30.** Hydrogen coordinates ( $\times 10^4$ ) and isotropic displacement parameters ( $\text{\AA}^2 \times 10^3$ ) for bis(5-nitroisophthalic acid)hexamethylenetetramine (**9**).

	x	y	z	U(eq)
H(1)	3281	2537	8319	51
H(6)	3119	8101	7467	59
H(7)	3108	4104	6524	51
H(12)	2051	1440	1487	66
H(15)	2494	4638	9941	47
H(13)	2631	7875	10161	40
H(11)	3170	5718	7781	50
H(32A)	4682	1964	6467	49
H(32B)	6283	1495	6977	49
H(34A)	145	1009	7411	62
H(34B)	982	1672	6734	62
H(41A)	5094	488	8016	54
H(41B)	2699	292	8222	54
H(40A)	876	-1557	6136	51
H(40B)	134	-901	7062	51
H(38A)	6179	-417	6652	50
H(38B)	4597	-1274	5894	50
H(36A)	2154	-591	5115	58
H(36B)	2208	713	5356	58
H(30)	2339	5556	5240	43
H(28)	1700	4907	2588	42
H(26)	2993	2552	3652	44



**Table 31.** Torsion angles [°] for bis(5-nitroisophthalic acid)hexamethylenetetramine (**9**).

O(1)-C(1)-C(2)-C(7)	177.6(10)	O(10)-N(6)-C(18)-C(17)	177.2(9)
O(2)-C(1)-C(2)-C(7)	-2.0(16)	O(9)-N(6)-C(18)-C(17)	-3.1(14)
O(1)-C(1)-C(2)-C(3)	-3.6(15)	C(21)-C(16)-C(17)-C(18)	1.5(14)
O(2)-C(1)-C(2)-C(3)	176.7(9)	C(15)-C(16)-C(17)-C(18)	180.0(9)
C(3)-C(2)-C(7)-C(6)	4.2(15)	C(19)-C(18)-C(17)-C(16)	-0.8(15)
C(1)-C(2)-C(7)-C(6)	-177.1(10)	N(6)-C(18)-C(17)-C(16)	-179.1(8)
C(2)-C(7)-C(6)-C(5)	-2.0(15)	N(2)-C(9)-N(1)-C(10)	-59.6(10)
C(2)-C(7)-C(6)-C(8)	-178.7(10)	N(2)-C(9)-N(1)-C(11)	60.6(10)
O(5)-C(8)-C(6)-C(7)	-176.2(10)	C(11)-N(1)-C(10)-N(3)	-58.8(10)
O(6)-C(8)-C(6)-C(7)	0.4(15)	C(9)-N(1)-C(10)-N(3)	59.6(10)
O(5)-C(8)-C(6)-C(5)	7.1(16)	N(1)-C(10)-N(3)-C(12)	58.3(11)
O(6)-C(8)-C(6)-C(5)	-176.3(8)	N(1)-C(10)-N(3)-C(14)	-58.4(10)
C(7)-C(6)-C(5)-C(4)	0.1(14)	C(12)-N(3)-C(14)-N(2)	-57.9(10)
C(8)-C(6)-C(5)-C(4)	177.0(9)	C(10)-N(3)-C(14)-N(2)	59.0(11)
C(6)-C(5)-C(4)-C(3)	-0.4(15)	N(3)-C(14)-N(2)-C(13)	58.3(11)
C(6)-C(5)-C(4)-N(5)	-177.9(8)	N(3)-C(14)-N(2)-C(9)	-60.5(10)
O(4)-N(5)-C(4)-C(5)	-2.4(13)	N(1)-C(9)-N(2)-C(13)	-59.6(10)
O(3)-N(5)-C(4)-C(5)	178.4(9)	N(1)-C(9)-N(2)-C(14)	59.9(10)
O(4)-N(5)-C(4)-C(3)	-180.0(9)	C(14)-N(2)-C(13)-N(4)	-57.4(10)
O(3)-N(5)-C(4)-C(3)	0.8(13)	C(9)-N(2)-C(13)-N(4)	62.0(11)
C(5)-C(4)-C(3)-C(2)	2.6(15)	N(2)-C(13)-N(4)-C(11)	-62.2(10)
N(5)-C(4)-C(3)-C(2)	-179.9(9)	N(2)-C(13)-N(4)-C(12)	55.1(10)
C(7)-C(2)-C(3)-C(4)	-4.4(15)	C(10)-N(3)-C(12)-N(4)	-60.1(11)
C(1)-C(2)-C(3)-C(4)	176.9(9)	C(14)-N(3)-C(12)-N(4)	57.2(10)
O(8)-C(15)-C(16)-C(17)	-174.1(10)	C(13)-N(4)-C(12)-N(3)	-56.2(10)
O(7)-C(15)-C(16)-C(17)	6.1(13)	C(11)-N(4)-C(12)-N(3)	60.3(10)
O(8)-C(15)-C(16)-C(21)	4.4(15)	C(13)-N(4)-C(11)-N(1)	60.8(10)
O(7)-C(15)-C(16)-C(21)	-175.4(8)	C(12)-N(4)-C(11)-N(1)	-56.3(10)
C(17)-C(16)-C(21)-C(20)	-3.2(14)	C(10)-N(1)-C(11)-N(4)	57.3(10)
C(15)-C(16)-C(21)-C(20)	178.3(9)	C(9)-N(1)-C(11)-N(4)	-61.3(10)
C(16)-C(21)-C(20)-C(19)	4.2(14)		
C(16)-C(21)-C(20)-C(22)	-175.2(9)		
O(12)-C(22)-C(20)-C(21)	8.3(15)		
O(11)-C(22)-C(20)-C(21)	-171.8(9)		
O(12)-C(22)-C(20)-C(19)	-171.0(9)		
O(11)-C(22)-C(20)-C(19)	8.9(14)		
C(21)-C(20)-C(19)-C(18)	-3.4(14)		
C(22)-C(20)-C(19)-C(18)	175.9(9)		
C(20)-C(19)-C(18)-C(17)	1.7(14)		
C(20)-C(19)-C(18)-N(6)	-180.0(9)		
O(10)-N(6)-C(18)-C(19)	-1.1(14)		
O(9)-N(6)-C(18)-C(19)	178.6(9)		

**Table 32.** Hydrogen bonds for bis(5-nitroisophthalic acid) hexamethylenetetramine (**9**) [Å and °]

D-H...A	d (D-H)	d (H...A)	d (D...A)	< (DHA)
O (1)-H (1...N (1)	0.84	1.85	2.680(10)	169.5
O (7)-H (7...O (2)	0.84	1.73	2.565(8)	174.1
O (12)-H (12...O (14)#1	0.84	2.21	2.872(10)	136.2
O (11)-H (6...O(13)	0.84	1.86	2.700(10)	176.7

Symmetry transformations used to generate equivalent atoms:

#1 -x+1,-y,-z+1. #2 x, y+1, z

**Table 33.** Crystal data and structure refinement for hexamethylenetetramine terephthalic acid (**10**).

Empirical formula	C <sub>28</sub> H <sub>36</sub> N <sub>8</sub> O <sub>8</sub>	
Formula weight	612.65g. mol <sup>-1</sup>	
Temperature	173(2) K	
Wavelength	0.71073 Å	
Crystal system	Monoclinic	
Space group	P2(1)	
Unit cell dimensions	a = 6.2820(6) Å	α = 90°
	b = 19.2870(19) Å	β = 90.577(6)°
	c = 17.2470(17) Å	γ = 90°
Volume	2089.6(4) Å <sup>3</sup>	
Z	2	
Density (calculated)	0.974 mg/m <sup>3</sup>	
Absorption coefficient	0.073 mm <sup>-1</sup>	
F(000)	648	
Theta range for data collection	1.58 to 29.25°	
Index ranges	-8 ≤ h ≤ 8, -26 ≤ k ≤ 25, -23 ≤ l ≤ 23	
Reflections collected	38639	
Independent reflections	10980 [R(int) = 0.0694]	
Completeness to theta = 29.25°	99.4 %	
Refinement method	Full-matrix least-squares on F <sup>2</sup>	
Data / restraints / parameters	10980 / 139 / 727	
Goodness-of-fit on F <sup>2</sup>	1.054	
Final R indices [I > 2σ(I)]	R1 = 0.0798, wR2 = 0.2375	
R indices (all data)	R1 = 0.1044, wR2 = 0.2655	
Absolute structure parameter	0.7(15)	
Largest diff. peak and hole	0.547 and -0.654 e.Å <sup>-3</sup>	

**Table 34.** Atomic coordinates ( $\times 10^4$ ) and equivalent isotropic displacement parameters ( $\text{\AA}^2 \times 10^3$ ) for hexamethylenetetramine terephthalic acid, (**10**).  $U(\text{eq})$  is defined as one third of the trace of the orthogonalized  $U_{ij}$  tensor.

	x	y	z	$U(\text{eq})$
O(1)	3299(5)	5363(2)	8112(2)	20(1)
O(2)	6733(5)	5633(2)	8375(2)	28(1)
O(3)	9857(4)	3496(2)	5352(2)	19(1)
O(4)	6488(4)	3230(2)	5092(2)	22(1)
O(5)	1990(5)	5345(2)	5180(2)	22(1)
O(6)	-1078(5)	5173(2)	4541(2)	27(1)
O(7)	4516(5)	3498(2)	1614(2)	29(1)
O(8)	7570(5)	3657(2)	2258(2)	30(1)
O(9)	-1029(9)	5375(3)	1666(3)	21(1)
O(10)	-4086(13)	5179(4)	1056(4)	38(2)
O(11)	1286(12)	3450(4)	-1847(5)	37(2)
O(12)	4493(9)	3656(3)	-1247(3)	20(1)
O(13)	-3177(9)	5323(3)	1242(3)	14(1)
O(14)	227(9)	5558(3)	1522(3)	24(1)
O(15)	3525(8)	3471(3)	-1521(3)	14(1)
O(16)	100(7)	3233(2)	-1843(3)	8(1)
N(1)	2586(6)	6365(2)	9093(2)	17(1)
N(2)	3228(6)	6878(2)	10370(2)	24(1)
N(3)	3239(6)	7609(2)	9208(2)	16(1)
N(4)	-102(6)	7147(2)	9660(2)	25(1)
N(5)	-121(5)	6293(2)	5923(2)	15(1)
N(6)	-94(6)	7099(2)	7016(2)	20(1)
N(7)	-623(5)	7532(2)	5697(2)	14(1)
N(8)	-3452(5)	6847(2)	6297(2)	22(1)
N(9)	-3614(7)	6216(2)	2425(3)	34(1)
N(10)	-3420(6)	6786(3)	3688(2)	34(1)
N(11)	-3948(8)	7459(2)	2533(2)	30(1)
N(12)	-6749(6)	6748(3)	2993(2)	43(1)
C(1)	5379(6)	5306(2)	8002(2)	15(1)
C(2)	6019(6)	4843(2)	7360(2)	12(1)
C(3)	8132(6)	4650(2)	7269(2)	15(1)
C(4)	8747(6)	4229(2)	6659(2)	16(1)
C(5)	7223(6)	4010(2)	6123(2)	12(1)
C(6)	5065(6)	4209(2)	6202(2)	13(1)
C(7)	4476(6)	4619(2)	6819(2)	12(1)
C(8)	7823(6)	3547(2)	5470(2)	13(1)
C(9)	257(7)	6525(2)	9181(3)	23(1)
C(10)	3584(7)	6984(2)	8736(2)	16(1)
C(11)	3568(6)	6274(2)	9880(2)	18(1)
C(12)	4165(6)	7478(2)	9998(2)	19(1)

C(13)	912(7)	7016(4)	10425(3)	39(1)
C(14)	916(7)	7724(2)	9280(2)	22(1)
C(15)	852(6)	5094(2)	4588(2)	14(1)
C(16)	2128(7)	4741(2)	3990(2)	17(1)
C(17)	4253(6)	4573(2)	4106(2)	15(1)
C(18)	5369(6)	4239(2)	3536(2)	15(1)
C(19)	4405(6)	4080(2)	2814(2)	15(1)
C(20)	2248(7)	4254(2)	2681(3)	20(1)
C(21)	1130(7)	4574(2)	3274(3)	19(1)
C(22)	5667(7)	3719(2)	2207(2)	20(1)
C(23)	-2483(6)	6226(2)	5999(2)	20(1)
C(24)	279(6)	6881(2)	5399(2)	17(1)
C(25)	759(7)	6456(2)	6698(2)	21(1)
C(26)	357(7)	7674(2)	6471(2)	21(1)
C(27)	-2439(7)	7012(3)	7063(2)	31(1)
C(28)	-2938(6)	7436(2)	5786(2)	18(1)
C(29)	-2228(14)	5126(4)	1101(5)	20(2)
C(30)	-883(17)	4759(5)	459(6)	11(2)
C(31)	1184(14)	4604(4)	595(5)	10(2)
C(32)	2315(11)	4249(4)	15(5)	5(1)
C(33)	1306(12)	4078(4)	-672(4)	5(1)
C(34)	-871(14)	4235(4)	-794(5)	8(2)
C(35)	-1960(20)	4579(7)	-52(8)	19(3)
C(36)	2534(13)	3698(4)	-1301(5)	18(1)
C(37)	-2603(10)	6229(3)	3222(3)	58(2)
C(38)	-3110(6)	6884(2)	2064(2)	18(1)
C(39)	-5972(10)	6172(4)	2511(4)	74(3)
C(40)	-2969(10)	7431(3)	3301(3)	45(2)
C(41)	-5698(7)	6719(2)	3749(2)	21(1)
C(42)	-6232(11)	7384(4)	2622(3)	64(2)
C(43)	-1094(11)	5255(3)	1129(4)	10(1)
C(44)	-404(16)	4787(5)	490(5)	8(2)
C(45)	1669(13)	4564(4)	425(5)	11(2)
C(46)	2269(12)	4147(4)	-221(5)	13(2)
C(47)	803(13)	3973(4)	-780(4)	9(2)
C(48)	-1386(16)	4197(5)	-700(6)	15(2)
C(49)	-1916(17)	4603(5)	-194(6)	7(2)
C(50)	1440(10)	3527(3)	-1432(4)	6(1)

**Table 35.** Bond lengths [Å] and angles [°] for hexamethylenetetramine terephthalic acid (**10**).

O(1)-C(1)	1.327(5)	O(3)-HO3	0.8400
O(1)-H(1)	0.8400	O(4)-C(8)	1.221(5)
O(2)-C(1)	1.234(5)	O(5)-C(15)	1.332(5)
O(3)-C(8)	1.300(4)	O(5)-H(5)	0.8400

O(6)-C(15)	1.224(5)	N(11)-C(42)	1.453(8)
O(7)-C(22)	1.318(5)	N(11)-C(40)	1.456(7)
O(7)-H#7	0.8400	N(11)-C(38)	1.474(6)
O(8)-C(22)	1.204(5)	N(12)-C(42)	1.422(10)
O(9)-C(29)	1.317(10)	N(12)-C(41)	1.457(6)
O(9)-H(9)	0.8400	N(12)-C(39)	1.475(7)
O(10)-C(29)	1.174(11)	C(1)-C(2)	1.482(5)
O(11)-C(36)	1.309(11)	C(2)-C(3)	1.389(5)
O(11)-H(11)	0.8400	C(2)-C(7)	1.407(5)
O(12)-C(36)	1.236(10)	C(3)-C(4)	1.388(5)
O(13)-C(43)	1.332(8)	C(3)-H(3)	0.9500
O(13)-H(13)	0.8400	C(4)-C(5)	1.390(5)
O(14)-C(43)	1.216(9)	C(4)-H(4)	1.05(4)
O(15)-C(50)	1.325(8)	C(5)-C(6)	1.417(5)
O(15)-H(15)	0.8400	C(5)-C(8)	1.488(5)
O(16)-C(50)	1.234(8)	C(6)-C(7)	1.379(5)
N(1)-C(10)	1.485(5)	C(6)-H(6)	1.01(4)
N(1)-C(11)	1.495(5)	C(7)-H(7)	0.91(4)
N(1)-C(9)	1.504(6)	C(9)-H(9A)	0.9900
N(2)-C(12)	1.450(6)	C(9)-H(9B)	0.9900
N(2)-C(11)	1.456(6)	C(10)-H(10A)	0.9900
N(2)-C(13)	1.483(6)	C(10)-H(10B)	0.9900
N(3)-C(10)	1.472(5)	C(11)-H(11A)	0.9900
N(3)-C(14)	1.483(5)	C(11)-H(11B)	0.9900
N(3)-C(12)	1.497(5)	C(12)-H(12A)	0.9900
N(4)-C(14)	1.444(6)	C(12)-H(12B)	0.9900
N(4)-C(9)	1.475(6)	C(13)-H(13A)	0.9900
N(4)-C(13)	1.482(6)	C(13)-H(13B)	0.9900
N(5)-C(25)	1.476(5)	C(14)-H(14A)	0.9900
N(5)-C(24)	1.474(5)	C(14)-H(14B)	0.9900
N(5)-C(23)	1.496(5)	C(15)-C(16)	1.478(5)
N(6)-C(25)	1.460(6)	C(16)-C(17)	1.386(6)
N(6)-C(27)	1.485(6)	C(16)-C(21)	1.416(6)
N(6)-C(26)	1.484(5)	C(17)-C(18)	1.373(5)
N(7)-C(28)	1.475(5)	C(17)-H(17)	1.17(4)
N(7)-C(24)	1.471(6)	C(18)-C(19)	1.413(5)
N(7)-C(26)	1.489(5)	C(18)-H(18)	1.02(4)
N(8)-C(23)	1.441(5)	C(19)-C(20)	1.413(5)
N(8)-C(28)	1.477(5)	C(19)-C(22)	1.491(6)
N(8)-C(27)	1.494(6)	C(20)-C(21)	1.391(6)
N(9)-C(38)	1.467(6)	C(20)-H(20)	0.95(4)
N(9)-C(39)	1.493(7)	C(21)-H(21)	0.99(6)
N(9)-C(37)	1.509(8)	C(23)-H(23A)	0.9900
N(10)-C(41)	1.442(6)	C(23)-H(23B)	0.9900
N(10)-C(40)	1.441(7)	C(24)-H(24A)	0.9900
N(10)-C(37)	1.440(8)	C(24)-H(24B)	0.9900

C(25)-H(25A)	0.9900	C(38)-H(38B)	0.9900
C(25)-H(25B)	0.9900	C(39)-H(39A)	0.9900
C(26)-H(26A)	0.9900	C(39)-H(39B)	0.9900
C(26)-H(26B)	0.9900	C(40)-H(40A)	0.9900
C(27)-H(27A)	0.9900	C(40)-H(40B)	0.9900
C(27)-H(27B)	0.9900	C(41)-H(41A)	0.9900
C(28)-H(28A)	0.9900	C(41)-H(41B)	0.9900
C(28)-H(28B)	0.9900	C(42)-H(42A)	0.9900
C(29)-C(30)	1.568(13)	C(42)-H(42B)	0.9900
C(30)-C(35)	1.157(17)	C(43)-C(44)	1.492(11)
C(30)-C(31)	1.351(13)	C(44)-C(45)	1.377(12)
C(31)-C(32)	1.410(11)	C(44)-C(49)	1.548(14)
C(31)-H(31)	0.9500	C(45)-C(46)	1.429(12)
C(32)-C(33)	1.378(10)	C(45)-H(45)	0.9500
C(32)-H(32)	0.9682	C(46)-C(47)	1.369(11)
C(33)-C(34)	1.414(11)	C(46)-H(32)	1.0872
C(33)-C(36)	1.524(10)	C(46)-H(46)	0.9500
C(34)-C(35)	1.600(17)	C(47)-C(48)	1.449(12)
C(34)-H(34)	0.9500	C(47)-C(50)	1.473(10)
C(35)-H(35)	0.9500	C(48)-C(49)	1.222(15)
C(37)-H(37A)	0.9900	C(48)-H(48)	0.9500
C(37)-H(37B)	0.9900	C(49)-H(49)	0.9500
C(38)-H(38A)	0.9900		
C(1)-O(1)-H(1)	109.5	C(25)-N(6)-C(27)	107.0(4)
C(8)-O(3)-HO3	109.5	C(25)-N(6)-C(26)	108.9(3)
C(15)-O(5)-H(5)	109.5	C(27)-N(6)-C(26)	108.3(3)
C(22)-O(7)-H#7	109.5	C(28)-N(7)-C(24)	108.3(3)
C(29)-O(9)-H(9)	109.5	C(28)-N(7)-C(26)	109.3(3)
C(36)-O(11)-H(11)	109.5	C(24)-N(7)-C(26)	108.2(3)
C(43)-O(13)-H(13)	109.5	C(23)-N(8)-C(28)	109.3(3)
C(50)-O(15)-H(15)	109.5	C(23)-N(8)-C(27)	108.4(3)
C(10)-N(1)-C(11)	107.4(3)	C(28)-N(8)-C(27)	105.7(4)
C(10)-N(1)-C(9)	107.0(3)	C(38)-N(9)-C(39)	108.1(5)
C(11)-N(1)-C(9)	109.0(3)	C(38)-N(9)-C(37)	106.4(4)
C(12)-N(2)-C(11)	108.6(3)	C(39)-N(9)-C(37)	108.6(4)
C(12)-N(2)-C(13)	106.7(4)	C(41)-N(10)-C(40)	108.2(4)
C(11)-N(2)-C(13)	109.3(4)	C(41)-N(10)-C(37)	109.5(5)
C(10)-N(3)-C(14)	108.6(3)	C(40)-N(10)-C(37)	108.2(4)
C(10)-N(3)-C(12)	107.9(3)	C(42)-N(11)-C(40)	108.0(4)
C(14)-N(3)-C(12)	108.9(3)	C(42)-N(11)-C(38)	109.9(5)
C(14)-N(4)-C(9)	107.6(3)	C(40)-N(11)-C(38)	108.7(4)
C(14)-N(4)-C(13)	110.3(4)	C(42)-N(12)-C(41)	109.4(5)
C(9)-N(4)-C(13)	107.1(4)	C(42)-N(12)-C(39)	108.5(5)
C(25)-N(5)-C(24)	109.0(3)	C(41)-N(12)-C(39)	109.1(5)
C(25)-N(5)-C(23)	107.6(3)	O(2)-C(1)-O(1)	123.9(3)
C(24)-N(5)-C(23)	107.2(3)	O(2)-C(1)-C(2)	120.4(4)

O(1)-C(1)-C(2)	115.6(3)	N(2)-C(13)-N(4)	112.7(3)
C(3)-C(2)-C(7)	119.7(4)	N(2)-C(13)-H(13A)	109.1
C(3)-C(2)-C(1)	120.9(3)	N(4)-C(13)-H(13A)	109.1
C(7)-C(2)-C(1)	119.3(3)	N(2)-C(13)-H(13B)	109.0
C(2)-C(3)-C(4)	121.1(4)	N(4)-C(13)-H(13B)	109.0
C(2)-C(3)-H(3)	119.5	H(13A)-C(13)-H(13B)	107.8
C(4)-C(3)-H(3)	119.5	N(4)-C(14)-N(3)	111.3(3)
C(3)-C(4)-C(5)	119.2(4)	N(4)-C(14)-H(14A)	109.4
C(3)-C(4)-H(4)	116(2)	N(3)-C(14)-H(14A)	109.4
C(5)-C(4)-H(4)	124(2)	N(4)-C(14)-H(14B)	109.4
C(4)-C(5)-C(6)	120.4(3)	N(3)-C(14)-H(14B)	109.4
C(4)-C(5)-C(8)	120.5(4)	H(14A)-C(14)-H(14B)	108.0
C(6)-C(5)-C(8)	119.1(3)	O(6)-C(15)-O(5)	121.9(3)
C(7)-C(6)-C(5)	119.6(3)	O(6)-C(15)-C(16)	123.7(4)
C(7)-C(6)-H(6)	115(2)	O(5)-C(15)-C(16)	114.3(3)
C(5)-C(6)-H(6)	125(2)	C(17)-C(16)-C(21)	119.3(4)
C(6)-C(7)-C(2)	120.0(4)	C(17)-C(16)-C(15)	122.4(4)
C(6)-C(7)-H(7)	123(3)	C(21)-C(16)-C(15)	118.3(4)
C(2)-C(7)-H(7)	117(3)	C(18)-C(17)-C(16)	120.3(4)
O(4)-C(8)-O(3)	123.4(3)	C(18)-C(17)-H(17)	122(2)
O(4)-C(8)-C(5)	121.7(3)	C(16)-C(17)-H(17)	117(2)
O(3)-C(8)-C(5)	114.9(3)	C(17)-C(18)-C(19)	121.0(4)
N(4)-C(9)-N(1)	112.2(3)	C(17)-C(18)-H(18)	118(2)
N(4)-C(9)-H(9A)	109.2	C(19)-C(18)-H(18)	121(2)
N(1)-C(9)-H(9A)	109.2	C(18)-C(19)-C(20)	119.6(4)
N(4)-C(9)-H(9B)	109.2	C(18)-C(19)-C(22)	119.6(3)
N(1)-C(9)-H(9B)	109.2	C(20)-C(19)-C(22)	120.8(3)
H(9A)-C(9)-H(9B)	107.9	C(21)-C(20)-C(19)	118.5(4)
N(3)-C(10)-N(1)	111.4(3)	C(21)-C(20)-H(20)	125(2)
N(3)-C(10)-H(10A)	109.4	C(19)-C(20)-H(20)	116(2)
N(1)-C(10)-H(10A)	109.4	C(20)-C(21)-C(16)	121.3(4)
N(3)-C(10)-H(10B)	109.4	C(20)-C(21)-H(21)	125(3)
N(1)-C(10)-H(10B)	109.3	C(16)-C(21)-H(21)	113(3)
H(10A)-C(10)-H(10B)	108.0	O(8)-C(22)-O(7)	124.1(4)
N(2)-C(11)-N(1)	111.8(3)	O(8)-C(22)-C(19)	122.0(4)
N(2)-C(11)-H(11A)	109.3	O(7)-C(22)-C(19)	113.8(4)
N(1)-C(11)-H(11A)	109.3	N(8)-C(23)-N(5)	112.5(3)
N(2)-C(11)-H(11B)	109.2	N(8)-C(23)-H(23A)	109.1
N(1)-C(11)-H(11B)	109.3	N(5)-C(23)-H(23A)	109.1
H(11A)-C(11)-H(11B)	107.9	N(8)-C(23)-H(23B)	109.1
N(2)-C(12)-N(3)	112.4(3)	N(5)-C(23)-H(23B)	109.1
N(2)-C(12)-H(12A)	109.1	H(23A)-C(23)-H(23B)	107.8
N(3)-C(12)-H(12A)	109.1	N(7)-C(24)-N(5)	111.9(3)
N(2)-C(12)-H(12B)	109.1	N(7)-C(24)-H(24A)	109.2
N(3)-C(12)-H(12B)	109.1	N(5)-C(24)-H(24A)	109.2
H(12A)-C(12)-H(12B)	107.9	N(7)-C(24)-H(24B)	109.2



N(5)-C(24)-H(24B)	109.2	C(34)-C(35)-H(35)	120.5
H(24A)-C(24)-H(24B)	107.9	O(12)-C(36)-O(11)	128.2(8)
N(6)-C(25)-N(5)	112.7(3)	O(12)-C(36)-C(33)	119.3(7)
N(6)-C(25)-H(25A)	109.1	O(11)-C(36)-C(33)	112.5(7)
N(5)-C(25)-H(25A)	109.1	N(10)-C(37)-N(9)	111.8(4)
N(6)-C(25)-H(25B)	109.1	N(10)-C(37)-H(37A)	109.3
N(5)-C(25)-H(25B)	109.0	N(9)-C(37)-H(37A)	109.3
H(25A)-C(25)-H(25B)	107.8	N(10)-C(37)-H(37B)	109.2
N(6)-C(26)-N(7)	110.5(3)	N(9)-C(37)-H(37B)	109.2
N(6)-C(26)-H(26A)	109.6	H(37A)-C(37)-H(37B)	107.9
N(7)-C(26)-H(26A)	109.6	N(9)-C(38)-N(11)	110.4(3)
N(6)-C(26)-H(26B)	109.5	N(9)-C(38)-H(38A)	109.6
N(7)-C(26)-H(26B)	109.5	N(11)-C(38)-H(38A)	109.6
H(26A)-C(26)-H(26B)	108.1	N(9)-C(38)-H(38B)	109.6
N(6)-C(27)-N(8)	112.9(3)	N(11)-C(38)-H(38B)	109.6
N(6)-C(27)-H(27A)	109.0	H(38A)-C(38)-H(38B)	108.1
N(8)-C(27)-H(27A)	109.0	N(12)-C(39)-N(9)	110.3(4)
N(6)-C(27)-H(27B)	109.0	N(12)-C(39)-H(39A)	109.6
N(8)-C(27)-H(27B)	109.0	N(9)-C(39)-H(39A)	109.6
H(27A)-C(27)-H(27B)	107.8	N(12)-C(39)-H(39B)	109.6
N(7)-C(28)-N(8)	112.3(3)	N(9)-C(39)-H(39B)	109.6
N(7)-C(28)-H(28A)	109.1	H(39A)-C(39)-H(39B)	108.1
N(8)-C(28)-H(28A)	109.1	N(10)-C(40)-N(11)	111.8(4)
N(7)-C(28)-H(28B)	109.1	N(10)-C(40)-H(40A)	109.3
N(8)-C(28)-H(28B)	109.1	N(11)-C(40)-H(40A)	109.3
H(28A)-C(28)-H(28B)	107.9	N(10)-C(40)-H(40B)	109.3
O(10)-C(29)-O(9)	125.3(9)	N(11)-C(40)-H(40B)	109.3
O(10)-C(29)-C(30)	122.4(8)	H(40A)-C(40)-H(40B)	107.9
O(9)-C(29)-C(30)	112.3(8)	N(10)-C(41)-N(12)	111.9(3)
C(35)-C(30)-C(31)	128.1(12)	N(10)-C(41)-H(41A)	109.2
C(35)-C(30)-C(29)	111.0(11)	N(12)-C(41)-H(41A)	109.2
C(31)-C(30)-C(29)	120.1(9)	N(10)-C(41)-H(41B)	109.2
C(30)-C(31)-C(32)	118.3(8)	N(12)-C(41)-H(41B)	109.2
C(30)-C(31)-H(31)	120.8	H(41A)-C(41)-H(41B)	107.9
C(32)-C(31)-H(31)	120.8	N(12)-C(42)-N(11)	111.4(4)
C(33)-C(32)-C(31)	119.7(7)	N(12)-C(42)-H(42A)	109.4
C(33)-C(32)-H(32)	118.1	N(11)-C(42)-H(42A)	109.4
C(31)-C(32)-H(32)	122.2	N(12)-C(42)-H(42B)	109.3
C(32)-C(33)-C(34)	120.8(7)	N(11)-C(42)-H(42B)	109.3
C(32)-C(33)-C(36)	119.6(7)	H(42A)-C(42)-H(42B)	108.0
C(34)-C(33)-C(36)	119.5(7)	O(14)-C(43)-O(13)	122.5(6)
C(33)-C(34)-C(35)	112.9(8)	O(14)-C(43)-C(44)	120.1(7)
C(33)-C(34)-H(34)	123.5	O(13)-C(43)-C(44)	117.4(7)
C(35)-C(34)-H(34)	123.6	C(45)-C(44)-C(43)	122.1(8)
C(30)-C(35)-C(34)	118.9(12)	C(45)-C(44)-C(49)	116.1(8)
C(30)-C(35)-H(35)	120.5	C(43)-C(44)-C(49)	121.4(8)

C(44)-C(45)-C(46)	119.8(8)	C(48)-C(47)-C(50)	120.8(7)
C(44)-C(45)-H(45)	120.1	C(49)-C(48)-C(47)	121.7(9)
C(46)-C(45)-H(45)	120.1	C(49)-C(48)-H(48)	119.1
C(47)-C(46)-C(45)	120.5(7)	C(47)-C(48)-H(48)	119.2
C(47)-C(46)-H(32)	155.5	C(48)-C(49)-C(44)	121.4(10)
C(45)-C(46)-H(32)	83.8	C(48)-C(49)-H(49)	119.3
C(47)-C(46)-H(46)	119.8	C(44)-C(49)-H(49)	119.3
C(45)-C(46)-H(46)	119.8	O(16)-C(50)-O(15)	124.4(6)
H(32)-C(46)-H(46)	36.2	O(16)-C(50)-C(47)	121.2(6)
C(46)-C(47)-C(48)	119.4(8)	O(15)-C(50)-C(47)	114.4
C(46)-C(47)-C(50)	119.6(7)		

**Table 36.** Anisotropic displacement parameters ( $\text{\AA}^2 \times 10^3$ ) for hexamethylenetetramine terephthalic acid, (10). the anisotropic displacement factor exponent takes the form:  $-2p^2[h^2 a^*2U^{11} + \dots + 2 h k a^* b^* U^{12}]$ .

	U <sup>11</sup>	U <sup>22</sup>	U <sup>33</sup>	U <sup>23</sup>	U <sup>13</sup>	U <sup>12</sup>
O(1)	21(1)	20(1)	19(1)	-13(1)	3(1)	-1(1)
O(2)	23(1)	19(1)	42(2)	-18(1)	-15(1)	4(1)
O(3)	12(1)	23(1)	23(1)	-14(1)	2(1)	-3(1)
O(4)	15(1)	31(2)	20(1)	-12(1)	-4(1)	-1(1)
O(5)	20(1)	25(1)	19(1)	-6(1)	3(1)	11(1)
O(6)	15(1)	32(2)	34(2)	-5(1)	-1(1)	5(1)
O(7)	24(2)	28(2)	34(2)	-24(1)	-11(1)	10(1)
O(8)	17(1)	44(2)	30(2)	-19(1)	-6(1)	10(1)
O(9)	20(1)	22(1)	21(1)	-1(1)	0(1)	-1(1)
O(10)	38(2)	39(2)	38(2)	-1(1)	1(1)	2(1)
O(11)	38(2)	37(2)	37(2)	-1(1)	0(1)	2(1)
O(12)	19(1)	21(1)	20(1)	1(1)	1(1)	0(1)
O(13)	12(1)	14(1)	16(1)	-3(1)	1(1)	-1(1)
O(14)	24(1)	25(1)	23(1)	-2(1)	-1(1)	0(1)
O(15)	14(1)	14(1)	13(1)	-2(1)	2(1)	0(1)
O(16)	7(1)	9(1)	8(1)	-3(1)	-1(1)	0(1)
N(1)	22(2)	16(2)	14(1)	-1(1)	-1(1)	-7(1)
N(2)	22(2)	39(2)	11(1)	2(1)	0(1)	1(2)
N(3)	22(2)	14(2)	13(1)	-2(1)	-1(1)	2(1)
N(4)	14(2)	44(2)	18(2)	0(1)	7(1)	6(1)
N(5)	11(1)	19(2)	17(1)	5(1)	0(1)	1(1)
N(6)	25(2)	25(2)	10(1)	3(1)	1(1)	3(1)
N(7)	11(1)	21(2)	9(1)	3(1)	0(1)	0(1)
N(8)	14(2)	30(2)	21(2)	10(1)	8(1)	2(1)
N(9)	45(2)	12(2)	47(2)	-7(2)	41(2)	-5(2)
N(10)	25(2)	59(3)	17(2)	19(2)	-4(1)	-4(2)
N(11)	61(3)	14(2)	16(2)	6(1)	18(2)	5(2)
N(12)	14(2)	87(4)	27(2)	-22(2)	2(1)	1(2)

C(1)	22(2)	10(2)	14(2)	-3(1)	-8(1)	1(1)
C(2)	13(2)	8(1)	16(2)	0(1)	-3(1)	-4(1)
C(3)	13(2)	13(2)	20(2)	1(1)	-6(1)	-1(1)
C(4)	12(2)	12(2)	24(2)	-1(1)	-5(1)	-1(1)
C(5)	18(2)	7(1)	11(2)	0(1)	-3(1)	-4(1)
C(6)	11(2)	15(2)	11(2)	-3(1)	2(1)	-1(1)
C(7)	13(2)	13(2)	11(2)	-1(1)	0(1)	-3(1)
C(8)	16(2)	12(2)	10(2)	-1(1)	3(1)	-5(1)
C(9)	17(2)	24(2)	27(2)	4(2)	1(2)	-8(2)
C(10)	24(2)	15(2)	9(2)	-1(1)	9(1)	5(2)
C(11)	19(2)	16(2)	20(2)	4(1)	-2(1)	-6(1)
C(12)	17(2)	24(2)	15(2)	-3(1)	-5(1)	5(1)
C(13)	23(2)	81(4)	14(2)	0(2)	10(2)	3(2)
C(14)	22(2)	29(2)	16(2)	-4(1)	-2(1)	12(2)
C(15)	13(2)	13(2)	18(2)	4(1)	4(1)	4(1)
C(16)	21(2)	9(2)	21(2)	1(1)	-1(1)	-1(1)
C(17)	15(2)	13(2)	17(2)	1(1)	0(1)	0(1)
C(18)	14(2)	15(2)	16(2)	6(1)	-3(1)	1(1)
C(19)	10(2)	10(2)	23(2)	-5(1)	-6(1)	3(1)
C(20)	16(2)	15(2)	27(2)	-5(1)	-9(2)	2(1)
C(21)	15(2)	14(2)	29(2)	-1(1)	-6(1)	-1(1)
C(22)	21(2)	16(2)	24(2)	-4(1)	-10(2)	0(1)
C(23)	11(2)	20(2)	28(2)	10(1)	1(1)	4(1)
C(24)	15(2)	24(2)	12(2)	4(2)	4(1)	4(2)
C(25)	23(2)	30(2)	11(2)	7(1)	0(1)	4(2)
C(26)	29(2)	21(2)	12(2)	1(1)	-2(1)	-2(2)
C(27)	28(2)	51(3)	14(2)	6(2)	14(2)	9(2)
C(28)	13(2)	19(2)	21(2)	2(1)	-1(1)	1(1)
C(29)	20(2)	19(2)	20(2)	0(1)	0(1)	1(1)
C(30)	11(2)	11(2)	11(2)	1(1)	1(1)	0(1)
C(31)	10(2)	10(2)	9(2)	-1(1)	0(1)	0(1)
C(33)	5(2)	5(2)	5(2)	0(1)	1(1)	0(1)
C(34)	9(2)	9(2)	7(2)	-1(1)	0(1)	-1(1)
C(35)	19(3)	19(3)	19(3)	0(1)	0(1)	0(1)
C(36)	19(2)	18(2)	18(2)	1(1)	1(1)	0(1)
C(37)	61(4)	55(4)	60(4)	45(3)	40(3)	49(3)
C(38)	19(2)	19(2)	16(2)	-2(2)	4(1)	6(2)
C(39)	55(4)	109(6)	59(4)	-74(4)	45(3)	-65(4)
C(40)	66(4)	48(3)	22(2)	-12(2)	11(2)	-48(3)
C(41)	27(2)	17(2)	18(2)	-4(1)	9(1)	-5(1)
C(42)	57(4)	112(6)	23(2)	11(3)	4(2)	68(4)
C(43)	11(1)	10(1)	10(1)	0(1)	-1(1)	0(1)
C(44)	8(2)	9(2)	8(2)	0(1)	-1(1)	-1(1)
C(45)	10(2)	12(2)	11(2)	0(1)	-1(1)	0(1)
C(46)	13(2)	13(2)	13(2)	0(1)	1(1)	0(1)
C(47)	9(2)	9(2)	9(2)	0(1)	0(1)	-1(1)

C(48)	14(2)	15(2)	15(2)	0(1)	-1(1)	0(1)
C(49)	7(2)	7(2)	8(2)	0(1)	0(1)	0(1)
C(50)	7(1)	5(1)	5(1)	0(1)	0(1)	0(1)

**Table 37.** Hydrogen coordinates ( $\times 10^4$ ) and isotropic displacement parameters ( $\text{\AA}^2 \times 10^3$ ) for hexamethylenetetramine terephthalic acid (**10**).

	x	y	z	U(eq)
H(1)	3073	5635	8482	24
HO3	10073	3230	4976	23
H(5)	1174	5538	5497	26
H#7	5309	3301	1293	35
H(9)	-1805	5564	1999	25
H(11)	2023	3245	-2179	45
H(13)	-3384	5591	1618	17
H(15)	3776	3215	-1904	17
H(3)	9173	4808	7631	18
H(9A)	-389	6597	8661	27
H(9B)	-459	6123	9423	27
H(10A)	5131	6903	8682	19
H(10B)	2971	7056	8211	19
H(11A)	2945	5861	10131	22
H(11B)	5116	6194	9826	22
H(12A)	5719	7406	9954	23
H(12B)	3936	7891	10327	23
H(13A)	687	7425	10763	47
H(13B)	213	6613	10671	47
H(14A)	664	8153	9581	26
H(14B)	280	7787	8757	26
H(23A)	-3114	6119	5484	23
H(23B)	-2804	5834	6349	23
H(24A)	1834	6938	5334	20
H(24B)	-353	6780	4883	20
H(25A)	435	6069	7056	25
H(25B)	2327	6495	6664	25
H(26A)	1916	7728	6416	25
H(26B)	-220	8112	6680	25
H(27A)	-3070	7444	7268	37
H(27B)	-2758	6634	7433	37
H(28A)	-3593	7357	5269	21
H(28B)	-3560	7865	6002	21
H(31)	1859	4731	1069	12
H(32)	3802	4127	76	12

H(34)	-1611	4146	-1267	10
H(35)	-3457	4635	-31	23
H(37A)	-2878	5782	3485	70
H(37B)	-1044	6282	3172	70
H(38A)	-3744	6902	1537	22
H(38B)	-1548	6932	2017	22
H(39A)	-6663	6191	1993	89
H(39B)	-6351	5724	2754	89
H(40A)	-1409	7486	3253	55
H(40B)	-3505	7821	3617	55
H(41A)	-6250	7097	4080	25
H(41B)	-6039	6273	4002	25
H(42A)	-6783	7775	2933	77
H(42B)	-6931	7400	2106	77
H(45)	2696	4687	809	13
H(46)	3696	3990	-263	16
H(48)	-2435	4023	-1049	18
H(49)	-3286	4811	-221	9
H(4)	10320(70)	4040(20)	6690(30)	18(11)
H(6)	3920(60)	4130(20)	5800(20)	6(8)
H(7)	3100(70)	4730(20)	6920(20)	11(9)
H(17)	5110(70)	4810(20)	4650(20)	19(11)
H(18)	6950(60)	4143(19)	3630(20)	2(8)
H(20)	1710(60)	4160(20)	2170(20)	8(9)
H(21)	-360(100)	4730(30)	3240(30)	51(17)

**Table 38.** Torsion angles [°] for hexamethylenetetramine terephthalic acid (**10**).

O(2)-C(1)-C(2)-C(3)	13.9(6)	C(6)-C(5)-C(8)-O(3)	167.6(3)
O(1)-C(1)-C(2)-C(3)	-169.2(3)	C(14)-N(4)-C(9)-N(1)	60.3(4)
O(2)-C(1)-C(2)-C(7)	-163.6(4)	C(13)-N(4)-C(9)-N(1)	-58.2(4)
O(1)-C(1)-C(2)-C(7)	13.4(5)	C(10)-N(1)-C(9)-N(4)	-58.4(4)
C(7)-C(2)-C(3)-C(4)	-1.0(5)	C(11)-N(1)-C(9)-N(4)	57.4(4)
C(1)-C(2)-C(3)-C(4)	-178.4(4)	C(14)-N(3)-C(10)-N(1)	-59.4(4)
C(2)-C(3)-C(4)-C(5)	1.2(6)	C(12)-N(3)-C(10)-N(1)	58.5(4)
C(3)-C(4)-C(5)-C(6)	-0.4(6)	C(11)-N(1)-C(10)-N(3)	-59.3(4)
C(3)-C(4)-C(5)-C(8)	-178.8(3)	C(9)-N(1)-C(10)-N(3)	57.5(4)
C(4)-C(5)-C(6)-C(7)	-0.6(5)	C(12)-N(2)-C(11)-N(1)	-59.4(4)
C(8)-C(5)-C(6)-C(7)	177.8(3)	C(13)-N(2)-C(11)-N(1)	56.7(4)
C(5)-C(6)-C(7)-C(2)	0.8(5)	C(10)-N(1)-C(11)-N(2)	59.6(4)
C(3)-C(2)-C(7)-C(6)	0.0(5)	C(9)-N(1)-C(11)-N(2)	-55.9(4)
C(1)-C(2)-C(7)-C(6)	177.5(3)	C(11)-N(2)-C(12)-N(3)	58.6(4)
C(4)-C(5)-C(8)-O(4)	164.1(4)	C(13)-N(2)-C(12)-N(3)	-59.2(4)
C(6)-C(5)-C(8)-O(4)	-14.2(5)	C(10)-N(3)-C(12)-N(2)	-58.2(4)
C(4)-C(5)-C(8)-O(3)	-14.1(5)	C(14)-N(3)-C(12)-N(2)	59.5(4)

C(12)-N(2)-C(13)-N(4)	58.0(6)	C(24)-N(7)-C(28)-N(8)	57.0(4)
C(11)-N(2)-C(13)-N(4)	-59.3(6)	C(26)-N(7)-C(28)-N(8)	-60.7(4)
C(14)-N(4)-C(13)-N(2)	-57.6(6)	C(23)-N(8)-C(28)-N(7)	-56.8(4)
C(9)-N(4)-C(13)-N(2)	59.2(6)	C(27)-N(8)-C(28)-N(7)	59.7(4)
C(9)-N(4)-C(14)-N(3)	-60.7(4)	O(10)-C(29)-C(30)-C(35)	2.1(15)
C(13)-N(4)-C(14)-N(3)	55.8(4)	O(9)-C(29)-C(30)-C(35)	-175.9(10)
C(10)-N(3)-C(14)-N(4)	61.0(4)	O(10)-C(29)-C(30)-C(31)	-168.6(9)
C(12)-N(3)-C(14)-N(4)	-56.2(4)	O(9)-C(29)-C(30)-C(31)	13.3(12)
O(6)-C(15)-C(16)-C(17)	-170.8(4)	C(35)-C(30)-C(31)-C(32)	8.4(17)
O(5)-C(15)-C(16)-C(17)	11.5(5)	C(29)-C(30)-C(31)-C(32)	177.4(7)
O(6)-C(15)-C(16)-C(21)	9.5(6)	C(30)-C(31)-C(32)-C(33)	0.9(12)
O(5)-C(15)-C(16)-C(21)	-168.2(3)	C(31)-C(32)-C(33)-C(34)	-2.1(11)
C(21)-C(16)-C(17)-C(18)	-1.0(6)	C(31)-C(32)-C(33)-C(36)	179.6(7)
C(15)-C(16)-C(17)-C(18)	179.3(4)	C(32)-C(33)-C(34)-C(35)	-2.9(11)
C(16)-C(17)-C(18)-C(19)	2.1(6)	C(36)-C(33)-C(34)-C(35)	175.4(8)
C(17)-C(18)-C(19)-C(20)	-1.3(6)	C(31)-C(30)-C(35)-C(34)	-14(2)
C(17)-C(18)-C(19)-C(22)	179.7(4)	C(29)-C(30)-C(35)-C(34)	176.2(9)
C(18)-C(19)-C(20)-C(21)	-0.6(6)	C(33)-C(34)-C(35)-C(30)	10.8(16)
C(22)-C(19)-C(20)-C(21)	178.4(4)	C(32)-C(33)-C(36)-O(12)	-12.7(11)
C(19)-C(20)-C(21)-C(16)	1.7(6)	C(34)-C(33)-C(36)-O(12)	168.9(7)
C(17)-C(16)-C(21)-C(20)	-0.9(6)	C(32)-C(33)-C(36)-O(11)	167.1(7)
C(15)-C(16)-C(21)-C(20)	178.8(4)	C(34)-C(33)-C(36)-O(11)	-11.2(10)
C(18)-C(19)-C(22)-O(8)	-12.2(6)	C(41)-N(10)-C(37)-N(9)	57.7(5)
C(20)-C(19)-C(22)-O(8)	168.8(4)	C(40)-N(10)-C(37)-N(9)	-60.0(6)
C(18)-C(19)-C(22)-O(7)	169.5(4)	C(38)-N(9)-C(37)-N(10)	60.1(5)
C(20)-C(19)-C(22)-O(7)	-9.5(6)	C(39)-N(9)-C(37)-N(10)	-56.1(6)
C(28)-N(8)-C(23)-N(5)	57.6(4)	C(39)-N(9)-C(38)-N(11)	57.4(5)
C(27)-N(8)-C(23)-N(5)	-57.2(4)	C(37)-N(9)-C(38)-N(11)	-59.1(4)
C(25)-N(5)-C(23)-N(8)	58.5(4)	C(42)-N(11)-C(38)-N(9)	-57.8(5)
C(24)-N(5)-C(23)-N(8)	-58.7(4)	C(40)-N(11)-C(38)-N(9)	60.2(5)
C(28)-N(7)-C(24)-N(5)	-59.2(4)	C(42)-N(12)-C(39)-N(9)	60.7(7)
C(26)-N(7)-C(24)-N(5)	59.1(4)	C(41)-N(12)-C(39)-N(9)	-58.4(7)
C(25)-N(5)-C(24)-N(7)	-57.0(4)	C(38)-N(9)-C(39)-N(12)	-59.2(7)
C(23)-N(5)-C(24)-N(7)	59.2(4)	C(37)-N(9)-C(39)-N(12)	55.9(7)
C(27)-N(6)-C(25)-N(5)	59.3(4)	C(41)-N(10)-C(40)-N(11)	-58.9(6)
C(26)-N(6)-C(25)-N(5)	-57.6(4)	C(37)-N(10)-C(40)-N(11)	59.6(6)
C(24)-N(5)-C(25)-N(6)	56.3(4)	C(42)-N(11)-C(40)-N(10)	59.4(7)
C(23)-N(5)-C(25)-N(6)	-59.6(4)	C(38)-N(11)-C(40)-N(10)	-59.9(6)
C(25)-N(6)-C(26)-N(7)	59.0(4)	C(40)-N(10)-C(41)-N(12)	57.5(5)
C(27)-N(6)-C(26)-N(7)	-57.0(4)	C(37)-N(10)-C(41)-N(12)	-60.2(5)
C(28)-N(7)-C(26)-N(6)	58.0(4)	C(42)-N(12)-C(41)-N(10)	-57.9(5)
C(24)-N(7)-C(26)-N(6)	-59.7(4)	C(39)-N(12)-C(41)-N(10)	60.7(5)
C(25)-N(6)-C(27)-N(8)	-57.6(5)	C(41)-N(12)-C(42)-N(11)	58.3(6)
C(26)-N(6)-C(27)-N(8)	59.7(5)	C(39)-N(12)-C(42)-N(11)	-60.6(6)
C(23)-N(8)-C(27)-N(6)	57.4(5)	C(40)-N(11)-C(42)-N(12)	-58.8(6)
C(28)-N(8)-C(27)-N(6)	-59.7(5)	C(38)-N(11)-C(42)-N(12)	59.6(5)

O(14)-C(43)-C(44)-C(45)14.3(12)  
O(13)-C(43)-C(44)-C(45)-165.9(7)  
O(14)-C(43)-C(44)-C(49)-157.9(8)  
O(13)-C(43)-C(44)-C(49)22.0(11)  
C(43)-C(44)-C(45)-C(46)-176.7(7)  
C(49)-C(44)-C(45)-C(46)-4.1(12)  
C(44)-C(45)-C(46)-C(47)0.6(12)  
C(45)-C(46)-C(47)-C(48)-1.9(12)  
C(45)-C(46)-C(47)-C(50)-178.4(7)  
C(46)-C(47)-C(48)-C(49)8.5(14)  
C(50)-C(47)-C(48)-C(49)-175.0(9)  
C(47)-C(48)-C(49)-C(44)-12.7(16)  
C(45)-C(44)-C(49)-C(48)10.7(15)  
C(43)-C(44)-C(49)-C(48)-176.7(9)  
C(46)-C(47)-C(50)-O(16)163.4(7)  
C(48)-C(47)-C(50)-O(16)-13.0(11)  
C(46)-C(47)-C(50)-O(15)-15.9(10)  
C(48)-C(47)-C(50)-O(15)167.6(7)



**Table 39.** Hydrogen bonds for hexamethylenetetramine terephthalic acid (**10**) [ $\text{\AA}$  and  $^\circ$ ]

D-H...A	d(D-H)	d(H...A)	d(D...A)	$\angle(\text{DHA})$
O(1)-H(1)...N(1)	0.84	1.79	2.611(4)	166.4
O(3)-HO3...N(7)#1	0.84	1.81	2.643(4)	169.1
O(5)-H(5)...N(5)	0.84	1.83	2.602(4)	153.1
O(7)-H#7...N(3)#1	0.84	1.84	2.643(4)	160.1
O(9)-H(9)...N(9)	0.84	1.85	2.650(7)	158.3
O(13)-H(13...N(9)	0.84	1.85	2.687(7)	175.0
O(15)-H(15)...N(11)#2	0.84	1.82	2.633(6)	162.0
O(11)-H(11)...N(11)#2	0.84	2.04	2.808(8)	152.7

Symmetry transformations used to generate equivalent atoms:  
 #1  $-x+1, y-1/2, -z+1$  #2  $-x, y-1/2, -z$

**Table 40.** Crystal data and structure refinement for [bis( $\mu_2$ -terephthalato)-( $\mu_2$ -hexamethylenetetramino)-diaqua-dinickel (II) dihydrate] (**11**).

Empirical formula	$\text{C}_{28} \text{H}_{56} \text{N}_8 \text{Ni} \text{O}_{10} \text{S}_4$	
Formula weight	795.31 $\text{g.mol}^{-1}$	
Temperature	208(2) K	
Wavelength	0.71073 $\text{\AA}$	
Crystal system	Triclinic	
Space group	$P-1$	
Unit cell dimensions	$a = 10.1851(9) \text{\AA}$ $b = 10.4428(8) \text{\AA}$ $c = 10.9767(8) \text{\AA}$	$\alpha = 67.589(5)^\circ$ $\beta = 74.153(6)^\circ$ $\gamma = 67.140(7)^\circ$
Volume	983.78(14) $\text{\AA}^3$	
Z	1	
Density (calculated)	1.342 $\text{mg/m}^3$	
Absorption coefficient	0.763 $\text{mm}^{-1}$	
F(000)	396	
Theta range for data collection	2.03 to 27.50 $^\circ$	
Index ranges	$-1 \leq h \leq 8, -12 \leq k \leq 12, -13 \leq l \leq 14$	
Reflections collected	3882	
Independent reflections	3238 [R(int) = 0.0242]	
Completeness to theta = 27.50 $^\circ$	71.4 %	
Refinement method	Full-matrix least-squares on F <sup>2</sup>	
Data / restraints / parameters	3238 / 0 / 244	

Goodness-of-fit on $F^2$	1.025
Final R indices [ $I > 2\sigma(I)$ ]	$R1 = 0.0408$ , $wR2 = 0.0886$
R indices (all data)	$R1 = 0.0579$ , $wR2 = 0.0964$
Largest diff. peak and hole	0.576 and -0.570 e.Å <sup>-3</sup>

**Table 41.** Atomic coordinates ( $\times 10^4$ ) and equivalent isotropic displacement parameters ( $\text{Å}^2 \times 10^3$ ) for [bis ( $\mu_2$ -terephthalato)-( $\mu_2$ -hexamethylenetetramino)-diaqua-dinickel (II) dihydrate] (11).  $U(\text{eq})$  is defined as one third of the trace of the orthogonalized  $U_{ij}$  tensor.

	x	y	z	$U(\text{eq})$
Ni(1)	0	0	0	16(1)
S(1)	-2135(1)	2156(1)	-4510(1)	43(1)
S(2)	2374(1)	2978(1)	-4815(1)	55(1)
O(1)	-517(3)	-750(2)	2025(2)	22(1)
O(2)	1808(2)	-1809(2)	84(2)	20(1)
O(3)	2646(2)	-1658(2)	-2056(2)	37(1)
O(4)	-1004(3)	2411(3)	-4088(2)	50(1)
O(5)	3742(4)	3337(4)	-5161(3)	78(1)
N(1)	-1307(3)	-1261(2)	-51(2)	18(1)
N(2)	-2124(3)	-2070(3)	-1463(3)	27(1)
N(3)	-3716(3)	-1535(3)	515(3)	27(1)
N(4)	-1584(3)	-3705(3)	762(3)	26(1)
C(1)	2687(3)	-2264(3)	-841(3)	20(1)
C(2)	3890(3)	-3686(3)	-402(3)	16(1)
C(3)	3941(3)	-4467(3)	939(3)	19(1)
C(4)	4967(3)	-4233(3)	-1347(3)	20(1)
C(5)	-2852(3)	-699(3)	511(3)	23(1)
C(6)	-3086(4)	-3067(3)	1297(3)	28(1)
C(7)	-3612(3)	-1480(3)	-867(3)	29(1)
C(8)	-1541(4)	-3592(3)	-626(3)	29(1)
C(9)	-750(3)	-2835(3)	755(3)	24(1)
C(10)	-1275(3)	-1237(3)	-1425(3)	24(1)
C(11)	-2403(5)	3453(5)	-6107(4)	60(1)
C(12)	-3775(5)	2974(5)	-3628(4)	63(1)
C(13)	1405(5)	4102(5)	-6170(4)	54(1)
C(14)	2816(5)	1270(5)	-5088(4)	66(1)

**Table 42.** Bond lengths [Å] and angles [°] for [bis ( $\mu_2$ -terephthalato)-( $\mu_2$ -

hexamethylenetetramino)-diaqua-dinickel (II) dihydrate] (11).

Ni(1)-O(1)	2.046(2)	C(2)-C(4)	1.396(4)
Ni(1)-O(1)#1	2.046(2)	C(3)-C(4)#2	1.385(4)
Ni(1)-O(2)	2.0556(18)	C(3)-H(3)	0.9400
Ni(1)-O(2)#1	2.0556(18)	C(4)-C(3)#2	1.385(4)
Ni(1)-N(1)	2.229(2)	C(4)-H(4)	0.9400
Ni(1)-N(1)#1	2.229(2)	C(5)-H(5A)	0.9800
S(1)-O(4)	1.495(3)	C(5)-H(5B)	0.9800
S(1)-C(12)	1.759(4)	C(6)-H(6A)	0.9800
S(1)-C(11)	1.774(4)	C(6)-H(6B)	0.9800
S(2)-O(5)	1.495(3)	C(7)-H(7A)	0.9800
S(2)-C(13)	1.770(4)	C(7)-H(7B)	0.9800
S(2)-C(14)	1.783(5)	C(8)-H(8A)	0.9800
O(1)-H(1)	0.76(4)	C(8)-H(8B)	0.9800
O(1)-H(2)	0.77(4)	C(9)-H(9A)	0.9800
O(2)-C(1)	1.264(3)	C(9)-H(9B)	0.9800
O(3)-C(1)	1.244(3)	C(10)-H(10A)	0.9800
N(1)-C(10)	1.490(3)	C(10)-H(10B)	0.9800
N(1)-C(5)	1.493(4)	C(11)-H(11A)	0.9700
N(1)-C(9)	1.499(3)	C(11)-H(11B)	0.9700
N(2)-C(10)	1.462(4)	C(11)-H(11C)	0.9700
N(2)-C(7)	1.465(4)	C(12)-H(12A)	0.9700
N(2)-C(8)	1.474(4)	C(12)-H(12B)	0.9700
N(3)-C(5)	1.460(4)	C(12)-H(12C)	0.9700
N(3)-C(6)	1.471(4)	C(13)-H(13A)	0.9700
N(3)-C(7)	1.471(4)	C(13)-H(13B)	0.9700
N(4)-C(9)	1.462(4)	C(13)-H(13C)	0.9700
N(4)-C(6)	1.465(4)	C(14)-H(14A)	0.9700
N(4)-C(8)	1.472(4)	C(14)-H(14B)	0.9700
C(1)-C(2)	1.517(4)	C(14)-H(14C)	0.9700
C(2)-C(3)	1.388(4)		
O(1)-Ni(1)-O(1)#1	180.0(2)	O(2)#1-Ni(1)-N(1)#1	90.02(8)
O(1)-Ni(1)-O(2)	89.77(8)	N(1)-Ni(1)-N(1)#1	180.00(11)
O(1)#1-Ni(1)-O(2)	90.23(8)	O(4)-S(1)-C(12)	105.37(19)
O(1)-Ni(1)-O(2)#1	90.23(8)	O(4)-S(1)-C(11)	105.57(18)
O(1)#1-Ni(1)-O(2)#1	89.77(8)	C(12)-S(1)-C(11)	97.3(2)
O(2)-Ni(1)-O(2)#1	180.00(15)	O(5)-S(2)-C(13)	105.9(2)
O(1)-Ni(1)-N(1)	85.18(9)	O(5)-S(2)-C(14)	106.9(2)
O(1)#1-Ni(1)-N(1)	94.82(9)	C(13)-S(2)-C(14)	97.8(2)
O(2)-Ni(1)-N(1)	90.02(8)	Ni(1)-O(1)-H(1)	106(3)
O(2)#1-Ni(1)-N(1)	89.98(8)	Ni(1)-O(1)-H(2)	134(3)
O(1)-Ni(1)-N(1)#1	94.82(9)	H(1)-O(1)-H(2)	105(4)
O(1)#1-Ni(1)-N(1)#1	85.18(9)	C(1)-O(2)-Ni(1)	130.31(18)
O(2)-Ni(1)-N(1)#1	89.98(8)	C(10)-N(1)-C(5)	107.1(2)

C(10)-N(1)-C(9)	106.8(2)	N(2)-C(8)-H(8A)	109.1
C(5)-N(1)-C(9)	106.9(2)	N(4)-C(8)-H(8B)	109.1
C(10)-N(1)-Ni(1)	112.71(18)	N(2)-C(8)-H(8B)	109.1
C(5)-N(1)-Ni(1)	112.34(16)	H(8A)-C(8)-H(8B)	107.8
C(9)-N(1)-Ni(1)	110.70(17)	N(4)-C(9)-N(1)	112.7(2)
C(10)-N(2)-C(7)	108.8(2)	N(4)-C(9)-H(9A)	109.1
C(10)-N(2)-C(8)	107.9(2)	N(1)-C(9)-H(9A)	109.1
C(7)-N(2)-C(8)	107.7(2)	N(4)-C(9)-H(9B)	109.1
C(5)-N(3)-C(6)	108.2(2)	N(1)-C(9)-H(9B)	109.1
C(5)-N(3)-C(7)	108.0(2)	H(9A)-C(9)-H(9B)	107.8
C(6)-N(3)-C(7)	108.2(2)	N(2)-C(10)-N(1)	112.9(2)
C(9)-N(4)-C(6)	108.4(2)	N(2)-C(10)-H(10A)	109.0
C(9)-N(4)-C(8)	108.1(2)	N(1)-C(10)-H(10A)	109.0
C(6)-N(4)-C(8)	107.8(2)	N(2)-C(10)-H(10B)	109.0
O(3)-C(1)-O(2)	126.1(2)	N(1)-C(10)-H(10B)	109.0
O(3)-C(1)-C(2)	118.1(2)	H(10A)-C(10)-H(10B)	107.8
O(2)-C(1)-C(2)	115.8(2)	S(1)-C(11)-H(11A)	109.5
C(3)-C(2)-C(4)	118.8(2)	S(1)-C(11)-H(11B)	109.5
C(3)-C(2)-C(1)	120.9(2)	H(11A)-C(11)-H(11B)	109.5
C(4)-C(2)-C(1)	120.3(2)	S(1)-C(11)-H(11C)	109.5
C(4)#2-C(3)-C(2)	121.2(3)	H(11A)-C(11)-H(11C)	109.5
C(4)#2-C(3)-H(3)	119.4	H(11B)-C(11)-H(11C)	109.5
C(2)-C(3)-H(3)	119.4	S(1)-C(12)-H(12A)	109.5
C(3)#2-C(4)-C(2)	119.9(3)	S(1)-C(12)-H(12B)	109.5
C(3)#2-C(4)-H(4)	120.0	H(12A)-C(12)-H(12B)	109.5
C(2)-C(4)-H(4)	120.0	S(1)-C(12)-H(12C)	109.5
N(3)-C(5)-N(1)	113.0(2)	H(12A)-C(12)-H(12C)	109.5
N(3)-C(5)-H(5A)	109.0	H(12B)-C(12)-H(12C)	109.5
N(1)-C(5)-H(5A)	109.0	S(2)-C(13)-H(13A)	109.5
N(3)-C(5)-H(5B)	109.0	S(2)-C(13)-H(13B)	109.5
N(1)-C(5)-H(5B)	109.0	H(13A)-C(13)-H(13B)	109.5
H(5A)-C(5)-H(5B)	107.8	S(2)-C(13)-H(13C)	109.5
N(4)-C(6)-N(3)	112.4(3)	H(13A)-C(13)-H(13C)	109.5
N(4)-C(6)-H(6A)	109.1	H(13B)-C(13)-H(13C)	109.5
N(3)-C(6)-H(6A)	109.1	S(2)-C(14)-H(14A)	109.5
N(4)-C(6)-H(6B)	109.1	S(2)-C(14)-H(14B)	109.5
N(3)-C(6)-H(6B)	109.1	H(14A)-C(14)-H(14B)	109.5
H(6A)-C(6)-H(6B)	107.8	S(2)-C(14)-H(14C)	109.5
N(2)-C(7)-N(3)	112.4(2)	H(14A)-C(14)-H(14C)	109.5
N(2)-C(7)-H(7A)	109.1	H(14B)-C(14)-H(14C)	109.5
N(3)-C(7)-H(7A)	109.1		
N(2)-C(7)-H(7B)	109.1		
N(3)-C(7)-H(7B)	109.1		
H(7A)-C(7)-H(7B)	107.9		
N(4)-C(8)-N(2)	112.6(2)		
N(4)-C(8)-H(8A)	109.1		

Symmetry transformations used to generate equivalent atoms:  
 #1 -x,-y,-z #2 -x+1,-y-1,-z

**Table 43.** Anisotropic displacement parameters ( $\text{\AA}^2 \times 10^3$ ) for [bis ( $\mu_2$ -terephthalato)-( $\mu_2$ -hexamethylenetetramino)-diaqua-dinickel (II) dihydrate] (11). The anisotropic displacement factor exponent takes the form:  $-2p^2[h^2 a^2 U_{11} + \dots + 2 h k a^* b^* U_{12}]$ .

	U11	U22	U33	U23	U13	U12
Ni(1)	12(1)	13(1)	20(1)	-5(1)	-4(1)	-1(1)
S(1)	45(1)	35(1)	47(1)	-3(1)	-19(1)	-11(1)
S(2)	67(1)	76(1)	33(1)	-18(1)	1(1)	-40(1)
O(1)	19(1)	19(1)	20(1)	-4(1)	-4(1)	-1(1)
O(2)	14(1)	16(1)	27(1)	-7(1)	-4(1)	-1(1)
O(3)	36(2)	31(1)	26(1)	-9(1)	-8(1)	10(1)
O(4)	33(2)	62(2)	47(2)	6(1)	-23(1)	-18(1)
O(5)	72(3)	103(3)	81(2)	-17(2)	-24(2)	-53(2)
N(1)	14(2)	14(1)	24(1)	-4(1)	-4(1)	-3(1)
N(2)	27(2)	25(1)	35(1)	-12(1)	-8(1)	-8(1)
N(3)	16(2)	23(1)	42(2)	-11(1)	-4(1)	-7(1)
N(4)	23(2)	19(1)	37(1)	-7(1)	-6(1)	-8(1)
C(1)	14(2)	16(1)	30(2)	-8(1)	-6(1)	-3(1)
C(2)	11(2)	12(1)	27(1)	-7(1)	-6(1)	-4(1)
C(3)	12(2)	19(1)	27(1)	-11(1)	-1(1)	-3(1)
C(4)	19(2)	17(1)	22(1)	-4(1)	-5(1)	-5(1)
C(5)	14(2)	22(2)	35(2)	-12(1)	-2(1)	-6(1)
C(6)	23(2)	24(2)	38(2)	-5(1)	-4(1)	-14(1)
C(7)	20(2)	25(2)	45(2)	-11(1)	-12(2)	-6(1)
C(8)	25(2)	22(2)	44(2)	-16(1)	-7(2)	-6(1)
C(9)	20(2)	17(1)	33(2)	-3(1)	-10(1)	-4(1)
C(10)	23(2)	22(2)	26(1)	-6(1)	-6(1)	-8(1)
C(11)	78(4)	67(3)	38(2)	-4(2)	-29(2)	-23(2)
C(12)	42(3)	87(3)	58(3)	-17(2)	-8(2)	-22(2)
C(13)	56(3)	68(3)	48(2)	-19(2)	1(2)	-36(2)
C(14)	74(4)	65(3)	55(3)	-14(2)	-5(2)	-26(3)

**Table 44.** Hydrogen coordinates ( $\times 10^4$ ) and isotropic displacement parameters ( $\text{\AA}^2 \times 10^3$ ) for [bis ( $\mu_2$ -terephthalato)-( $\mu_2$ -hexamethylenetetramino)-Diaqua-Dinickel (II) dihydrate] (11).

	x	y	z	U(eq)
H(3)	3220	-4105	1581	23
H(4)	4951	-3718	-2259	24
H(5A)	-2909	-728	1427	27
H(5B)	-3258	324	-12	27
H(6A)	-3137	-3118	2219	34
H(6B)	-3656	-3643	1308	34
H(7A)	-4184	-2041	-883	34
H(7B)	-4021	-464	-1403	34
H(8A)	-2098	-4168	-638	35
H(8B)	-542	-4008	-1005	35
H(9A)	256	-3250	391	29
H(9B)	-774	-2895	1673	29
H(10A)	-1646	-221	-1979	29
H(10B)	-274	-1640	-1808	29
H(11A)	-2644	4428	-6056	90
H(11B)	-3185	3394	-6405	90
H(11C)	-1528	3247	-6732	90
H(12A)	-3779	2465	-2682	95
H(12B)	-4566	2918	-3915	95
H(12C)	-3884	3991	-3803	95
H(13A)	1226	5121	-6283	81
H(13B)	494	3923	-5993	81
H(13C)	1964	3878	-6976	81
H(14A)	3420	1286	-5943	99
H(14B)	1939	1108	-5082	99
H(14C)	3329	489	-4386	99
H(1)	-1120(40)	-120(40)	2220(40)	39(11)
H(2)	-70(50)	-1160(40)	2610(40)	53(13)

**Table 45.** Torsion angles [°] for [bis ( $\mu_2$ -terephthalato)-( $\mu_2$ -hexamethylenetetramino)-diaqua-dinickel (II) dihydrate], (**11**).

O(1)-Ni(1)-O(2)-C(1)	171.0(3)
O(1)#1-Ni(1)-O(2)-C(1)	-9.0(3)
O(2)#1-Ni(1)-O(2)-C(1)	-109(100)
N(1)-Ni(1)-O(2)-C(1)	85.9(3)
N(1)#1-Ni(1)-O(2)-C(1)	-94.1(3)
O(1)-Ni(1)-N(1)-C(10)	-175.77(18)
O(1)#1-Ni(1)-N(1)-C(10)	4.23(18)
O(2)-Ni(1)-N(1)-C(10)	-86.01(17)
O(2)#1-Ni(1)-N(1)-C(10)	93.99(17)
N(1)#1-Ni(1)-N(1)-C(10)	136(100)
O(1)-Ni(1)-N(1)-C(5)	63.15(18)
O(1)#1-Ni(1)-N(1)-C(5)	-116.85(18)
O(2)-Ni(1)-N(1)-C(5)	152.91(18)
O(2)#1-Ni(1)-N(1)-C(5)	-27.09(18)
N(1)#1-Ni(1)-N(1)-C(5)	15(100)
O(1)-Ni(1)-N(1)-C(9)	-56.27(18)
O(1)#1-Ni(1)-N(1)-C(9)	123.73(18)
O(2)-Ni(1)-N(1)-C(9)	33.49(18)
O(2)#1-Ni(1)-N(1)-C(9)	-146.51(18)
N(1)#1-Ni(1)-N(1)-C(9)	-104(100)
Ni(1)-O(2)-C(1)-O(3)	1.6(5)
Ni(1)-O(2)-C(1)-C(2)	-178.13(18)
O(3)-C(1)-C(2)-C(3)	-175.6(3)
O(2)-C(1)-C(2)-C(3)	4.1(4)
O(3)-C(1)-C(2)-C(4)	4.3(4)
O(2)-C(1)-C(2)-C(4)	-175.9(3)
C(4)-C(2)-C(3)-C(4)#2	-0.1(5)
C(1)-C(2)-C(3)-C(4)#2	179.9(3)
C(3)-C(2)-C(4)-C(3)#2	0.1(5)
C(1)-C(2)-C(4)-C(3)#2	-179.9(3)
C(6)-N(3)-C(5)-N(1)	58.4(3)
C(7)-N(3)-C(5)-N(1)	-58.5(3)
C(10)-N(1)-C(5)-N(3)	57.1(3)
C(9)-N(1)-C(5)-N(3)	-57.0(3)
Ni(1)-N(1)-C(5)-N(3)	-178.64(18)
C(9)-N(4)-C(6)-N(3)	58.9(3)
C(8)-N(4)-C(6)-N(3)	-58.0(3)
C(5)-N(3)-C(6)-N(4)	-58.8(3)
C(7)-N(3)-C(6)-N(4)	58.1(3)
C(10)-N(2)-C(7)-N(3)	-58.3(3)
C(8)-N(2)-C(7)-N(3)	58.3(3)
C(5)-N(3)-C(7)-N(2)	58.6(3)
C(6)-N(3)-C(7)-N(2)	-58.3(3)



C(9)-N(4)-C(8)-N(2)	-58.6(3)
C(6)-N(4)-C(8)-N(2)	58.4(3)
C(10)-N(2)-C(8)-N(4)	58.7(3)
C(7)-N(2)-C(8)-N(4)	-58.6(3)
C(6)-N(4)-C(9)-N(1)	-58.3(3)
C(8)-N(4)-C(9)-N(1)	58.4(3)
C(10)-N(1)-C(9)-N(4)	-57.6(3)
C(5)-N(1)-C(9)-N(4)	56.8(3)
Ni(1)-N(1)-C(9)-N(4)	179.42(18)
C(7)-N(2)-C(10)-N(1)	57.7(3)
C(8)-N(2)-C(10)-N(1)	-58.8(3)
C(5)-N(1)-C(10)-N(2)	-56.3(3)
C(9)-N(1)-C(10)-N(2)	57.9(3)
Ni(1)-N(1)-C(10)-N(2)	179.66(17)

Symmetry transformations used to generate equivalent atoms:

#1 -x,-y,-z #2 -x+1,-y-1,-z

**Table 46.** Hydrogen bonds for [bis ( $\mu_2$ -terephthalato)-( $\mu_2$ -hexamethylenetetramino)-diaqua-dinickel (II) dihydrate] (**11**) [ $\text{\AA}$  and  $^\circ$ ].

D-H...A	d(D-H)	d(H...A)	d(D...A)	$\angle(\text{DHA})$
O(1)-H(1) ...O(3)#1	0.76(4)	1.88(4)	2.610(3)	159(4)
O(1)-H(2) ...O(4)#1	0.77(4)	1.94(4)	2.715(3)	173(4)
C(12)-H(12B...O(5)#3	0.97	2.30	3.234(5)	162.3

Symmetry transformations used to generate equivalent atoms:

#1 -x,-y,-z. #2 -x+1,-y-1,-z. #3 x-1,y,z

**Table 47.** Crystal data and structure refinement for-[bis ( $\mu_2$ -terephthalato) - ( $\mu_2$ -hexamethylenetetramino)-diaqua-dizinc (II) dihydrate] (**12**).

Empirical formula	$\text{C}_{28} \text{H}_{42} \text{N}_8 \text{O}_{13} \text{Zn}_2$	
Formula weight	$829.44 \text{ g mol}^{-1}$	
Temperature	298(2) K	
Wavelength	0.71073 $\text{\AA}$	
Crystal system	monoclinic	
Space group	$P2_1/m$	
Unit cell dimensions	$a = 10.0437(15) \text{ \AA}$ $b = 16.964(3) \text{ \AA}$ $c = 10.6795(15) \text{ \AA}$	$\alpha = 90^\circ$ $\beta = 114.123(11)^\circ$ $\gamma = 90^\circ$
Volume	$1660.7(4) \text{ \AA}^3$	
Z	2	

Density (calculated)	1.659 mg/m <sup>3</sup>
Absorption coefficient	1.523 mm <sup>-1</sup>
F(000)	860
Crystal size	? x ? x ? mm <sup>3</sup>
Theta range for data collection	2.09 to 25.35°.
Index ranges	-1 ≤ h ≤ 12, -1 ≤ k ≤ 20, -12 ≤ l ≤ 12
Reflections collected	3981
Independent reflections	3152 [R(int) = 0.0375]
Completeness to theta = 25.35°	100.0 %
Refinement method	Full-matrix least-squares on F <sup>2</sup>
Data / restraints / parameters	3152 / 4 / 276
Goodness-of-fit on F <sup>2</sup>	1.051
Final R indices [I > 2σ(I)]	R1 = 0.0526, wR2 = 0.1011
R indices (all data)	R1 = 0.0931, wR2 = 0.1148
Largest diff. peak and hole	0.737 and -0.482 e.Å <sup>-3</sup>

**Table 48.** Atomic coordinates ( $\times 10^4$ ) and equivalent isotropic displacement parameters ( $\text{\AA}^2 \times 10^3$ ) for [bis ( $\mu_2$ -terephthalato)-( $\mu_2$ -hexamethylenetetramino)-diaqua-dizinc (II) dihydrate] (**12**). U(eq) is defined as one third of the trace of the orthogonalized  $U^{ij}$  tensor.

	x	y	z	U(eq)
Zn(1)	2471(1)	2500	2410(1)	25(1)
Zn(2)	0	5000	5000	24(1)
O(1)	1867(3)	5061(2)	6724(3)	27(1)
O(2)	2445(4)	3798(2)	7212(3)	50(1)
O(3)	3945(5)	2500	4424(4)	27(1)
O(4)	5863(5)	2500	3891(5)	46(2)
O(5)	8609(8)	2500	11363(6)	94(3)
O(6)	10498(6)	2500	10854(5)	39(1)
O(7)	235(4)	6197(2)	4680(4)	31(1)
O(8)	3695(8)	2500	1365(7)	53(2)
N(1)	2321(4)	3793(2)	2619(4)	22(1)
N(2)	3645(4)	5032(2)	3502(4)	28(1)
N(3)	1406(4)	5048(2)	1418(4)	28(1)
N(4)	1295(4)	4791(2)	3637(4)	23(1)
C(1)	5299(7)	2500	4733(7)	24(2)
C(2)	6301(7)	2500	6254(6)	22(2)
C(3)	7795(7)	2500	6691(6)	23(2)
C(4)	8729(7)	2500	8057(7)	29(2)
C(5)	8151(7)	2500	9047(6)	23(2)
C(6)	9153(9)	2500	10550(7)	33(2)

C(7)	6665(7)	2500	8614(7)	27(2)
C(8)	5738(7)	2500	7241(7)	27(2)
C(9)	1567(6)	4197(3)	1263(5)	29(1)
C(10)	3776(5)	4191(3)	3327(5)	28(1)
C(11)	1470(5)	3944(3)	3441(4)	22(1)
C(12)	2775(5)	5147(3)	4303(5)	26(1)
C(13)	572(5)	5156(3)	2241(5)	29(1)
C(14)	2861(5)	5390(3)	2145(5)	33(1)
C(15)	2637(5)	4514(3)	7485(5)	29(1)
C(16)	3860(5)	4765(3)	8784(5)	24(1)
C(17)	4795(4)	4214(3)	9674(3)	29(1)
O(9)	8568(4)	2500(3)	13780(3)	37(1)
O(10)	2801(4)	2500(3)	-1231(3)	67(2)
C(18)	4072(5)	5552(3)	9142(5)	30(1)

**Table 49.** Bond lengths [Å] and angles [°] for [bis ( $\mu_2$ -terephthalato)-( $\mu_2$ -hexamethylenetetramino)-diaqua-dizinc (II) dihydrate] (**12**).

Zn(1)-O(8)	1.968(7)	N(1)-C(10)	1.503(6)
Zn(1)-O(6)#1	1.999(5)	N(2)-C(10)	1.453(6)
Zn(1)-O(3)	2.053(4)	N(2)-C(12)	1.464(6)
Zn(1)-N(1)	2.216(4)	N(2)-C(14)	1.468(6)
Zn(1)-N(1)#2	2.216(4)	N(3)-C(13)	1.452(6)
Zn(2)-O(1)#3	2.024(3)	N(3)-C(14)	1.466(6)
Zn(2)-O(1)	2.024(3)	N(3)-C(9)	1.470(6)
Zn(2)-O(7)#3	2.089(4)	N(4)-C(11)	1.474(5)
Zn(2)-O(7)	2.089(4)	N(4)-C(12)	1.488(5)
Zn(2)-N(4)#3	2.342(4)	N(4)-C(13)	1.499(5)
Zn(2)-N(4)	2.342(4)	C(1)-C(2)	1.521(9)
O(1)-C(15)	1.266(6)	C(2)-C(3)	1.377(9)
O(2)-C(15)	1.247(6)	C(2)-C(8)	1.386(9)
O(3)-C(1)	1.262(8)	C(3)-C(4)	1.374(8)
O(4)-C(1)	1.243(8)	C(3)-H(3)	0.9300
O(5)-C(6)	1.200(9)	C(4)-C(5)	1.399(9)
O(6)-C(6)	1.253(9)	C(4)-H(4)	0.9300
O(6)-Zn(1)#4	1.999(5)	C(5)-C(7)	1.370(9)
O(7)-HO7A	0.810(19)	C(5)-C(6)	1.507(9)
O(7)-HO7B	0.80(2)	C(7)-C(8)	1.378(9)
O(8)-HO8A	0.84(10)	C(7)-H(7)	0.9300
O(8)-HO8B	0.62(7)	C(8)-H(8)	0.9300
N(1)-C(11)	1.476(5)	C(9)-H(9A)	0.9700
N(1)-C(9)	1.498(5)	C(9)-H(9B)	0.9700

C(10)-H(10A)	0.9700	C(15)-C(16)	1.490(6)
C(10)-H(10B)	0.9700	C(16)-C(18)	1.381(7)
C(11)-H(11A)	0.9700	C(16)-C(17)	1.391(6)
C(11)-H(11B)	0.9700	C(17)-C(18)#5	1.369(6)
C(12)-H(12A)	0.9700	C(17)-H(17)	0.9300
C(12)-H(12B)	0.9700	O(9)-HO9A	0.80(2)
C(13)-H(13A)	0.9700	O(9)-HO9B	0.77(2)
C(13)-H(13B)	0.9700	O(10)-HO10	0.73(6)
C(14)-H(14A)	0.9700	C(18)-C(17)#5	1.369(6)
C(14)-H(14B)	0.9700	C(18)-H(18)	0.9300
O(8)-Zn(1)-O(6)#1	99.5(3)	C(11)-N(1)-C(10)	107.7(3)
O(8)-Zn(1)-O(3)	104.1(2)	C(9)-N(1)-C(10)	106.5(4)
O(6)#1-Zn(1)-O(3)	156.3(2)	C(11)-N(1)-Zn(1)	108.1(3)
O(8)-Zn(1)-N(1)	98.12(10)	C(9)-N(1)-Zn(1)	112.6(3)
O(6)#1-Zn(1)-N(1)	89.92(10)	C(10)-N(1)-Zn(1)	113.7(3)
O(3)-Zn(1)-N(1)	86.79(10)	C(10)-N(2)-C(12)	108.2(4)
O(8)-Zn(1)-N(1)#2	98.12(10)	C(10)-N(2)-C(14)	108.6(4)
O(6)#1-Zn(1)-N(1)#2	89.92(10)	C(12)-N(2)-C(14)	108.3(4)
O(3)-Zn(1)-N(1)#2	86.79(9)	C(13)-N(3)-C(14)	109.1(4)
N(1)-Zn(1)-N(1)#2	163.57(19)	C(13)-N(3)-C(9)	108.1(4)
O(1)#3-Zn(2)-O(1)	180.000(1)	C(14)-N(3)-C(9)	108.5(4)
O(1)#3-Zn(2)-O(7)#3	88.56(14)	C(11)-N(4)-C(12)	108.0(3)
O(1)-Zn(2)-O(7)#3	91.44(13)	C(11)-N(4)-C(13)	107.4(3)
O(1)#3-Zn(2)-O(7)	91.44(13)	C(12)-N(4)-C(13)	106.9(4)
O(1)-Zn(2)-O(7)	88.56(14)	C(11)-N(4)-Zn(2)	111.4(3)
O(7)#3-Zn(2)-O(7)	180.000(1)	C(12)-N(4)-Zn(2)	110.0(3)
O(1)#3-Zn(2)-N(4)#3	91.68(13)	C(13)-N(4)-Zn(2)	112.9(3)
O(1)-Zn(2)-N(4)#3	88.32(13)	O(4)-C(1)-O(3)	124.9(6)
O(7)#3-Zn(2)-N(4)#3	85.22(14)	O(4)-C(1)-C(2)	118.2(6)
O(7)-Zn(2)-N(4)#3	94.78(14)	O(3)-C(1)-C(2)	116.8(6)
O(1)#3-Zn(2)-N(4)	88.32(13)	C(3)-C(2)-C(8)	117.9(6)
O(1)-Zn(2)-N(4)	91.68(13)	C(3)-C(2)-C(1)	121.1(6)
O(7)#3-Zn(2)-N(4)	94.78(14)	C(8)-C(2)-C(1)	121.0(6)
O(7)-Zn(2)-N(4)	85.22(14)	C(4)-C(3)-C(2)	122.4(6)
N(4)#3-Zn(2)-N(4)	180.000(1)	C(4)-C(3)-H(3)	118.8
C(15)-O(1)-Zn(2)	130.0(3)	C(2)-C(3)-H(3)	118.8
C(1)-O(3)-Zn(1)	120.8(4)	C(3)-C(4)-C(5)	119.2(6)
C(6)-O(6)-Zn(1)#4	144.3(5)	C(3)-C(4)-H(4)	120.4
Zn(2)-O(7)-HO7A	102(4)	C(5)-C(4)-H(4)	120.4
Zn(2)-O(7)-HO7B	133(4)	C(7)-C(5)-C(4)	118.4(6)
HO7A-O(7)-HO7B	116(6)	C(7)-C(5)-C(6)	121.4(6)
Zn(1)-O(8)-HO8A	138(7)	C(4)-C(5)-C(6)	120.1(6)
Zn(1)-O(8)-HO8B	113(8)	O(5)-C(6)-O(6)	125.1(7)
HO8A-O(8)-HO8B	110(10)	O(5)-C(6)-C(5)	117.8(7)
C(11)-N(1)-C(9)	108.0(3)	O(6)-C(6)-C(5)	117.1(7)

C(5)-C(7)-C(8)	121.9(6)	N(4)-C(12)-H(12B)	109.1
C(5)-C(7)-H(7)	119.0	H(12A)-C(12)-H(12B)	107.8
C(8)-C(7)-H(7)	119.0	N(3)-C(13)-N(4)	112.6(4)
C(7)-C(8)-C(2)	120.1(6)	N(3)-C(13)-H(13A)	109.1
C(7)-C(8)-H(8)	120.0	N(4)-C(13)-H(13A)	109.1
C(2)-C(8)-H(8)	120.0	N(3)-C(13)-H(13B)	109.1
N(3)-C(9)-N(1)	112.1(4)	N(4)-C(13)-H(13B)	109.1
N(3)-C(9)-H(9A)	109.2	H(13A)-C(13)-H(13B)	107.8
N(1)-C(9)-H(9A)	109.2	N(3)-C(14)-N(2)	112.0(4)
N(3)-C(9)-H(9B)	109.2	N(3)-C(14)-H(14A)	109.2
N(1)-C(9)-H(9B)	109.2	N(2)-C(14)-H(14A)	109.2
H(9A)-C(9)-H(9B)	107.9	N(3)-C(14)-H(14B)	109.2
N(2)-C(10)-N(1)	112.6(4)	N(2)-C(14)-H(14B)	109.2
N(2)-C(10)-H(10A)	109.1	H(14A)-C(14)-H(14B)	107.9
N(1)-C(10)-H(10A)	109.1	O(2)-C(15)-O(1)	124.6(4)
N(2)-C(10)-H(10B)	109.1	O(2)-C(15)-C(16)	119.1(4)
N(1)-C(10)-H(10B)	109.1	O(1)-C(15)-C(16)	116.3(4)
H(10A)-C(10)-H(10B)	107.8	C(18)-C(16)-C(17)	118.5(4)
N(4)-C(11)-N(1)	112.6(4)	C(18)-C(16)-C(15)	120.6(4)
N(4)-C(11)-H(11A)	109.1	C(17)-C(16)-C(15)	120.9(4)
N(1)-C(11)-H(11A)	109.1	C(18)#5-C(17)-C(16)	120.7(4)
N(4)-C(11)-H(11B)	109.1	C(18)#5-C(17)-H(17)	119.7
N(1)-C(11)-H(11B)	109.1	C(16)-C(17)-H(17)	119.7
H(11A)-C(11)-H(11B)	107.8	HO9A-O(9)-HO9B	93(8)
N(2)-C(12)-N(4)	112.7(4)	C(17)#5-C(18)-C(16)	120.8(4)
N(2)-C(12)-H(12A)	109.1	C(17)#5-C(18)-H(18)	119.6
N(4)-C(12)-H(12A)	109.1	C(16)-C(18)-H(18)	119.6
N(2)-C(12)-H(12B)	109.1		

---

Symmetry transformations used to generate equivalent atoms:

#1  $x-1, y, z-1$ . #2  $x, -y+1/2, z$ . #3  $-x, -y+1, -z+1$ . #4  $x+1, y, z+1$ . #5  $-x+1, -y+1, -z+2$

**Table 50.** Anisotropic displacement parameters ( $\text{\AA}^2 \times 10^3$ ) for [bis ( $\mu_2$ -terephthalato)-( $\mu_2$ -hexamethylenetetramino)-diaqua-dizinc (II) dihydrate] (**12**). The anisotropic displacement factor exponent takes the form:  $-2p^2[h^2 a^*2U_{11} + \dots + 2hk a^* b^* U_{12}]$ .

	U <sub>11</sub>	U <sub>22</sub>	U <sub>33</sub>	U <sub>23</sub>	U <sub>13</sub>	U <sub>12</sub>
Zn(1)	23(1)	28(1)	20(1)	0	4(1)	0
Zn(2)	22(1)	21(1)	19(1)	1(1)	-2(1)	-1(1)
O(1)	19(2)	31(2)	19(2)	2(2)	-4(1)	0(2)
O(2)	47(2)	29(2)	38(2)	-3(2)	-20(2)	5(2)
O(3)	26(3)	28(3)	19(2)	0	3(2)	0
O(4)	29(3)	86(4)	21(3)	0	7(2)	0
O(5)	66(5)	195(9)	20(3)	0	15(3)	0
O(6)	33(3)	35(3)	30(3)	0	-7(2)	0
O(7)	31(2)	25(2)	30(2)	-1(2)	4(2)	-3(2)
O(8)	32(4)	98(6)	26(3)	0	8(3)	0
N(1)	23(2)	19(2)	22(2)	2(2)	7(2)	2(2)
N(2)	27(2)	26(2)	30(2)	-2(2)	9(2)	-4(2)
N(3)	31(2)	24(2)	24(2)	3(2)	8(2)	2(2)
N(4)	19(2)	21(2)	24(2)	-1(2)	5(2)	0(2)
C(1)	21(4)	17(3)	30(4)	0	5(3)	0
C(2)	24(4)	16(3)	20(3)	0	3(3)	0
C(3)	22(4)	24(4)	24(3)	0	10(3)	0
C(4)	19(4)	30(4)	29(4)	0	2(3)	0
C(5)	29(4)	18(3)	21(3)	0	8(3)	0
C(6)	36(5)	32(4)	28(4)	0	10(4)	0
C(7)	26(4)	32(4)	25(3)	0	11(3)	0
C(8)	19(4)	35(4)	27(4)	0	10(3)	0
C(9)	34(3)	27(3)	25(2)	4(2)	10(2)	7(2)
C(10)	21(3)	33(3)	27(3)	4(2)	8(2)	3(2)
C(11)	20(2)	22(2)	21(2)	1(2)	7(2)	0(2)
C(12)	22(3)	20(3)	31(3)	1(2)	8(2)	-2(2)
C(13)	28(3)	27(3)	31(3)	3(2)	10(2)	5(2)
C(14)	35(3)	33(3)	33(3)	4(2)	16(2)	-5(2)
C(15)	23(3)	39(3)	20(2)	-1(2)	5(2)	-2(2)
C(16)	19(3)	30(3)	19(2)	3(2)	5(2)	-1(2)
C(17)	27(3)	26(3)	25(3)	-1(2)	2(2)	-1(2)
O(9)	30(3)	47(3)	34(3)	0	14(3)	0
O(10)	118(7)	44(4)	32(3)	0	24(4)	0
C(18)	25(3)	31(3)	23(2)	7(2)	-1(2)	7(2)

**Table 51.** Hydrogen coordinates ( $\times 10^4$ ) and isotropic displacement parameters ( $\text{\AA}^2 \times 10^3$ ) for [bis ( $\mu_2$ -terephthalato)-( $\mu_2$ -hexamethylenetetramino)-diaqua-dizinc (II) dihydrate] (**12**).

	x	y	z	U(eq)
H(3)	8187	2500	6038	28
H(4)	9733	2500	8320	34
H(7)	6270	2500	9264	33
H(8)	4733	2500	6978	32
H(9A)	2122	4113	715	35
H(9B)	610	3964	778	35
H(10A)	4295	3950	4220	33
H(10B)	4349	4107	2795	33
H(11A)	513	3706	2987	26
H(11B)	1954	3695	4331	26
H(12A)	2679	5707	4427	31
H(12B)	3283	4913	5203	31
H(13A)	-387	4924	1766	35
H(13B)	442	5716	2341	35
H(14A)	2768	5953	2252	40
H(14B)	3422	5315	1600	40
H(17)	4650	3680	9464	35
H(18)	3437	5927	8572	36
HO10	2810(60)	2150(40)	-1620(60)	80(20)
HO7A	-550(30)	6300(30)	4070(40)	36(16)
HO7B	650(60)	6550(20)	5180(50)	60(20)
HO8A	3580(100)	2500	540(100)	80(40)
HO8B	4350(80)	2500	1740(80)	30(30)
HO9A	8350(100)	2500	12970(30)	90(40)
HO9B	7760(30)	2500	13690(50)	0(15)



**Table 52.** Torsion angles [°] for [bis ( $\mu_2$ -terephthalato)-( $\mu_2$ -hexamethylenetetramino)-diaqua-dizinc (II) dihydrate] (**12**).

O(1)#3-Zn(2)-O(1)-C(15)	-55(94)	O(1)-Zn(2)-N(4)-C(11)	93.0(3)
O(7)#3-Zn(2)-O(1)-C(15)	10.7(4)	O(7)#3-Zn(2)-N(4)-C(11)	1.4(3)
O(7)-Zn(2)-O(1)-C(15)	-169.3(4)	O(7)-Zn(2)-N(4)-C(11)	-178.6(3)
N(4)#3-Zn(2)-O(1)-C(15)	95.9(4)	N(4)#3-Zn(2)-N(4)-C(11)	13(73)
N(4)-Zn(2)-O(1)-C(15)	-84.1(4)	O(1)#3-Zn(2)-N(4)-C(12)	153.2(3)
O(8)-Zn(1)-O(3)-C(1)	0.00(1)	O(1)-Zn(2)-N(4)-C(12)	-26.8(3)
O(6)#1-Zn(1)-O(3)-C(1)	180.00(1)	O(7)#3-Zn(2)-N(4)-C(12)	-118.4(3)
N(1)-Zn(1)-O(3)-C(1)	-97.57(10)	O(7)-Zn(2)-N(4)-C(12)	61.6(3)
N(1)#2-Zn(1)-O(3)-C(1)	97.57(10)	N(4)#3-Zn(2)-N(4)-C(12)	-107(73)
O(8)-Zn(1)-N(1)-C(11)	-177.9(3)	O(1)#3-Zn(2)-N(4)-C(13)	33.9(3)
O(6)#1-Zn(1)-N(1)-C(11)	82.5(3)	O(1)-Zn(2)-N(4)-C(13)	-146.1(3)
O(3)-Zn(1)-N(1)-C(11)	-74.1(3)	O(7)#3-Zn(2)-N(4)-C(13)	122.3(3)
N(1)#2-Zn(1)-N(1)-C(11)	-6.9(8)	O(7)-Zn(2)-N(4)-C(13)	-57.7(3)
O(8)-Zn(1)-N(1)-C(9)	62.9(4)	N(4)#3-Zn(2)-N(4)-C(13)	134(74)
O(6)#1-Zn(1)-N(1)-C(9)	-36.7(3)	Zn(1)-O(3)-C(1)-O(4)	0.000(2)
O(3)-Zn(1)-N(1)-C(9)	166.7(3)	Zn(1)-O(3)-C(1)-C(2)	180.000(2)
N(1)#2-Zn(1)-N(1)-C(9)	-126.1(6)	O(4)-C(1)-C(2)-C(3)	0.000(2)
O(8)-Zn(1)-N(1)-C(10)	-58.3(4)	O(3)-C(1)-C(2)-C(3)	180.000(2)
O(6)#1-Zn(1)-N(1)-C(10)	-157.9(3)	O(4)-C(1)-C(2)-C(8)	180.000(3)
O(3)-Zn(1)-N(1)-C(10)	45.5(3)	O(3)-C(1)-C(2)-C(8)	0.000(2)
N(1)#2-Zn(1)-N(1)-C(10)	112.6(7)	C(8)-C(2)-C(3)-C(4)	0.000(2)
O(1)#3-Zn(2)-N(4)-C(11)	-87.0(3)	C(1)-C(2)-C(3)-C(4)	180.000(3)
C(2)-C(3)-C(4)-C(5)	0.000(3)	C(14)-N(2)-C(10)-N(1)	-58.8(5)
C(3)-C(4)-C(5)-C(7)	0.000(4)	C(11)-N(1)-C(10)-N(2)	-57.8(5)
C(3)-C(4)-C(5)-C(6)	180.000(4)	C(9)-N(1)-C(10)-N(2)	57.9(5)
Zn(1)#4-O(6)-C(6)-O(5)	0.000(6)	Zn(1)-N(1)-C(10)-N(2)	-177.6(3)
Zn(1)#4-O(6)-C(6)-C(5)	180.000(4)	C(12)-N(4)-C(11)-N(1)	-57.4(4)
C(7)-C(5)-C(6)-O(5)	0.000(4)	C(13)-N(4)-C(11)-N(1)	57.6(5)
C(4)-C(5)-C(6)-O(5)	180.000(3)	Zn(2)-N(4)-C(11)-N(1)	-178.3(2)
C(7)-C(5)-C(6)-O(6)	180.000(3)	C(9)-N(1)-C(11)-N(4)	-57.6(4)
C(4)-C(5)-C(6)-O(6)	0.000(4)	C(10)-N(1)-C(11)-N(4)	57.0(4)
C(4)-C(5)-C(7)-C(8)	0.000(3)	Zn(1)-N(1)-C(11)-N(4)	-179.7(3)
C(6)-C(5)-C(7)-C(8)	180.000(3)	C(10)-N(2)-C(12)-N(4)	-58.8(5)
C(5)-C(7)-C(8)-C(2)	0.000(3)	C(14)-N(2)-C(12)-N(4)	58.8(5)
C(3)-C(2)-C(8)-C(7)	0.000(3)	C(11)-N(4)-C(12)-N(2)	57.9(5)
C(1)-C(2)-C(8)-C(7)	180.000(3)	C(13)-N(4)-C(12)-N(2)	-57.4(5)
C(13)-N(3)-C(9)-N(1)	-58.9(5)	Zn(2)-N(4)-C(12)-N(2)	179.7(3)
C(14)-N(3)-C(9)-N(1)	59.2(5)	C(14)-N(3)-C(13)-N(4)	-58.1(5)
C(11)-N(1)-C(9)-N(3)	57.7(5)	C(9)-N(3)-C(13)-N(4)	59.7(5)
C(10)-N(1)-C(9)-N(3)	-57.7(5)	C(11)-N(4)-C(13)-N(3)	-58.8(5)
Zn(1)-N(1)-C(9)-N(3)	177.0(3)	C(12)-N(4)-C(13)-N(3)	56.9(5)
C(12)-N(2)-C(10)-N(1)	58.6(5)	Zn(2)-N(4)-C(13)-N(3)	178.0(3)

C(13)-N(3)-C(14)-N(2)	58.5(5)	
C(9)-N(3)-C(14)-N(2)	-59.0(5)	C(17)-C(16)-C(18)-C(17)#5 2.0(8)
C(10)-N(2)-C(14)-N(3)	58.9(5)	C(15)-C(16)-C(18)-C(17)#5 179.2(4)
C(12)-N(2)-C(14)-N(3)	-58.5(5)	
Zn(2)-O(1)-C(15)-O(2)	8.0(8)	
Zn(2)-O(1)-C(15)-C(16)	-172.7(3)	Symmetry transformations used to
O(2)-C(15)-C(16)-C(18)	-177.6(5)	generate equivalent atoms:
O(1)-C(15)-C(16)-C(18)	3.0(7)	#1 x-1,y,z-1 #2 x,-y+1/2,z #3 -x,-
O(2)-C(15)-C(16)-C(17)	1.2(8)	y+1,-z+1 #4 x+1,y,z+1 #5 -x+1,-
O(1)-C(15)-C(16)-C(17)	-178.2(4)	y+1,-z+2
C(18)-C(16)-C(17)-C(18)#5	-2.0(8)	
C(15)-C(16)-C(17)-C(18)#5	179.2(4)	

**Table 53.** Hydrogen bonds for [bis ( $\mu_2$ -terephthalato)-( $\mu_2$ -hexamethylenetetramino)-diaqua-diZinc (II) dihydrate] (**12**) [ $\text{\AA}$  and  $^\circ$ ].

D-H...A	d(D-H)	d(H...A)	d(D...A)	$\angle(\text{DHA})$
O(8)-HO8A...O(10)	0.84(10)	1.73(10)	2.541(7)	163(10)
O(8)-HO8B...O(4)	0.62(7)	2.18(8)	2.687(8)	142(10)
O(9)-HO9A...O(5)	0.80(2)	1.84(4)	2.598(7)	158(10)
O(7)-HO7A...O(2)#3	0.810(19)	1.84(3)	2.623(5)	161(5)
O(7)-HO7A...O(2)#3	0.810(19)	1.84(3)	2.623(5)	161(5)

Symmetry transformation used to generate equivalent atoms

#1 x-1,y,z-1. #2 x,-y+1/2,z. #3 -x,-y+1,-z+1. #4 x+1,y,z+1. #5 -x+1,-y+1,-z+2

